School of Electrical and Data Engineering
Faculty of Engineering and Information Technology

A Dissertation submitted in fulfilment of the requirements for the degree of Doctor of Philosophy

D2D Communications in 5G Mobile Cellular Networks

We propose and validate a novel approach to mobility management

Autumn 2018

by
Shouman Barua

Supervisor

Professor Robin Braun

Professor of Telecommunications Engineering, School of Electrical and Data Engineering.
Core Member, Global Big Data Technologiy Centre
University of Technology Sydney

Co-supervisor

Associate Professor Mehran Abolhasan

Deputy Head of School, School of Electrical and Data Engineering
Core Member, Global Big Data Technology Centre
University of Technology Sydney

To my lovely parents...

Declaration

To the best of my knowledge and belief this work was prepared without aid from any other sources except where indicated. Any reference to material previously published by any other person has been duly acknowledged.

Signature: Production Note: Signature removed prior to publication. .....

Place: University of Technology Sydney

Date: 6th July, 2018

Acknowledgements

This work would have never been finished without the help of many great inspiring people around me.

Firstly, I would like to mention the most inspiring person of my PhD period, my great supervisor Professor Robin Braun. I would like to express my sincere gratitude to him. His scholastic guidance inspired me every moment to get the work done on time. He was my excellent source of motivation, encouragement and always made me go the extra mile even when I was feeling upset. He guided me in resolving my problems with his solid advice and extensive experience. His vast knowledge of mathematics, simulation and wireless theory helped me to get the topic so quickly. I learned many things from him apart from my research. I am again grateful to him and thank him for everything he has done for me. His trust and patience towards me will always be appreciated and acknowledged. I feel lucky, and it has been my privilege to be able to have him as my supervisor.

I would like to thank my co-supervisor Associate Professor Mehran Abolhasan for agreeing to supervise me and for supporting me throughout the research period.

I would like to thank the Australian Government and the University of Technology Sydney for selecting me for an Australian Post-Graduate Award (APA) Scholarship. I was sincerely honored to have been selected as a recipient of this prestigious scholarship

I was also pleased to have Dr Pakawat Pupatwibul as my research colleague as well as my friend at all times. He inspired me to keep pace and stay calm during the candidature confirmation and the later stages. Thank you, Dr Pakawat, for your great support.

I would like to acknowledge the support of the Graduate Research School (GRS), University of Technology Sydney throughout my UTS doctoral studies and express sincere gratitude to the members of the Centre of Real Time Information (CRIN) for all their support.

My sincere gratitude to the School of Electrical and Data Engineering and Faculty of Engineering and Information Technology for all kinds of support with funding to travel locally and abroad to present my papers.

I am genuinely indebted to the UTS CISCO course co-ordinator Max Hendriks for giving me the scope to teach his course at UTS. Teaching is always an exciting undertaking and I gained valuable experience by teaching here.

I am grateful to all the people on Level Six of the Engineering Building for a lot of support, fun and memorable times. You are surely amazing guys who made my early days easier.

I would like to thank my friends Ashis, junior Pantha, Emon, Afaz and many others for their inspiration and co-operation at all times.

I would like to thank all my friends from school, college, the 01 EEE batch of Chittagong University of Engineering and Technology, Bangladesh and all the well-wishers from Germany during my Masters studies there.

Last but by no means the least, I would like to give credit to my lovely parents and family for loving, inspiring and trusting me that I could make this happen. It's been a long time and thank you for encouraging me at all times to attain the highest degree that one can achieve in life. Credit also goes to my relatives and my great well-wisher, my maternal uncle Ajay Kanti Barua and his family who give me and my family so much love and support at all times.

Thank you once again to all of my well-wishers who always trust me and love me beyond the limit.

Abstract

Fifth Generation (5G) stands for future fitness combined with flexible technical solutions that combine with the latest wireless technology. 5G is expected to multiply a thousand times (1000x) in data speed with 20.4 billion devices (IoT) connected to the network by 2020. This literally means everything connecting to everything. From the network point of view, lower latency along with high flexibility is not limited just to 5G. It is already being implemented in real networks. The number of wireless devices connected to networks has increased remarkably over the last couple of decades. Ubiquitous voice and data connections are the fundamental requirements for the next generation of wireless technology.

Device-to-Device communication is widely known as D2D. It is a new paradigm for cellular communication. It was initially proposed to boost network performance. It is considered to be an integral part of the next generation (5G) of telecommunications networks. It takes place when two devices communicate directly without significant help from the base station. In a cellular network, Device-to-Device communication has been viewed as a promising technology overcoming many existing problems. These include capacity, quality and scarce spectrum resources. However, this comes at the price of increased interference and complex mobility issues, even though it was proposed as a new paradigm to enhance network performance. Nevertheless, it is still a challenge to manage devices that are moving. Cellular devices without well-managed mobility are hardly acceptable. Considering in-band underlay D2D communication, a well-managed mobility system in cellular communication should have lower latency, lower power consumption and higher data rates. In this dissertation, we review existing mobility management systems for LTE-Advanced technology and propose an algorithm to be used over the current system so that lower signalling overheads and less delay, along with uninterrupted D2D communication, are guaranteed. We model and simulate our algorithm, comparing the results with mathematical models based on Markov theory.

As in other similar communication systems, mobility management for D2D communication is yet to be explored fully. There are few research papers published so far. What we can say is that the intention of such systems in cellular networks are to enable lower latency, lower power consumption, less complexity and, last but not least, uninterrupted data connections. Our simulation results validate our proposed model and highlight D2D communication and its mobility issues.

An essential element of our proposal is to estimate the user's location. We can say that a mobility management system for D2D communication is hardly workable if the location of the users is not realisable. This dissertation also shows some latest techniques for estimating the direction of arrival (DOA) with mathematical models and simulation results. Smart antenna systems are proposed. It is possible to determine the location of a user by considering the uplink transmission system. Estimating the channel and actual path delay is also an important task, which might be done by using 1D uniform linear array (ULA) or 2D Uniform Rectangular (URA) array antenna systems. In this chapter, 1D ULA is described utilising some well-known techniques. The channel characteristics largely determine the performance of an end-to-end communication system. It determines the signal transformation while propagating through the channel between receivers and transmitters. Accurate channel information is crucial for both the transmitter and receiver ends to perform at their best. The ultimate focus of this part is to estimate the channel based on 2D parameter estimation. Uniform Rectangular Array (URA) is used to perform the 2D parameter estimation. It is possible to estimate azimuth and elevation of a source by using the URA model.

The problem of mobility in this context has been investigated in few papers, with no reliable solutions as yet. We propose a unique algorithm for mobility management for D2D communications. In this dissertation, we highlight and explain the mobility model mathematically and analytically, along with the a simulation of the Markovian model. A Markov model is essentially a simplified approach to describing a system that occupies a discrete state at any point in time. We also make a bridge between our mobility algorithm and a Markovian model.

Research Structure

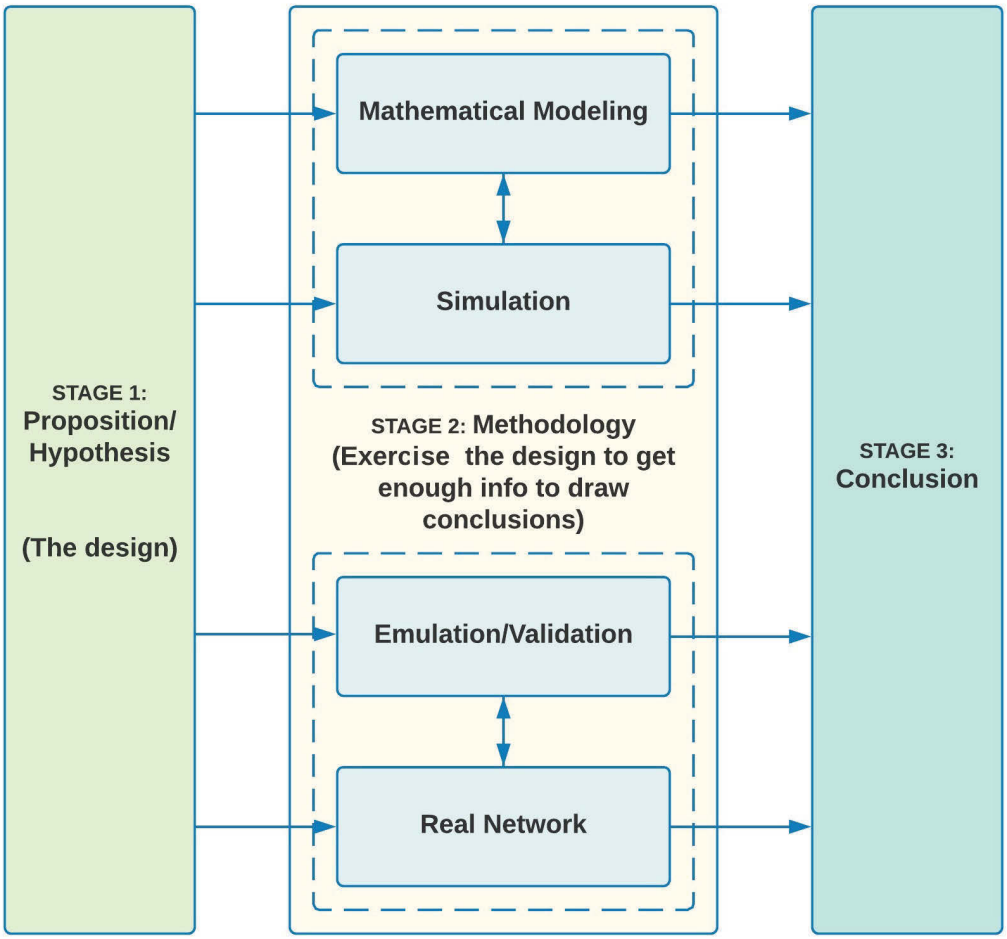

Figure 1: Stages and structure of the overall research

List of Publications

Most of the theories, technical discussions and contributions in this dissertation are based on the following publications written by the author in which others are the co-authors.

A. International Conference Publications:

[$C1$] S. Barua and R. Braun, "Mobility management of D2D communication for the 5G cellular network system: A study and result," 2017 17th International Symposium on Communications and Information Technologies (ISCIT), Cairns, QLD, 2017, pp. 1-6. doi: 10.1109/ISCIT.2017.8261187, IEEE.

[$C2$] S. Barua and R. Braun, "A novel approach of mobility management for the D2D communications in 5G mobile cellular network system," 2016 18th Asia-Pacific Network Operations and Management Symposium (APNOMS), Kanazawa, 2016, pp. 1-4. doi: 10.1109/APNOMS.2016.7737272, IEEE.

[$C3$] S. Barua and R. Braun, "A Markovian Approach to the Mobility Management for the D2D Communication in 5G Cellular Network System," 2017 5th Asia Pacific International Conference on Computer Assisted and System Engineering (APCASE 2017) ISBN 978-0-9924518-0-6.

[$C4$] S. Barua, Sinh Cong Lam, P. Ghosa, Shiqi Xing and K. Sandrasegaran, "A survey of Direction of Arrival estimation techniques and implementation of channel estimation based on SCME," 2015, 12th International Conference on Electrical Engineering/Electronics, Computer, Telecommunications and Information Technology (ECTI-CON), Hua Hin, 2015, pp. 1-5. doi: 10.1109/ECTICon.2015.7206986, IEEE.

[$C5$] S. C. Lam, R. Subramanian, K. Sandrasegaran, P. Ghosal and S. Barua, "Performance of well-known frequency reuse algorithms in LTE downlink 3GPP LTE systems," 2015, 9th International Conference on Signal Processing and Communication Systems (ICSPCS), Cairns, QLD, 2015, pp. 1-5. doi: 10.1109/ICSPCS.2015.7391766, IEEE.

[$C6$] Daeinabi, A., K. Sandrasegaran, and S. Barua. "A dynamic almost blank subframe scheme for video streaming traffic model in heterogeneous networks." 2015, 12th International Conference on Electrical Engineering/Electronics, Computer, Telecommunications and Information

Technology (ECTI-CON), IEEE.

B. International Book Chapter Publications:

[*B*1] S. Barua and R. Braun, "*Direction of Arrival (DOA) and Channel Estimation.*" Self-Organized Mobile Communication Technologies and Techniques for Network Optimization. IGI Global, 2016. 216-235.

C. International Journal Publications:

[*J*1] S. Barua, F. Afroz, S. S. Islam, A. U. Ahmed, P. Ghosal, and K. Sandrasegaran. "Comparative study on priority based QOS aware MAC protocols for WSN." International Journal of Wireless and Mobile Networks 6, no. 5 (2014): p175.

[*J*2] G, Pantha, S. Barua, R. Subramanian, S. Xing, and K. Sandrasegaran. "A novel approach for mobility management in LTE femtocells." International Journal of Wireless and Mobile Networks 6, no. 5 (2014): p45.

[*J*3] K. Haider Ali, S. Barua, P. Ghosal, and K. Sandrasegaran. "Macro with Pico Cells (HetNets) System Behavior Using Well-known scheduling Algorithms." arXiv preprint arXiv:1411.2140 (2014).

[*J*4] F. Afroz, S. Barua, and K. Sandrasegaran. "Performance analysis of FLS, EXP, LOG AND M-LWDF packet scheduling algorithms in downlink 3GPP LTE system." International Journal of Wireless and Mobile Networks 6, no. 5 (2014): p77.

[*J*5] X. Shiqi, P. Ghosal, S. Barua, R. Subramanian, and K. Sandrasegaran. "System level simulation for two tier macro-femto cellular networks." International Journal of Wireless and Mobile Networks 6, no. 6 (2014): p1.

[*J*6] D. Suman, S. Barua, and J. Sen. "Auto default gateway settings for virtual machines in servers using default gateway weight settings protocol (DGW)." International Journal of Wireless and Mobile Networks 6, no. 5 (2014): p133.

[*J*7] S. Ramprasad, S. Barua, S. C. Lam, P. Ghosal, and K. San-

drasegaran. “Group Based Algorithm to Manage Access Technique in the Vehicular Networking to Reduce Preamble ID Collision and Improve RACH allocation in ITS.” International Journal of Wireless and Mobile Networks 6, no. 5 (2014): p1.

Contents

List of Figures

List of Tables

Abbreviations and Acronyms

1G	First Generation System
2G	Second Generation System
3G	Third Generation System
3GPP	3rd Generation Partnership Project.
3GPP2	3rd Generation Partnership Project 2
4G	Fourth Generation System
5G	Fifth Generation System
8PSK	8-Phase Shift Keying
AMPS	Advanced Mobile Phone System
BBU	Baseband Unit
BDMA	Beam Division Multiple Access
CA	Carrier Aggregation
CDMA	Code Division Multiple Access
CDMA2000	Code Division Multiple Access 2000
CoMP	Coordinated Multi-point Transmission
CUE	Cellular User's Equipment
D2D	Device-to-Device
DOA	Direction of Arrival
DUE	D2D User's Equipment
EDGE	Enhanced Data rates for GSM Evolution (EDGE)
eNodeB	Evolved NodeB
eNB	Evolved NodeB
EPC	Evolved Packet Core
ESPRIT	Estimation of Signal Parameters via Rotational Invariance Technique
EV-DO	Evolution-Data Optimised
FDD	Frequency Division Duplex
FDMA	Frequency Division Multiple Access
GFDM	Generalized Frequency Division Multiplexing
GPRS	General Packet Radio Service
GPS	Global Positioning System
GSM	Global System for Mobile Communications
GTP-U	GPRS Tunnelling Protocol for User Plane

HDTV	High Definition TV
HO	Handover
HSDPA	High Speed Downlink Packet Access
HSPA+	Evolved High-Speed Packet Access
HSUPA	High Speed UplinkPacket Access
IMT-Advanced	International Mobile Telecommunications Advanced
IoT	Internet of Things
IPV6	Internet Protocol Version 6
ITU-R	International Telecommunications Union-Radio communications sector
KPI	Key Performance Indicator
LAS-CDMA	Large Area Synchronised Code Division Multiple Access
LOS	Line of Sight
LRAPs	Light RAPs
LTE	Long Term Evolution
LTE-A	LTE-Advanced
LTE-Hi	LTE Hotspot Improvement
MC-CDMA	Multi-Carrier Code Division Multiple Access
MDT	Minimisation of Drive Test
MIMO	Multiple Input, Multiple Output
MME	Mobility Management Entity
MMS	Multimedia Message System
MTC	Machine type communication
Multi-RAT	Multiple Radio Access Technology
MUSIC	Multiple Signal Classication
MVDR	Minimum Variance Distortionless Response
NFV	Network Function Virtualisation
NLOS	Non-Line of Sight
NMT	Nordic Mobile Telephone
NTT	Nippon Telegraph and Telephone
OFDM	Orthogonal Frequency Division Multiplexing
OFDMA	Orthogonal Frequency-Division Multiple Access
PAPR	Peak-to-Average Power Ratio
P-GW	Packet Data Network Gateway
PGW-C	Packet Data Network Gateway Control Plane
PGW-D	Packet Data Network Gateway Data Plane
PRBs	Physical Resource Blocks
PSTN	Public Switched Telephone Network
RACE	Random Access Channel
RAPs	Radio Access Points
RAT	Radio Access Technologies

RoF	Radio-over-Fiber
RSRP	Reference Signal Receive Power
RSRQ	Reference Signal Received Quality
RSSI	Received Signal Strength Indicator
SAS	Smart Antenna System
SCMA	Sparse Code Multiple Access
SDN	Software Defined Networking
S-GW	Serving Gateway
SMS	Short Message Services
SMTP	Simple Mail Transfer Protocol
SNR	Signal-to-Noise Ratio
TACS	Total Access Communication System
TDD	Time Division Duplex
TDMA	Time Division Multiple Access
TD-SCDMA	Time Division Synchronous Code Division Multiple Access
UCA	Uniform Circular Array
UCE	Unified Control Entity
UDW	Unified Data Gateway
UE	User Equipment
ULA	Uniform Linear Array
UMTS	Universal Mobile Telecommunication System
URA	Uniform Rectangular Array
V2V	Vehicle-to-Vehicle
VoIP	Voice over Internet Protocol
W-CDMA	Wideband Code Division Multiple Access
WiFi	Wireless Fidelity
WiMAX	Worldwide Interoperability for Microwave Access
ZC	Zado-Chu Sequence.

Part I

Introduction and Background

Chapter 1

Introduction

In this chapter, the overall research methodology and structure of this dissertation are described. In addition to this, the motivation of this research topic is explained. Some promising research questions are mentioned, and the solutions are also proposed. This chapter presents the objectives and scopes of this dissertation.

1.1 Background of Mobility Management

Nowadays, mobile cellular communication without smooth mobility management is not acceptable. Device-to-Device (D2D) communication is a prospective technology that is yet to be implemented to the real network. A smooth handover method is always a preference for any cellular system, and many methods were developed from the 2G to the 4G mobile system. A heterogeneous network is the latest trend, and a perfect handover system is a key to making it superb for customers. A basic handover system is shown as a line diagram in Figure 1.1. Here, different signalling messages are shown from among the UE, Source eNodeB, and Target eNodeB. Our proposed model for the D2D communication follows this basic model. However, I extended the algorithm to fit it for D2D communication. Detailed description is beyond the scope of this chapter.

1.2 Research Motivation

The major motivations for this dissertation could be considered from three different perspectives. As mentioned in the topic of this dissertation, I studied the motivation from three significant points of view. They are the mo-

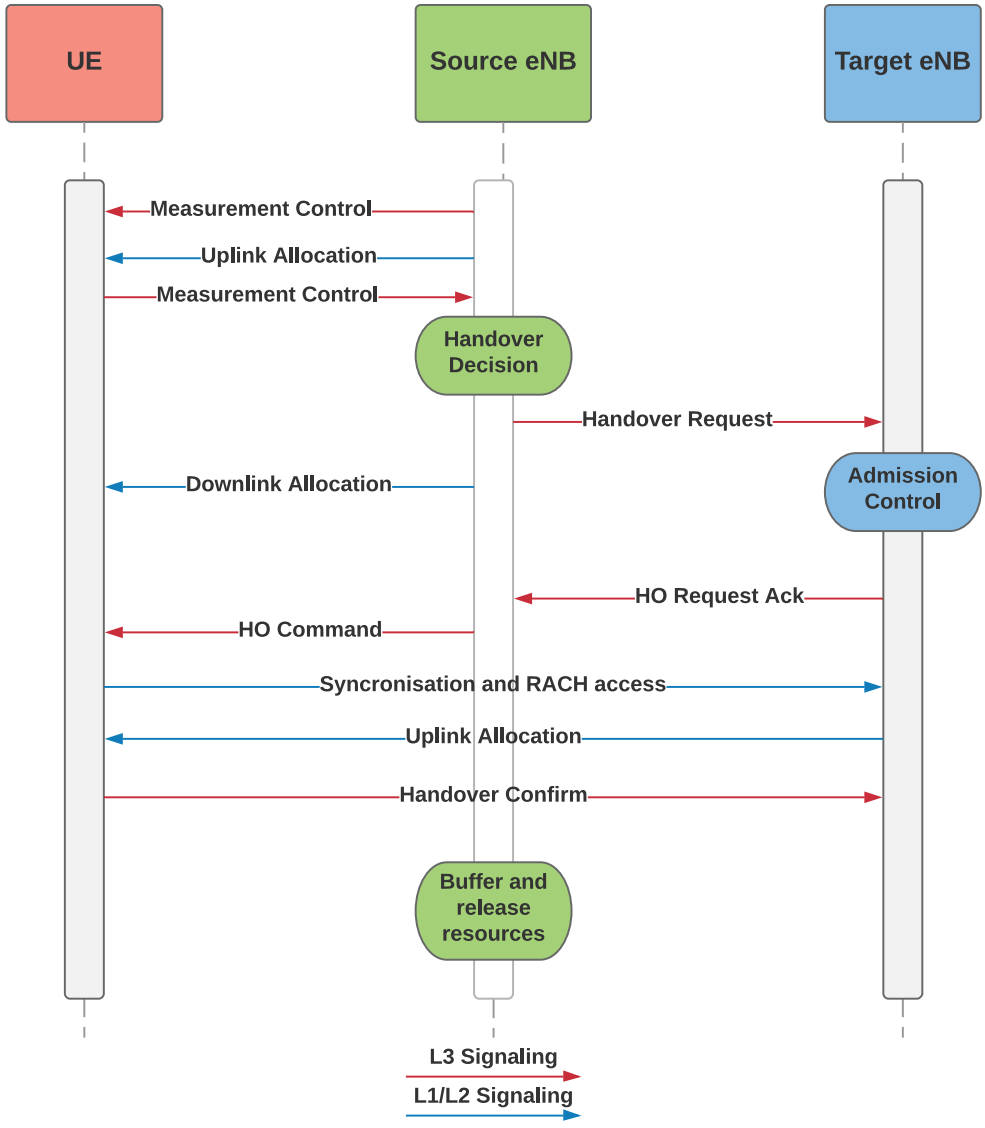

Figure 1.1: Basic handover model for the cellular network system.

bility management process, the prospective 5G cellular system and the D2D communication system.

1.2.1 Motivation from the Mobility Management Process

As mentioned in the previous section, a perfect mobility management system is yet to be developed for D2D communication. As the D2D communication method is one of the prospective technologies for the 5G cellular network, it needs a perfect algorithm to manage the mobility of the devices so that continuous data and voice connection can be maintained. Low latency and low complexity combined with a compatible system with the previous technologies are the main challenges.

1.2.2 Motivation from the Prospective 5G Cellular System

The 5G network is currently the most anticipated technology and it is one that will change the human lifestyle significantly. A lot of research, experiments and tests have already been done to sort out how the 5G network will be realised. It is still an ongoing process. Many new technologies are proposed and considered as the prospective technologies for the 5G network. Three use cases [17, 18] are considered to drive the 5G revolution.

1.2.2.1 Enhance Mobile Broadband

The low latency of fewer than one millisecond and promising 10Gbps connectivity is no longer a dream of the 5G network.

1.2.2.2 The Internet of Things (IoT)

The 5G network is assumed to be a pivotal driver to implement the IoT. Massive data delivery is a pre-requisite for the IoT and 5G is almost ready to handle the challenge.

1.2.2.3 High Reliability

The 5G network will open a new door to network reliability, enabling driverless cars, a virtual reality network and expanding many more applications will enhance the horizons of a unique lifestyle. Only a reliable network can promise all the advantages.

1.2.3 Motivation From the D2D Communication System

D2D communication is included in but not limited to prospective 5G technologies. Implementation of D2D technology in a network can substantially reduce network congestion and increase the data rates including high-spectrum efficiencies. As the technology is new, proper implementation mechanism is yet to come.

1.3 Research Objectives and Scopes

This research aims to develop a model or algorithm for the mobility management of the D2D communications system. However, it is not very straightforward to implement in a real network. The objectives and scope of this dissertation are as follows:

1.3.1 Research Objectives

The target of this research work is to test an algorithm we have developed that allows D2D users to move from one place in different directions without major interruptions to the communication between them. When D2D users are in cellular mode, handover should take place smoothly without compromising quality. This research considers different mobility scenarios when two devices move in two different directions from each other with respect to their base stations. This research also explores the handover possibilities from one base station to other base stations by keeping two devices under the same base station. This research also considers the D2D communications where two devices might be attached to two different base stations.

So far, mobility management for any wireless system is a challenging process, and only a smart algorithm can make it smooth. Although we have reliable handover processes for modern heterogeneous 4G technologies, a more intelligent algorithm would be required to manage the entire mobility for D2D communication in the 5G cellular network system. In Chapter 7, a model of D2D implementation in a mobile network has been shown, and my objective is to extend and develop it by including the mobility issues of real network scenarios.

It is essential to know the location of devices for D2D communication to be possible. I also enhance the state-of-the-art methods to estimate

the direction of arrival by analysing the channel.

Another objective is to explain the mobility of devices analytically using the popular Markov Chain model. Finally, this research aims to develop a novel approach for D2D communications for the 5G mobile cellular network.

1.3.2 Research Scope

Simulation tools like PS-3 and LTE Sim are not able to simulate D2D communication system without modification. I therefore used the MATLAB-2017 to simulate the proposed algorithm. For some simulations, I also used the LTE system simulation toolbox. To simulate analytically, I demonstrated the Markov Chain model and used MATLAB-2017. An implementation of this model in a real network and detailed analysis of the DOA are beyond the scope of this dissertation.

1.4 Problem Statement

Nowadays mobile devices are part and parcel of our daily life. The number of devices attached to the network is not only increasing but the enormous data requirements are also increasing exponentially. Networks should have the ability to contact each other from anywhere at any time. 5G technology is assumed to be a promising next-generation mobile cellular system that should be able to handle this massive amount of data requirements.

Wireless network capabilities need to be extended to meet the demand and expectation of 5G networks. D2D communication is a proposed solution that can solve many problems of internet data speed and can improve spectrum efficiency too. 5G can be defined by three primary KPIs [18]: device connection density is higher than one million per kilometre square (IoT), pick data rate is faster than 10Gbps (enhance mobile broadband use case) and latency is below 1ms. D2D communication can play a significant role in maintaining these KPIs. As the heterogeneous network is already a trend and the footprint of the network is a must, it is essential to offload the eNB as much as possible. The D2D communication system is a promising technology to offload the network infrastructure in this regard.

Mobility is an essential criterion for any wireless network. When D2D communication takes place, the network performance data speed ramps

up. However, when one or both of the devices change location, it not still unknown how this mobility how this mobility and smooth handover would be managed. It is crucial solving the problem of mobility management to maintain the network connection uninterrupted for D2D devices. I have classified five modes based on the moving direction of the D2D users from the eNB. They are as follows:

- D2D mode
- Cellular mode
- Relay mode
- Call waiting mode
- Call drop

1.4.1 Research Question

Based on the movement probability of D2D users, I have formulated and discussed four possible directions in this dissertation. There are four directions when we can raise a question to solve the mobility issues seamlessly.

- D2D transmitter is moving towards another eNB
- D2D receiver is moving towards another eNB.
- Both D2D users are moving towards each other under the same eNB.
- Both D2D users are moving apart towards different eNBs.

From the network point of view, mobility management is the same for all the directions. I therefore consider only one direction to analyse in depth.

1.4.2 Proposition Derived From the Research Question

Considering underlay inband D2D communication, I propose the group handover when one or both devices are moving, i.e., both devices are handled by the same eNB to reduce the overhead and latency while maintaining the maximum data speed. If some D2D communication is not feasible due to the distance from each other or distance from the eNB, some different modes are proposed. Total received power and the data sum-rate of the D2D users can be the primary criterion for selecting a possible option.

1.5 Approach and Methodology

Figure 1.2 shows the approach and methodology used for the research objectives to be accomplished. They follow certain steps until the final result is found. This methodology considers the background of the topic by reviewing the scholarly literature, theoretical knowledge enhancement, increasing the proficiency of simulation tools and finally simulating the proposed model. The significant steps are as follows:

1. Literature reviews and enhance the knowledge of technical background.
2. Identifying and understanding the existing problem.
3. Developing the technical knowledge regarding the existing problem and proposing a solution algorithm.
4. Developing a simulation model using the MATLAB simulation tool.
5. Implementing and validating the proposed algorithm through simulations.
6. Analysing simulation performance, undertaking a comparison and updating the model if required.
7. Making recommendations, reaching conclusions, writing the dissertation and preparing it for submission..

1.6 Statement of Contributions

In this dissertation, a new approach for mobility management has been investigated. For this investigation, I first reviewed the literature and relevant background regarding the topic. Chapters 2, 3 and 4 are the relevant literature review. References have been cited where applicable. However, the tables are the overall summary based on the literature reviews, and the figures are innovative and unless cited in the caption drawn by the author of this dissertation.

Chapters 5, 6, and 7 describe the main proposal of this dissertation. Unless cited, these chapters are the contributions of this dissertation that represent the proposed theory and relevant mathematical derivation contributed by the author. All the pictures are drawn by the author unless cited otherwise in the caption.

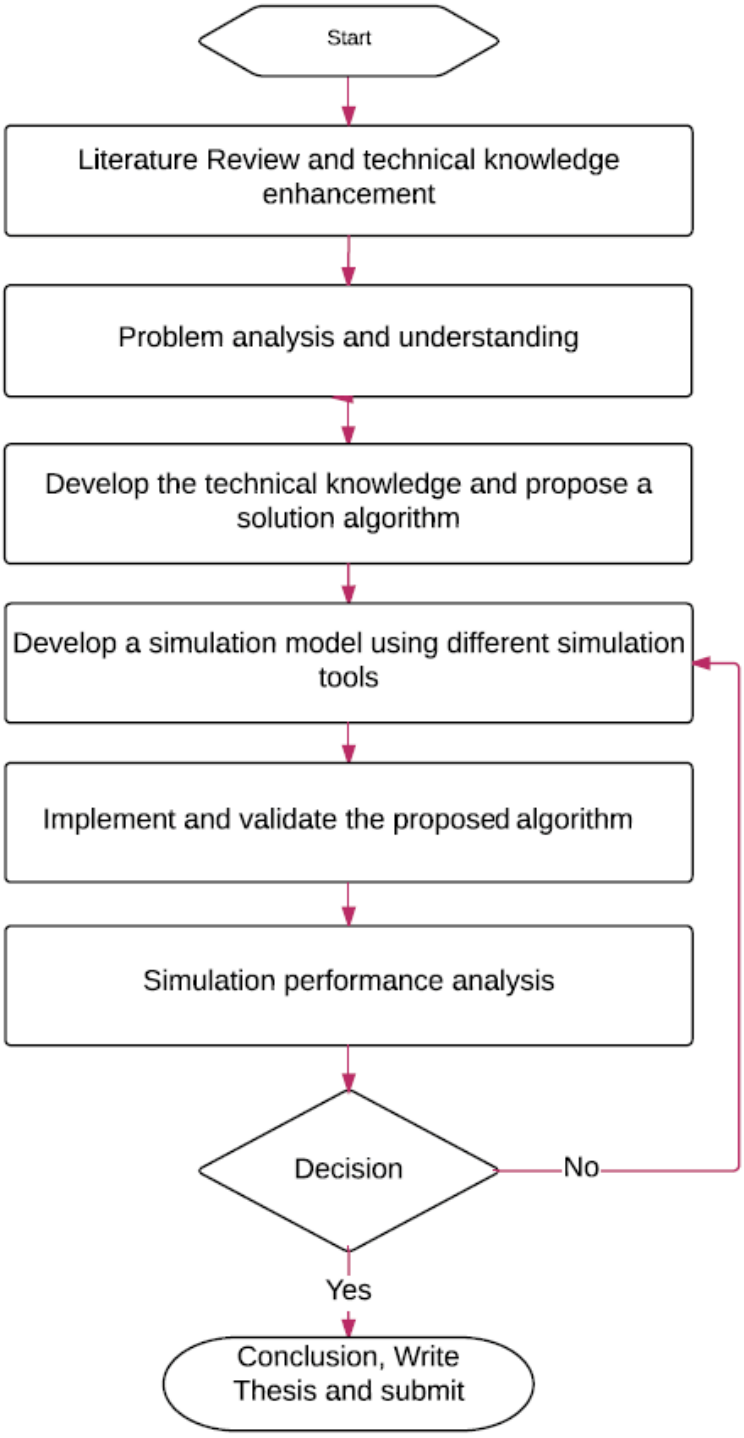

Figure 1.2: Flowchart of approach and methodology

Chapters 8, 9, and 10 are the simulations and results that are done on MATLAB 2017b. The author has contributed the simulation and results. The proposed model is unique and might be helpful for future researchers and can be a trial to implement in the real network for the 5G cellular network system.

1.7 Overview and Outline of Dissertation Structure

Figure 1.3 shows the overall structure of the dissertation. This dissertation consists in total of 11 chapters. After introducing the basic ideas about the whole dissertation in Chapter 1, I have organized the rest of the chapters as follows:

Chapter 2 - This chapter represents the history of telecommunication till now. Starting from the prehistoric era, this chapter describes all the generations of the telecommunication system.

Chapter 3 - This chapter is dedicated exclusively to the issues of the 5G network system. This chapter highlights all the prospective technologies that might be an integral part of the 5G cellular network system.

Chapter 4 - In this chapter, I have tried to give a brief description of the D2D communication system. It includes basics and total types of D2D communication and their pros and cons.

Chapter 5 -This chapter is an in-depth extension of my published paper [19] and book chapter [20] based on the direction of arrival and channel estimation for it. It describes state-of-the-art technologies to estimate the DOA by analysing the channel.

Chapter 6 - A brief explanation of mobility management for D2D communication, including problems and proposed solutions along with the algorithm are described in this chapter. This chapter is based on my published conference paper [21, 22].

Chapter 7 - This chapter validates the mobility management from the Markovian Chain model point of view. It describes in-depth theory based on the mobility probability of D2D users. This chapter is based on my published paper [23].

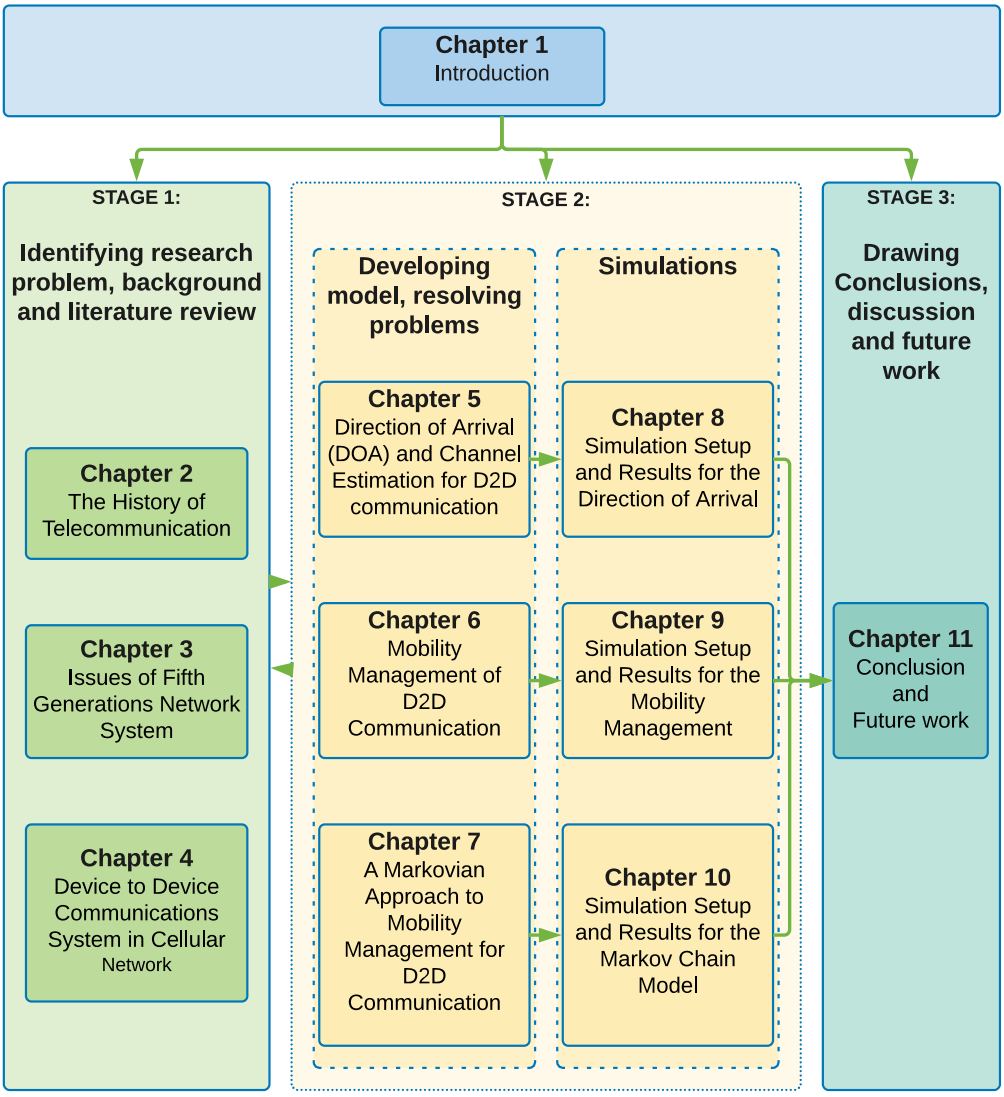

Figure 1.3: Overview and outline of dissertation structure

Chapter 8 - This chapter describes the setting up the simulation and results based on the theory of DOA and the channel estimation described in Chapter 5.

Chapter 9 - The simulation setup and results for the proposed theory detailed in Chapter 6 are described in this chapter.

Chapter 10 - This chapter is dedicated to the simulation results for the Markovian model described in Chapter 7. It also simulates different types of walking models.

Chapter 11 - This final chapter summarises and concludes the dissertation and suggests the scope of future research.

1.8 Mathematical Conventions

Some mathematical conventions are stated here in order to be consistent throughout the dissertation. Scalars are denoted by lower case letters, vectors and matrices are denoted by lower case and upper case bold letters respectively. Hermitian, transpose and pseudo-inverse of a matrix are denoted by $\{.\}^H$, $\{.\}^T$ and $\{.\}^\dagger$, respectively. The elements of a $K \times L$ matrix are denoted by $\{.\}_{k,l}$, for $k = 1, \ldots, K$ and $l = 1, \ldots, L$, respectively. Khatri-Rao product, Kronecker product, Hadamard and dot product are denoted by $\circ$, $\otimes$, $\odot$, and $\cdot$, respectively. $E\{.\}$ denotes statistical expectation, $\{.\}^*$ represents conjugate, vec$\{.\}$ is vectorization operator, and $\lfloor z \rfloor$ rounds off z to the largest integer number not greater than z. $\Re\{.\}$ and $\Im\{\}$ returns the real and imaginary values, respectively.

Chapter 2

The History of Telecommunication

Telecommunication is defined as an exchange of information between two end users over distance through one or more mediums. The history of telecommunication is not limited to the last couple of decades. Exchanging information from a distance started even earlier than when Alexander Graham Bell invented the telephone system in 1876, when the first telephone patent was issued. The telecommunication system from prehistoric man with fire signals to the current smartphone with millions of applications is still key to humanity's success and survival.

The following timelines illustrate the major communication eras and the communication methods used. [24] [25]:

In the prehistoric era: fire, smoke signals, beacons and horns had been used.

6th Century BCE: mail.

5th century BCE: pigeon post.

4th century BCE: Hydraulic semaphore.

Circa 490 BCE: heliographs.

15th century CE: maritime flag semaphore.

1672: first experimental acoustic telephone.

1838: electrical telegraph.

1858: first trans Atlantic telegraph cable.

1867: signal lamps.

1876: telephones.

1877: acoustic phonograph.

1880: telephony via light-beam photophones.

1893: wireless telegraphy.

1896: radio.

1915: first North American transcontinental telephone calling.

1927: television.

1927: first UK-US radio-telephone service.

1930: first experimental videophones.

1934: first commercial radio-telephone service, US,Japan.

1936: world's first public videophone network.

1946: limited-capacity mobile telephone service for automobiles.

1956: transatlantic telephone cable.

1962: commercial telecommunications satellite.

1964: first published paper on fiber-optic telecommunications.

1969: computer networking.

1973: first modern-era mobile phone.

1981: first mobile phone network.

1982: simple Mail Transfer Protocol (SMTP) email.

1983: internet.

2003: Voice over Internet Protocol (VoIP) telephony.

2.1 History of Mobile Cellular Communication

Mobile communication is regarded as a recent innovation, and most of its features were introduced after the 1980s. The first mobile phone network was established in 1981, and later on, it improved enormously in what is still an ongoing process. The era of cellular communication has been divided into several generations. It is observed that we get a new generation of the mobile period almost every 10 years. Table 2.1 shows the time-line of mobile generations. Short descriptions of the mobile age are illustrated in the next sections.

2.2 First Generation System

First Generation (1G) system before the 1980s was referred to as an analog system that used only Frequency Division Multiple Access (FDMA) technology. Different types of the mobile network were introduced in the 1G as mentioned in Table 2.2.

The 1G mobile system faced many problems. The fact is that it belonged to many standards, and different countries followed different standards. Consequently, they were incompatible with each other. Apart from this, whole systems were based on analog technology, and that is why quality and efficiency were considerably low.

THe 1G network was also vulnerable in terms of security. In fact, it was quite insecure. With only a little bit of effort, people with an all-band receiver could easily listen to other people's conversations. It was almost impossible to transfer enormous volume of data using 1G standard technology since the data transfer rate was extremely low, such as 1200bps.

Generations	1G	2G	3G	4G	5G
Design Began(aprox.)	1970	1980	1990	2000	2010
Implementation (aprox.)	1984	1991	2002	2010	2020
Service	Analog voice	Digital voice, short messages, higher capacity packetised data	Higher capacity broadband data	Higher capacity, completely IP, multimedia data	Massive MIMO, cloud RAN, Device-to-Device, etc.
Technologies	AMPS, TACS, NMT, etc.	TDMA, CDMA, GSM, PDC, GPRS, EDGE.	WCDMA, CDMA2000	Single standard	Not standardised.
Data bandwidth	1.9 Kbps	384 Kbps	2 Mbps	200Mbps	Not defined, expected to boost 1000x
Multiplexing	FDMA	TDMA, CDMA	CDMA	CDMA	Not defined yet
Core Network	PSTN	PSTN, Packet network	Packet network	Internet	Not defined

Table 2.1: Generations of Mobile Telephone Technologies.

1979	NTT's (Nippon Telegraph and Telephone) system in Tokyo
1981	Nordic Mobile Telephone (NMT) (450) in the nordic countries
1982	Advanced Mobile Phone System (AMPS) in Northern America, Australia in 1987
1985	Total Access Communication System (TACS) in the UK
1985	NMT(900)

Table 2.2: Examples of 1G standard technologies.

A new era of telecommunication system called Second Generation (2G) technologies was introduced to overcome the problems that existed in 1G. 2G was based entirely on digital technology.

2.3 Second Generation System

With the development of digital technology, the 2G cellular mobile system brought tremendous change to people in their daily lives. 2G fixed so many problems experienced with 1G that it became popular within a very short time. First, 2G cellular networks were commercially launched in 1991 [26], although 2G was introduced in the late 1980s through the giant mobile technologies GSM in Europe and Code Division Multiple Access (CDMA) in the United States. Figure 2.1 depicts the 2G standard technologies and their features. Detailed description of each term is outside the scope of this chapter.

2G had several advantages over 1G, such as its ability to encrypt conversation digitally. Short Message Services (SMS) was introduced in 2G first. In term of spectral efficiency, 2G allowed more users at the same time and same place. As a result of this greater spectral efficiency, 2G technology significantly improved data rates. Consequently, it enables various services like picture messages, multimedia messages, etc. The 2G technology used advanced source and channel coding compared with any earlier technologies to make the signal even more robust against interference. New access technologies like Time Division Multiple Access (TDMA) and improved hand-off control mechanisms were incorporated into 2G. In addition, 2G's power emission was greatly reduced and its privacy enhanced by reducing fraud scope. Table 2.3 shows some 2G standard technologies.

Before stepping into the new generation, this technology achieved a couple of milestones within 2G which were further versioned with, for example, 2.5G and 2.75G.

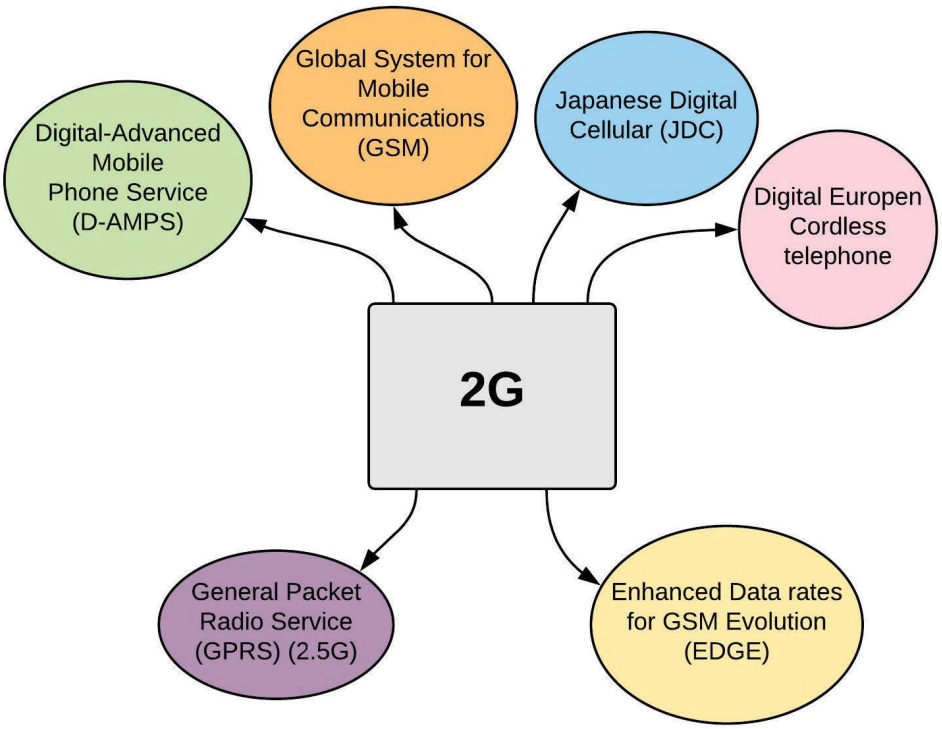

Figure 2.1: 2G Technologies and features.

2.3.1 2.5G

The 2.5G (Second and a Half Generation) is described as the combination of packet-switched and circuit domain. The major contribution of 2.5G was the introduction of General Packet Radio Service (GPRS) for the GSM system. The equivalent CDMA evolution for the 2.5G technologies was CDMA2000. Theoretical maximum capacities of GPRS were 85.6 Kbps for the upload and 21.4 Kbps for the upload.

2.3.2 2.75G

The 2.75G standard was achieved with the introduction of Enhanced Data rates for GSM Evolution (EDGE) in addition to GPRS in the GSM system. In order to get it done, 8PSK (8-Phase Shift Keying) encoding method

Name of the system	Country
Digital-Advanced Mobile Phone Service (D-AMPS)	North America
Global System for Mobile Communications (GSM)	First in Europe and later spread in many countries outside of Europe
Japanese Digital Cellular(JDC)	Japan
Cordless Telephone-2	United Kingdom (UK)
Digital Europen Cordless telephone	Europe

Table 2.3: Examples of 2G standard technologies.

was used. 3rd Generation Partnership Project (3GPP) standardised EDGE as part of the GSM technology. It enabled users three times the capacity compared to GPRS networks. The maximum theoretical capacity of EDGE was 236.8 Kbps for the download and 59.2 Kbps for the upload.

2.4 Third Generation System

The 3G, short for the Third Generation of mobile telecommunication technology, came with incredible changes and promises. It consisted of various standards for end users that comply with the IMT-2000 (International Mobile Telecommunications - 2000) specifications set by the IUT (International Telecommunication Union) [27]. Figure 2.2 shows the technological standard of the 3G cellular system. A brief description is outside the scope of this chapter.

This technology enables many more features than the 2G system. Mobile internet became extremely user-friendly; video calls and mobile TV are just examples of 3G applications. The era of smartphone technologies started with the introduction of 3G mobile network systems.

The first branded 3G standard was the Universal Mobile Telecommunications System (UMTS), which was first offered in 2000. UMTS was standardised by the 3GPP and first used in Europe, Japan and China. The original radio technology used in 3G was Wideband Code Division Multiple Access (W-CDMA). In 2009, China commercialised the Time Division Synchronous Code Division Multiple Access (TD-SCDMA) radio interface. Evolved High-Speed Packet Access, or HSPA+, the latest release of UMTS

network, could provide peak data rates of up to 22 Mbps for the uplink and 56 Mbps for the downlink.

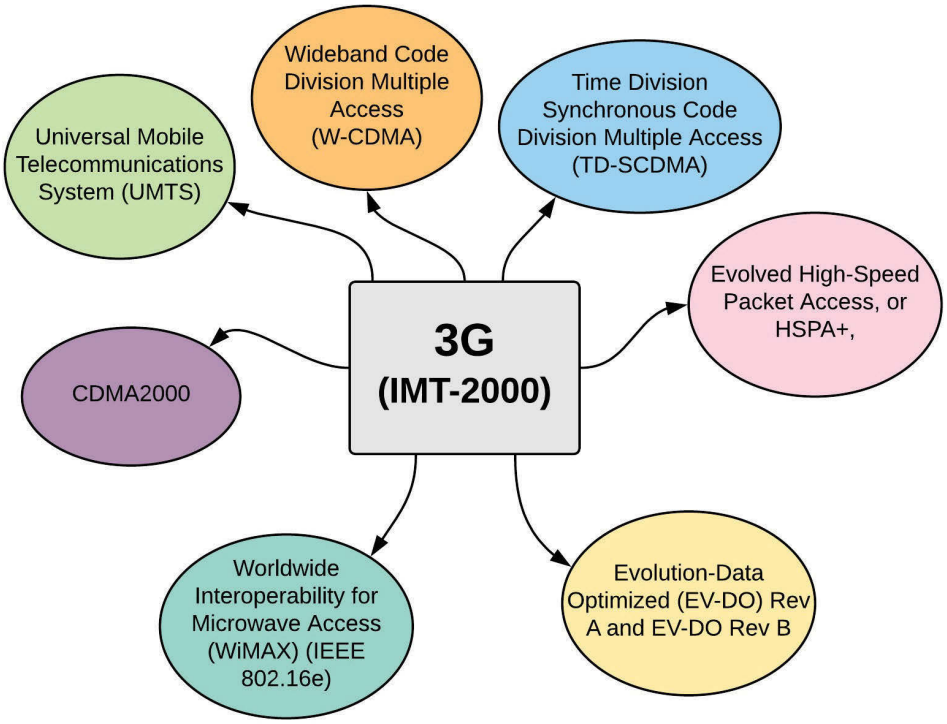

Figure 2.2: 3G Technologies and features.

In 2002, the CDMA2000 system was standardised by 3rd Generation Partnership Project 2 (3GPP2). It was used in South Korea and North America by sharing with the IS-95 standard infrastructure. The radio technology used in this system was based on spread spectrum.

The 3G network used packet-switched network communication mechanism, which is connectionless. In packet switched networks, data are split into many packets, and headers are added to identify the source and destination. The 3G system enabled people to use so many modern applications, like Multimedia Message System (MMS). It was an extended version of SMS where a picture could be sent directly. It is to be noted that MMS could be sent to the 2G network, but due to slow network speeds, it was impractical to send a picture using the 2G network. 3G is could also provide seamless video calling and video streaming, video conferencing,

Global Positioning System (GPS), location-based services, telemedicine, etc. 3G was more secure than any earlier technologies since it used a robust encrypted system. Similar to 2G, 3G was also extended in further versions.

2.4.1 3.5G

This was a standard that was an interim step towards further technologies like 4G. It provided better speed and quality performance to the end users. The leading technologies of 3.5G were Evolved HSPA, High-Speed Downlink Packet Access (HSDPA), High-Speed UplinkPacket Access (HSUPA) standardized by 3GPP. Similar technologies standardised by 3GPP2 were Evolution-Data Optimized (EV-DO) Rev A and EV-DO Rev B.

2.4.2 3.9G

Some debate existed about choosing the standard for 3.9G which is sometimes associated with 3.5G or 4G. However, LTE is sometimes called 3.9G technology standardised by 3GPP. Other significant technologies were mobile Worldwide Interoperability for Microwave Access (WiMAX) (IEEE 802.16e) and Flash-OFDM, Orthogonal Frequency Division Multiplexing (IEEE 802.20).

2.5 Forth Generation System

This is the latest standard in wireless mobile communication system succeeding 3G. The architecture of Fourth Generation System (4G) is entirely different from any earlier standard, and as a result, it is non-backward compatible. This technology added new higher frequencies bands. 4G technologies are the most secure technologies for both end-users and operators. A pictorial view of 4G standard technologies are mentioned in Figure 2.3. It is outside the scope of this dissertation to describe each technology even briefly in this chapter.

The first 4G technical requirements, named the International Mobile Telecommunications Advanced (IMTAdvanced), were specified by the International Telecommunications Union-Radio communications sector (ITU-R) in March 2008. The peak speed was set for 4G services at 100 Mbps for high mobility communications and ay 1Gbps for the less mobile or stationary users.

4G is a more secure and comprehensive all-IP-based mobile standard broadband solution for the end services like a laptop, modem, smartphone, and other similar devices. This standard facilitates ultra-broadband internet service which enables gaming services, streamed multimedia service, and IP telephony, i.e., IP-based voice data, High Definition TV (HDTV) and many more.

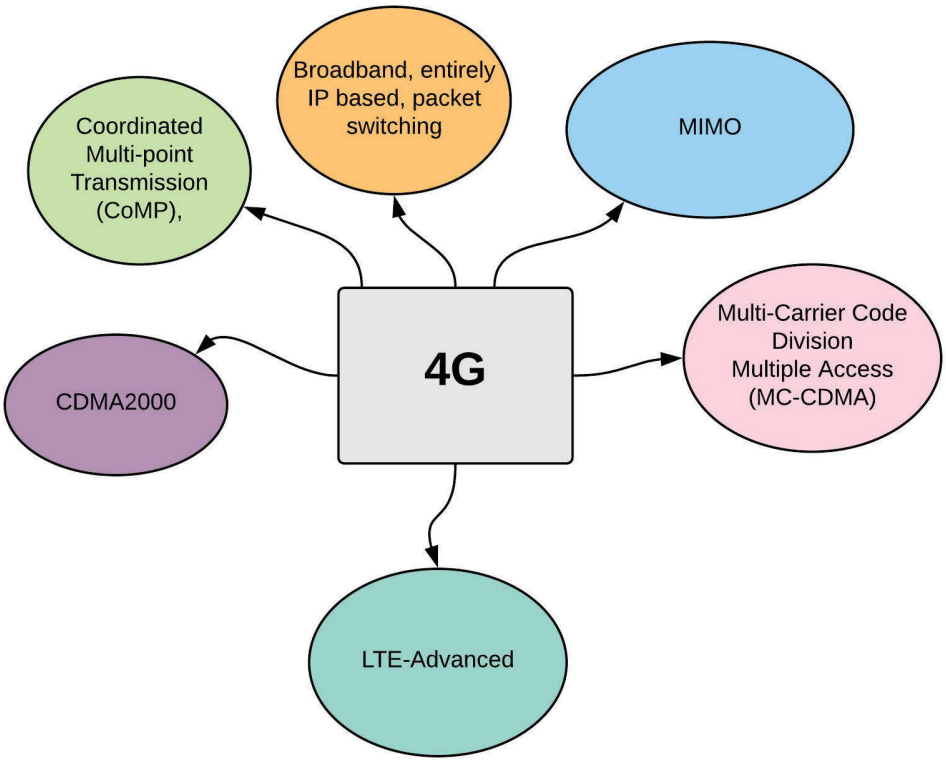

Figure 2.3: 4G Technologies and features.

Two giants among the latest technologies, such as Multiple Input, Multiple Output (MIMO) and Orthogonal Frequency-Division Multiple Access (OFDMA), enable 4G mobile networks to provide this amazing speed. Smart antenna systems use MIMO, and the OFDMA replaces the conventional spread spectrum radio technology used in 3G. The spectral efficiency in 4G is the best compared with any previous standards. It was possible because of the MIMO and OFDMA systems in it. The MIMO system is based on spatial multiplexing, which helps 4G to achieve long-range communications, high data rate and high reliability. By contrast, OFDMA

Items	3G	4G
Speed	Up to 2Mbps	Low Mobility: Up to 1Gbps, Full Mobility: Up to 100Mbps
Core Network	Circuit and packet switching, wide area concept	Broadband, entirely IP-based, packet switching
Services	Difficulty with global roaming	Smooth roaming
Technologies	WCDMA, CDMA2000, TD-SCDMA	All access convergence, including OFDMA, Multi-Carrier Code Division Multiple Access (MC-CDMA), Large Area Synchronised Code Division Multiple Access (LAS-CDMA)

Table 2.4: A comparison between 3G and 4G.

is robust against fading, enhances scalability and provides higher data rates where signals are multiplexed orthogonally. Detailed descriptions of MIMO and OFDMA are beyond the scope of this dissertation. The requirements set for the 4G offer the highest quality services for next-generation multimedia support. Coordinated Multi-point Transmission (CoMP), advanced technology for 4G, also allows more system capacity to cope with massive data speed requirement.

LTE-Advanced (LTE-A) is the latest telecommunication system used extensively nowadays as a 4G standard technology. It was standardised by 3GPP as a part of Release 10 as an enhancement of LTE. Similarly, standard 802.16m, i.e., WiMAX, was standardised by IEEE.

Unlike 3G, as an All-IP standard, 4G supports Internet Protocol version 6 (IPv6). Since a large number of devices are expected to be connected in the 4G system, IPV4 is not quite sufficient to meet the requirements. A comparison between 3G and 4G is given in Table 2.4.

2.6 Fifth Generation System

The Fifth Generation (5G) mobile network refers to the next major phase of mobile telecommunications systems beyond the currently available IMT-

Advanced/4G standards. 5G is expected to fulfill significant demand for data services in the telecommunication system along with the new era of the Internet of Things (IoT). It is expected that the rollout of 5G to meet market demands will be available by 2020 and vendors/operators are preparing to launch the 5G standard network for the first time accordingly. Nowadays, a lot of researchers from universities and institutes are carrying out the research to debut a possible standard for the 5G mobile telecommunication system. The next chapter is dedicated to the issues of 5G.

Chapter 3

Issues of the Fifth Generation Network System

Future fit demand and flexible solutions combined with high quality services is expected in the 5G telecommunications technology. In recent years, scientists and researchers have proposed many new technologies which might be an integral part of 5G. Nowadays telecommunication technologies are not limited only to voice and data although meeting the enormous increase in data requirements is the key target. In this chapter, I will highlight some features and technological enhancements for which it is only a matter of time before they are added to next generation of mobile communications. However, to reflect the expected outcomes in 5G, technological improvement is the key challenge. Some issues that are expected to play a key roles in 5G are reviewed as well as proposed in this chapter.

Wireless devices connected with networks have been increasing remarkably for the last couple of decades. Ubiquitous internet connection is the key requirement for the next generation of wireless technology. According to CISCO, it is expected that 50 billion devices will be connected by 2020s and almost everything will be connected (Internet of Things) in the network.

As 5G has not been defined yet, it is still an open question whether it will fit all technologies in order to address all uses and requirements. 5G is assumed to be about not only boosting the data rate in 4G but also the massive connections. If we think about the 2G, it was all coverage-oriented. In 3G and 4G, it was all capacity-oriented, although coverage has also been an issue. However, it is believed that 5G will be based on green and smart technologies. Total energy consumption per area per user will be less than any earlier technologies. Smartness indicates the ability to deal with massive

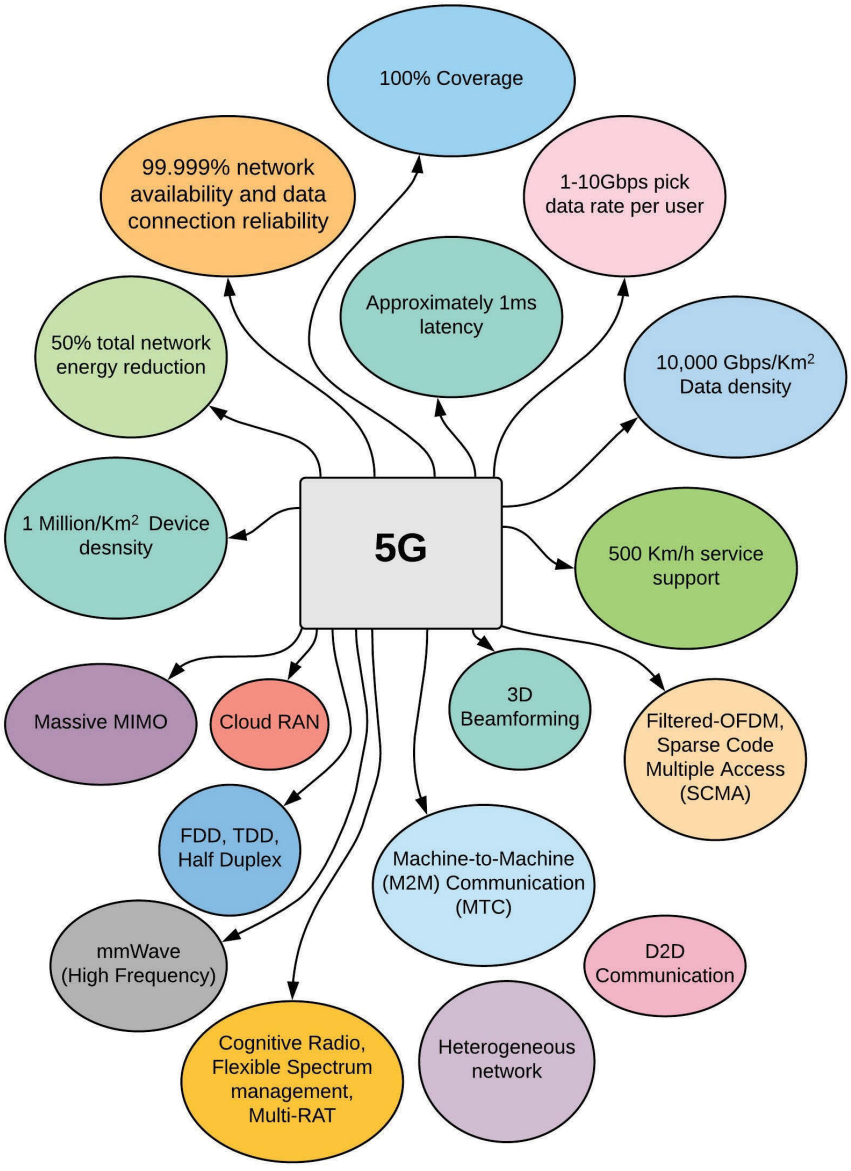

Figure 3.1: A pictorial view of proposed 5G techonogies and features.

Generations	Analog/ Digital	Service	Access method	Cell size
1G	Analog	Voice	FDMA	Macro (coverage-oriented)
2G	Digital	Voice	TDMA	Macro (coverage-oriented)
3G	Digital	Data	CDMA	Macro/Micro (spectrum efficient-oriented)
4G	Digital	Video	OFDMA	Micro/Femto (spectrum efficient-oriented
5G	Digital	Video/ Machine to Machine	Beam Division Multiple Access (BDMA)/Sparse Code Multiple Access (SCMA)	Hyper (spectrum efficient and energy-efficient oriented)

Table 3.1: A paradigm shift of cellular architecture [16]

connections maintaining low signalling and global optimisation. It also means how fast connectivity can be achieved and how reliable the network is.

Figure 3.1 shows what 5G is assumed to be at a glance. Coverage improvement is presumed to be 100 percent along with 99.999 percent network availability and data connection reliability. The latency should be no more than 1ms. Peak data rate should be 1-10 Gbps per user with 10,000 Gbps per kilometer square data density. 5G expects user mobility speeds to be up to 500Km per hour without compromising the service. It will also improve the network energy consumption by up to 50 percent. The enhanced technologies that can enable those conditions are described in the next sections. The architecture of a 5G network including network architecture, physical layer and MAC layer perspectives are as in Figure 3.2. [1].

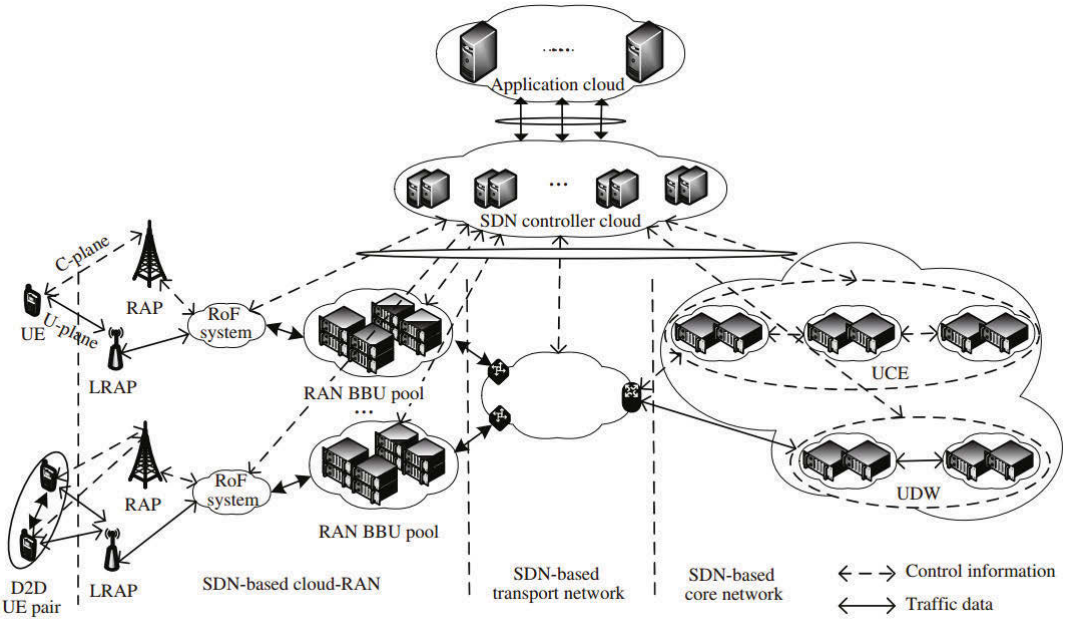

Figure 3.2: A proposed 5G cellular archetecture [1]. [UCE (Unified Control Entity), UDW (Unified Data Gateway), SGW-C (Service Gateway Control Plane), PGW-C (Packet Data Network Gateway Control Plane), GTP-U (GPRS Tunnelling Protocol for User Plane), SGW-D (Integrates Service Gateway Data Plane), PGW-D (Packet Data Network Gateway Data Plane), SDN (Software Defined Network), RoF (Radio-over-Fiber), BBU (Baseband Unit), RAPs (Radio Access Points), LRAPs (Light RAPs)] Image Source: [1]

Detailed explanation of this architecture is beyond the scope of this dissertation. Table 3.1 [16] also shows a paradigm shift in the cellular architecture.

In [28], Traffic-Aware Network planning and Green Operation (TANGO) have been proposed by Zhisheng Niu (2011) for the 5G telecommunication network where C-plane would be larger, and D-plane would be smaller, i.e., decoupling of control coverage and traffic coverage was suggested. Control coverage should be seamless, and traffic coverage should be elastic, i.e., reconfigurable. A base station will go into sleep mode and consume almost no energy once it has no active user. On the other hand, it could hand over the user to the nearest convenient base station so that it could save energy and can go into sleep mode.

A lot of researchers have proposed possible technological enhancement for the 5G network. Some big projects like METIS [29] and 5GNOW [30] have already progressed significantly towards 5G. In [31], Federico at al. (2014) highlight five disruptive technology directions for the 5G network, as follows:

- Device-centric architecture
- Millimeter wave (mmWave)
- Massive MIMO
- Smarter devices
- Native support for machine-to-machine (M2M) communications

In [9], Jeffrey G. et al. (2014) highlight what 5G would be. The authors set out three big technologies like mmWave, ultra-densification, and massive MIMO. Major engineering requirements like data rate, latency, energy, and cost were also highlighted. Some design issues like access technologies, spectrum sharing and regulations were also considered.

In [2], the authors discuss the key challenges for radio access technologies in 5G. Here seven technology enhancement directions are listed also shown graphically in Figure 3.3. The directions are as follows:

- RAT evolution
- Cell shrinking
- Composite wireless infrastructure

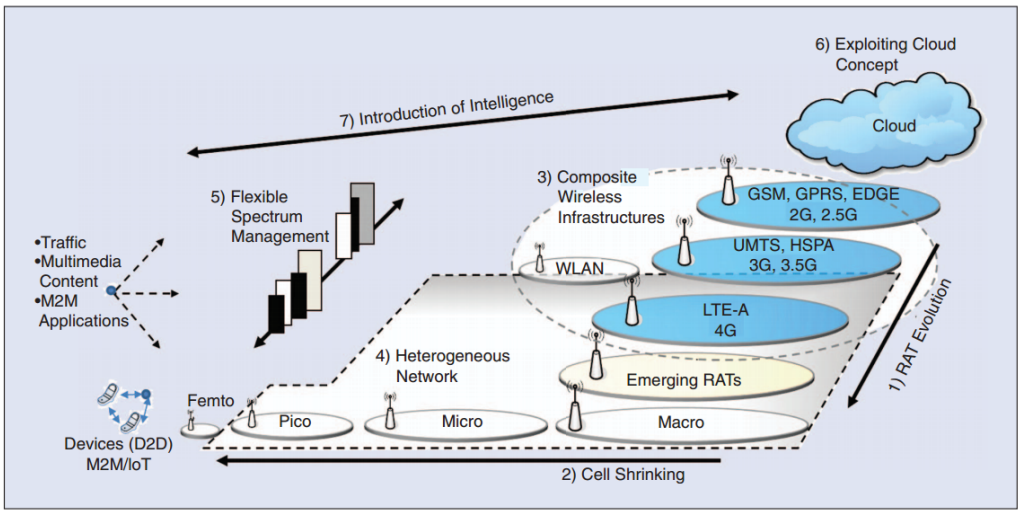

Figure 3.3: Seven technical direction of cellular network proposed in [2].

- Heterogeneous network
- Flexible spectrum management
- Exploiting cloud concept
- Introduction of intelligence

The authors in [5] discuss network densification for the wireless evolution into 5G. With their mathematical model, the authors clarify that network densification is a combination of spectral aggression and spatial densification. In the case of spatial densification, the authors consider heterogeneous networks, cell range expansion and advanced interference cancellation receivers. For the spectral aggregation, some other aspects, like spectrum availability, multiband operation and RF transceiver design challenges, are also described. On the other hand, the authors also mention device-to-device communication (discussed in detail in the next chapter), small neighborhood cells, mmWave technology and backhaul densification.

A multi-tier 5G wireless cellular network from an interference management perspective is suggested in [10]. In this paper, the vision and requirements for the 5G multi-tier network are discussed that are as follows:

- Data rate and latency
- Machine Type Communication (MTC) devices
- mmWave communication

- Multiple RATS
- Base station densification
- Prioritised spectrum access
- Network-assisted D2D communication
- Energy harvesting for energy-efficient communication.

The authors also clearly mention some challenges for 5G interference management. The major challenges are designing efficient methods to support simultaneous association to multiple BSs, designing efficient methods for cooperation and coordination among multiple tiers, designing optimised cell association and power control methods for multi-tier networks. The authors propose some design guidelines for the joint prioritized power control and resource-aware cell association schemes for the 5G multi-tier cellular network.

Some general enhancements, like 3D beamforming, new carrier type, enhancement for coordinated multi-point communications (eCoMP), LTE hotspot improvement (LTE-Hi), spectrum efficiency enhancements for small cell, Frequency Division Duplex (FDD)/Time Division Duplex (TDD) joint operation, Multi-Radio Access Technology (Multi-RAT) operation enhancement i.e., Wireless Fidelity (WiFi) interworking, Minimization of Drive Test (MDT), services and enablers of new services, i.e., Machine Type Communication (MTC), proximity-based services (ProSe) are discussed in [32] by Huawei Technologies which they named LTE-B or the second phase of LTE-advanced.

Under the METIS project [33], scenarios for 5G communication network were projected, and the requirements, challenges and prospects also considered. In [34], a co-operative distributed optimisation mechanism has been proposed to deploy hyper-dense small cell.

3.1 Architectural Change, Extreme Densification

The existing architecture needs to be changed considerably to achieve the 1000x data rate. Mobile cellular communication has been designed historically based on cells as the primary units for the radio access network to ensure the necessary coverage and capacity. Network densification is a

significant trend of any cellular generation. As a heterogeneous network was a major modification in the 4G network, the 5G network is assumed to change into device-centric architecture [31]. It will change the network densification in different directions. Apparently, no-edge network, i.e., uniform network solution, is both the trend and challenge for the 5G network.

Allocation of a different spectrum with higher frequencies or use of cognitive radios will require total architectural change in the network so that coupling of uplink and downlink communication can flow through different sets of nodes [31]. Proposal for the phantom cell [35], where data transferred through the small low power cell nodes and signalling or control information might be sent high power cells, can effectively play a significant role in the 5G network.

Some technological changes, e.g., cooperative multipoint (CoMP), relay node, will facilitate the shift in architecture, although they are part of 4G technologies. Moreover, using smarter devices can effectively change the concept of architecture since D2D or M2M (discussed later in this chapter) are going to be important day to day.

A uniform coverage proposed in [28] would require a massive change in network architecture where green operation and traffic-aware network are the key achievements.

An architectural design towards 5G in terms of spatial densification has been discussed in [5]. It is yet to be confirmed what architectural change might appear in the next cellular generation. However, a realistic proposition is required, and all the research efforts so far in simulation should be tested in a real network.

A pictorial view of the network architectural trend for the seven directions has been highlighted in [2], as stated earlier in Figure 3.3.

3.2 Massive MIMO

Multiple Input Multiple Output (MIMO) has already been incorporated into WiFi technology and LTE systems. MIMO is the technology that has already boosted the data rate and increased spectral efficiency in quite a significant way, and it is clearly a potential technology for the next

generation network as well. MIMO is now a mature technology, and a lot of researchers have already investigated the future of MIMO as a probable solution to achieve the target data rates and spectral efficiency [31] for 5G technology. Actually, the more antennas as transmitters or receivers are engaged, the more signal paths there are to facilitate more reliability and higher data rates. But this comes at the price of increased complexity like hardware, power consumptions, and proper techniques to decode the data. Figure 3.4 [3] shows a concept of Massive MIMO. Here, a sufficient number of antennas are installed at the base station, and by using beamforming technique, the base station can transmit the data directed to the data users. Chapter 5 discusses the different beamforming techniques to estimate the direction of the users, which is also important to locate the D2D users properly.

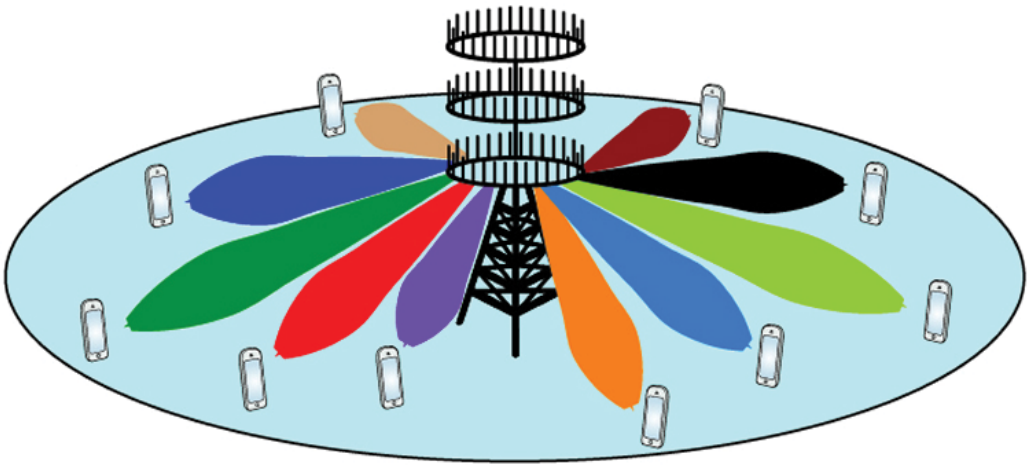

Figure 3.4: A concept of Massive MIMO [3]. Image credit: Linkoping University

Massive MIMO, also widely known as Very Large MIMO, Full-Dimension MIMO, Large-Scale Antenna Systems, Hyper MIMO, means a large number of antennas (e.g., hundreds or thousands) are used simultaneously as transmitters or receivers or both.

Detail theoretical discussion is beyond the scope of this report. However, extensive analysis has been done in [36] to achieve the considerable advantage of massive MIMO. Other issues, e.g., channel estimation, precoding and detection schemes have also been discussed. Some other benefits, like reduced latency, robustness against jamming, use of inexpensive low-power components and MAC-layer simplification, were also discussed in [37].

In [31], some potential issues for massive MIMO to be attached to the 5G network based on the Henderson-Clark framework were discussed. The authors state that it would be a scalable technology compared with 4G, which in many aspects is not scalable. On the other hand, deployment and architectural issues are not that challenging with the existing infrastructures. This is because they can be replaced with a couple of base stations since they can provide higher data rates and serve more users at the same time.

The spectral benefits of massive MIMO with the increased number of base stations and the power efficiency improvements are discussed in [38, 39]

Although massive MIMO seems to be an integral part of 5G, it has some challenges and difficulties for deployment in a real network. Some problems are addressed in [9, 40, 41, 42]. Pilot contamination and overhead reductions [43, 44], architectural challenges [45], full-dimensional MIMO and elevation beamforming, channel models [46, 47], coexistence with small cells [48, 49] and mmWave [50] are the major challenges to be solved.

3.3 mmWave

A frequency spectrum is a scarce resource. Telecommunication operators have to cost huge capital expenses for the allocated spectrum band. It is also difficult for the regulators to find new spectrum bandwidth to assign to operators. Currently, terrestrial wireless operators are highly restricted in their operations to the allocated microwave frequencies, which are relatively small in range. The available frequencies used for telecommunication extends from several hundred megahertz to a few gigahertz and in terms of wavelengths, in the range of a few centimeters to about a meter. By now, this spectral band is almost fully occupied, and it is time to search for the new spectrum band to be allocated to the next-generation wireless system. The fact is that an immense amount of relatively idle frequency band is still available in the range of 30-300GHz [51, 52], where the wavelength is approximately from one to 10 millimeters. Figure 3.5 [4] shows the available spectrum that can be allocated for the 5G network. The mmWave range is from 24GHz to 100GHz. The Federal Communications Commission (FCC) stated in the FCC Fact Sheet on this proposal, “Building on a tried-and-true approach to spectrum policy that enabled the explosion of 4G (LTE), the Chairmans rules would set in motion the United States rapid advancement to next-generation 5G networks and technologies.”

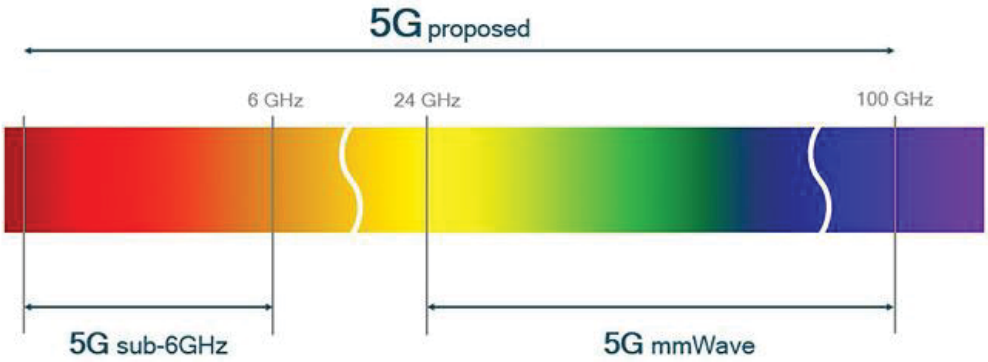

Figure 3.5: Available millimeter wave spectrum proposed for 5G. [4].

The mmWave range is still idle due to a range of reasons. These include strong path loss, hostile propagation qualities, rain and atmospheric absorption, strong phase noise, low penetration through objects and diffraction around obstacles, large arrays, narrow beams and link acquisition. The authors also illustrate how these could be resolved in the 5G network. A constraint of semiconductor technology was also an inevitable issue for mmWave to be deployed. Nowadays, there is almost no problem in producing hardware for mmWave technologies.

Since network densification is a clear trend of the cellular communication system, the heterogeneous network requires smaller cells that can cover a radius from 4 to 200 meters. The mmWave might be a reliable spectrum solution for these smaller cells, like Pico or Femtocells. As it is a high-frequency spectrum band, it requires smaller antenna size to cover the same area compared with lower spectrum bands if to be used for the smaller area. The power issue is also managed as long as it covers a small area.

A very directional beam that improves the link adaptability which enables very dense spatial reuse through spatial or angular isolation is illustrated in Figure 3.6 [5]. A mmWave base station could be deployed for the short range. It might be an overlapping coverage but no strong inter-cell interference by using massive orthogonalisation that leads to a different cellular architecture.

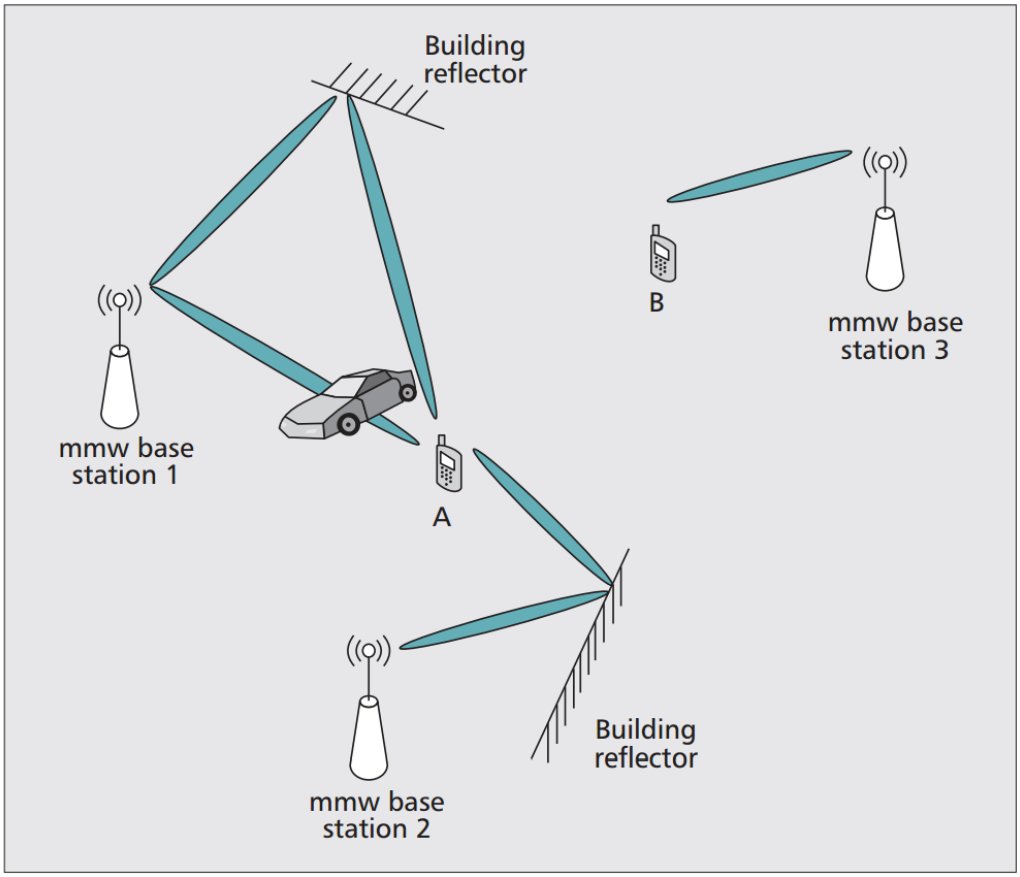

Figure 3.6: Example of millimeter wave cellular mobile access [5].

3.4 Cloud RAN

The idea of Cloud Radio Access Network (C-RAN) is a centralised solution for cellular mobile network operators. Cloud-based radio access network is a completely new technology and has never been used in the real network. It is a new direction to improve cost efficiency further by making the network flexible, nimble and scalable. A cloud computing resource that is shared for massive storage is an architecture that enables a couple of main characteristics like Centralized Processing, Clean, Real-time Cloud, and Collaborative Radio Access Network [53]. Sometimes, C-RAN is referred to as Centralized-RAN.

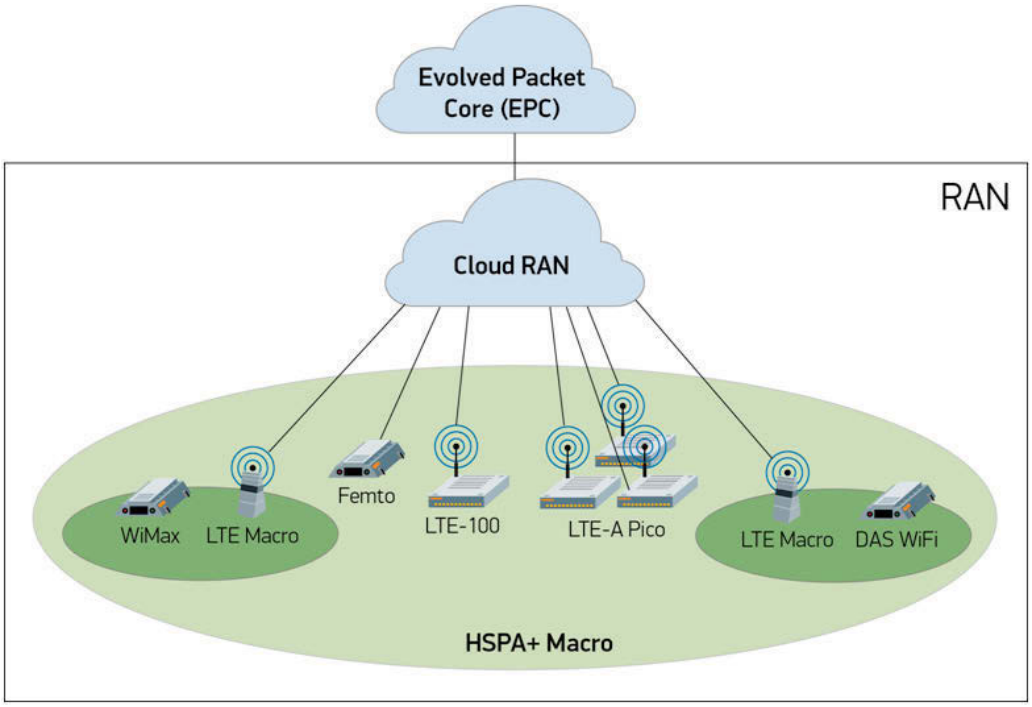

Figure 3.7: Could RAN in the next generation network [6].

In terms of the wireless network, information technology, and recent progress in the optical network, C-RAN may be regarded as an architectural evolution, a combination of all those technologies with distributed base station system and its signal processing into a large-scale centralised deployment. Major characteristics of C-RAN are large-scale centralized control of the base station, native supports to collaborate radio access technologies and real-time virtualisation capability based on the open platform.

A pictorial view of the C-RAN concept has been given in 3.7 [6]. Detail of co-operative transmission in C-RAN considering processing constraints and fronthaul capacity has been stated in [54]. Two paramount technology trends that are assumed to play roles in the era of C-RAN are Network Function Virtualization (NFV) and Software Defined Networking (SDN)[9]. Details of those architectures are beyond the scope of this chapter but are described in [55, 56, 57, 58].

3.5 Cognitive Radio and Multi-band Operation

Radio management in cellular communication has always been considered a challenging job regardless of the spectrum allocation. Since spectrum is a scarce resource, it is quite a vital issue to plan the spectrum in such a way that the quality of the air interface is optimal without compromising the service. In view of the enormous increase in data requirements, allocated bandwidth is going to be critical to ensure the increased data rate. Flexible spectrum management could be a potential solution to improve the overall problem of spectral issues. However, it will have to overcome many challenges in a real network. Figure 3.8 depicts the concept architecture of cognitive radio [7, 8]. Here, unlicensed spectrum is also used parallel with license band. Cognitive radio could be used for secondary networks with or without network infrastructure.

Carrier Aggregation (CA) technology has already been used in LTE-A (Rel-10), which facilitates non-contiguous spectrum utilisation. It enables much more bandwidth by combining different component carriers. Some component carriers with flexible/on-demand bandwidth utilisation might be used to improve further that are parts of an NCT work item in Rel-12.

Utilisation of cognitive radio is going to be a clear trend since a wireless system consists of various technology and all the technologies like WiFi, TV, cellular, have different spectrum bands, and sometimes they are underutilised. It is possible to share the spectrum of one technology with another when they are not used actively.

No doubt spectrum policy and allocation will play an essential role in the 5G cellular system. Regarding spectrum regulation and standardisation of 5G, four options, such as Exclusive Licence, Unlicensed Spectrum,

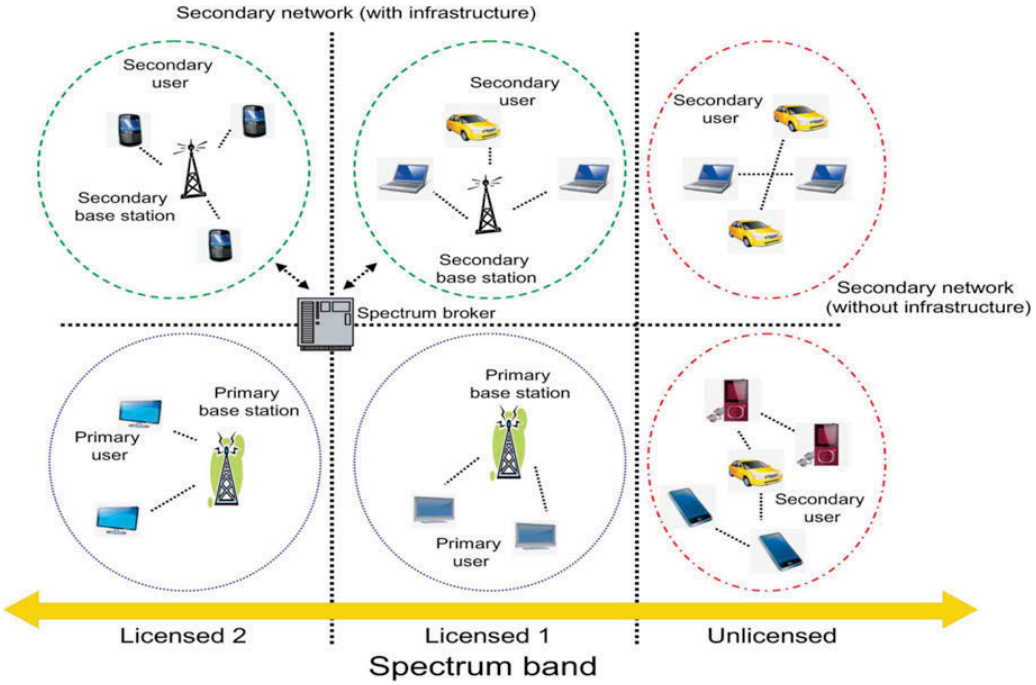

Figure 3.8: Cognitive Radio Architecture [7, 8].

Spectrum Sharing and Market-Based Approaches to Spectrum Allocation, are mentioned in [9]. Detailed discussions of each option are beyond the scope of this chapter. Some other aspects, like economic considerations with infrastructure sharing, offloading, mobile virtual network operating, backhaul, etc, are also highlighted in [9].

3.6 Multi-RAT

Heterogeneous networks that already exist for the 4G cellular system will continue to decrease the size of the cell as we move towards 5G. The 5G network should be able to handle different types of Radio Access Technologies (RAT) systems. It should ensure that devices can handle earlier technologies like 4G or 3G. It is also assumed to be a combination of different types of technologies, like WiFi and device-to-device communications. Different radio access systems are used in various wireless systems. 5G should support all the radio access technologies, and therefore it needs to extend the ability to handle all complex tasks for the network with different spectrum bands. A multi-RAT network with many frequency networks is difficult to achieve. A simplified model is shown in [9] as in Figure 3.9. A RAT selection process is proposed using an interesting game-theoretic approach in [59] where Pareto-efficiency of convergence to Nash equilibria are studied.

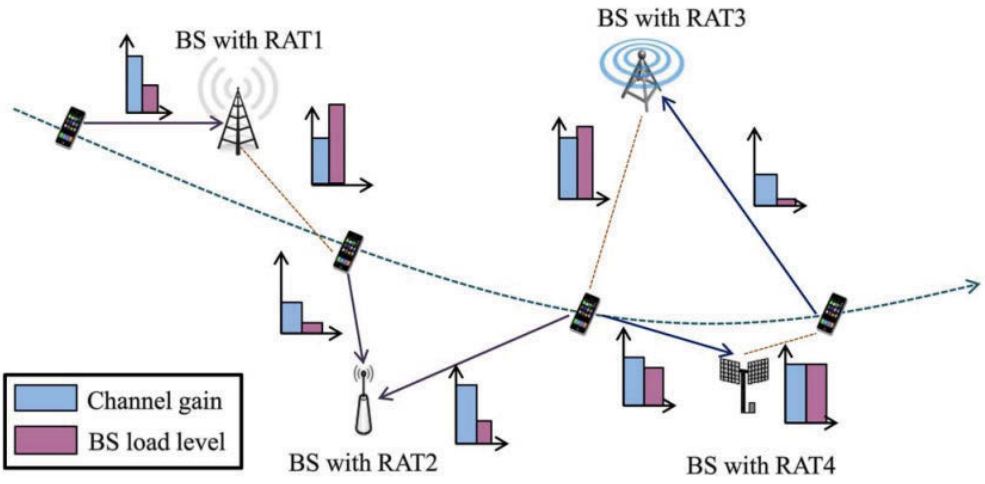

Figure 3.9: Example of Multi-RAT system [9].

3.7 Device to Device Communications

Device-to-device, widely known as D2D communication is another direction of the wireless communication system where a device directly communicates with another device to increase the overall throughput and spectrum efficiency by offloading the base station traffic.

In the traditional system, a device establishes a connection with any other device through the base station irrespective of the location of any device. In the cellular communication system, it is unlikely that two users are in close proximity when they are involved with voice or data communication. However, when two devices are close to each other and willing to establish a connection to transfer data, video conferencing, gaming or social networking, it is possible to get them to communicate directly with or without the active involvement of network base station.

Another aspect of D2D communication is that a device can act as a relay to forward the traffic from the cell-edge device to the base station or from the base station to the cell-edge devices where the cell-edge devices might be located out of the coverage as well. The SINR of cell-edge devices is usually low, and some devices may locate out of coverage of the base station but may be located at proximity distance from the network attached devices. In that case, a network-attached device can perform the role of a relay for the other device which is less than the SINR threshold to attach with the base station and still have adequate data throughput.

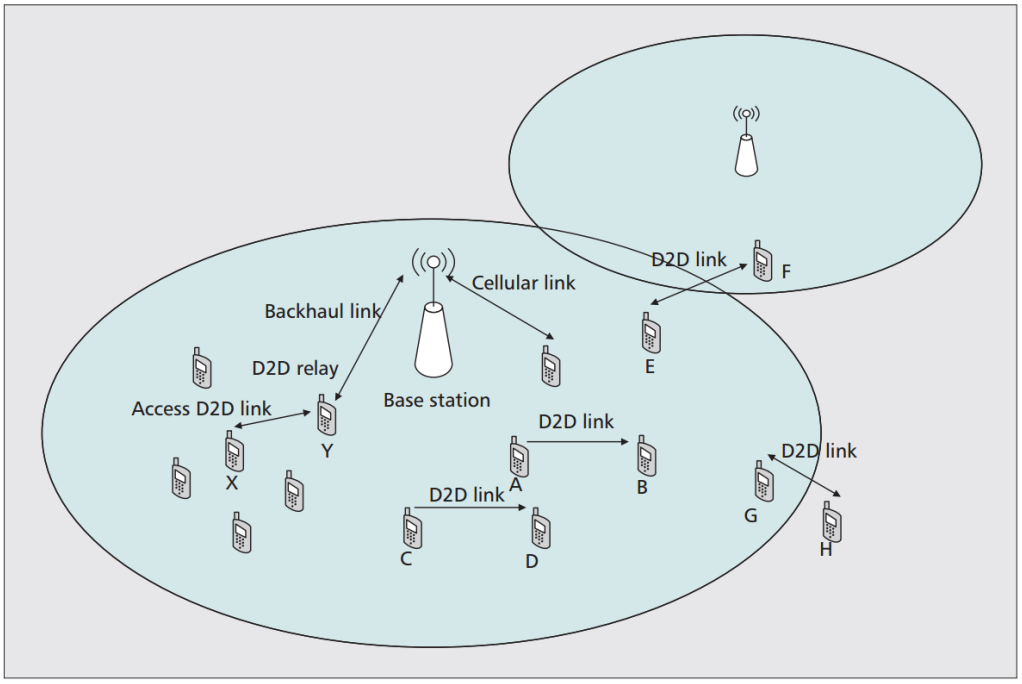

Figure 3.10: Example of Multi-hop relay service and D2D proximity communication system [5].

Paper [5] outlines D2D communication as shown in Figure 7.1. Here multiple device links that share the same bandwidth simultaneously increase the overall spectral efficiency considerably. On the other hand, they reduce the latency and power consumptions.

D2D communication still requires efficient protocols and algorithms to handle these communication scenarios. Major challenges of D2D communication are to find the real opportunities to establish the connection, duplexing structure of uplink/downlink communication, designing devices that are D2D-enabled from both protocol and hardware perspectives and accounting for the extra overheads to control the communication and estimating the channel [31]. A complete feature and an opportunity for D2D communication for the next generation cellular network is discussed full in Chapter 4.

3.8 Some Other Enhancement

The 5G network may have some other aspects. Some of them are included as follows but the network is not limited to these.

3.8.1 3-Dimentional Beamforming

In a recent development of active antenna system, it is possible to estimate the elevation of the user in addition to the direction by controlling the beamforming [32]. Since higher frequency is an option for the next generation cellular system, it enables more antennas to be installed with reduced size. SU-MIMO and MU-MIMO could be used for spatial resolution, and traditional antenna tilting might disappear in 5G.

3.8.2 Enhancement for Co-ordinated Multipoint Communications (eCoMP)

The 5G network is assumed to be a "No-Edge" network, which means a network provides stable coverage irrespective of the position of a user. CoMP is a prominent feature used in LTE-A for improving user experience at cell-edge. However, enhancement of this technology will also facilitate a seamless network for non-ideal backhaul scenarios. Cell-edge throughput and mobility management should be more efficient in 5G and eCoMP might be a solution for this.

3.8.3 FDD/TDD joint operation

TDD is a better option for achieving higher-resource assignment, considering huge fluctuation of downlink/uplink traffic in a high-frequency band. On the other hand, FDD is a unique choice for the low-frequency band in a macro coverage area. As cell size is reducing and mmWave could be used in 5G, a joint operation of FDD and TDD is a good choice to get the maximum benefit from each technology. In that case, UE should support both technologies. This joint operation will also improve the throughput of cell-edge users.

3.8.4 WiFi Interworking

Some giant operators have already started to deploy WiFi in their coverage areas to boost cellular network capacity. This is because of the significant increase of data and mobile broadband users. It would be very unusual to see a WiFi working jointly with the cellular network without any interruption of services. Although WiFi interworking requires huge authentication complexity, access point discovery mechanism, regulation issues and radio management system, significant research is already going on.

3.8.5 Enabling of New Services

Every generation of cellular network introduced new sorts of services that enabled greater user-friendliness than their predecessor. As shown by the latest advances in smartphone technology, nowadays, cellular operators are not only able to provide services like voice and data but also other application-based services like tracking, positioning, congestion control, etc.

Large penetration of smartphones causes user plane congestion in RAN, and it is a severe problem for operators. To reduce congestion, it is possible to control the packets of different quality services with the recent development of multi-antenna arrays, heterogeneous network, eCoMP, 3D beamforming capability and huge availability of applications. Traditional positioning systems will be replaced with new positioning solutions which will be more precise and perfect.

Apart from this, new business opportunities will be explored by introducing Machine Type Communication (MTC), proximity-based services and group communication services in the 5G cellular network.

3.9 Design Issues of 5G Network

The design issue for any network generation has always been considered a vital issue. To support a 1000x higher data rate, the 5G network must not be the same with the existing network system. This network must have lower energy consumption, decreased latencies and lower cost compared with any earlier cellular network generations. Some design issues are discussed in detail in [9]. Authors start with most fundamental design aspect like physical layer and then step into the evaluation of virtualised network architectures. There is a possibility that the transition to 5G could involve different signaling and multiple access systems and design architecture.

OFDM is a unique choice for cutting-edge wireless technologies. However, OFDMA also has some drawbacks, like higher Peak-to-Average Power Ratio (PAPR). Spectral efficiency is significantly reduced in OFDM (although better than earlier technologies) by introducing Cyclic Prefix (CP) and strictly maintaining orthogonality. Paper [60] discussed an approach to reduce this effect, which increases the downlink cell-edge rate. A potential alternative to OFDM is mentioned in [9][61], where time-frequency packing, non-orthogonal signal, multicarrier, Generalized Frequency Division

Multiplexing (GFDM), single carrier, Tunable OFDM are discussed in detail.

As cloud-based networking is a trend, it is also important to consider this concept in designing the 5G network. Renewable energy is the future, and solar power will be used in 5G extensively. So, energy harvesting BSs [62] are more likely to be used in 5G, as efficient energy utilization is a significant research area nowadays.

The 5G network is not standardised yet. A lot of researchers are engaged in drawing the network that might be feasible in the real system. The issues that are discussed here are just some focus directions of researchers towards 5G. It is not sure yet which technology we will actually experience in the 2020s.

As D2D communication is a part of this dissertation, next Chapter is all about D2D communications and its issues.

Chapter 4

Device-to-Device Communications System in a Cellular Network

Device-to-device communication, widely known as D2D communication is a new paradigm of cellular communication initially proposed to boost network performance. It is a communication technology that facilitates any device to communicate directly with another device without the support of major infrastructure, i.e., a base station during the data transfer period. Base stations only control the devices to enable the communication between them. A position of the D2D communication system in a multitier cellular network architecture is mentioned in [10], as shown in Figure 4.1.

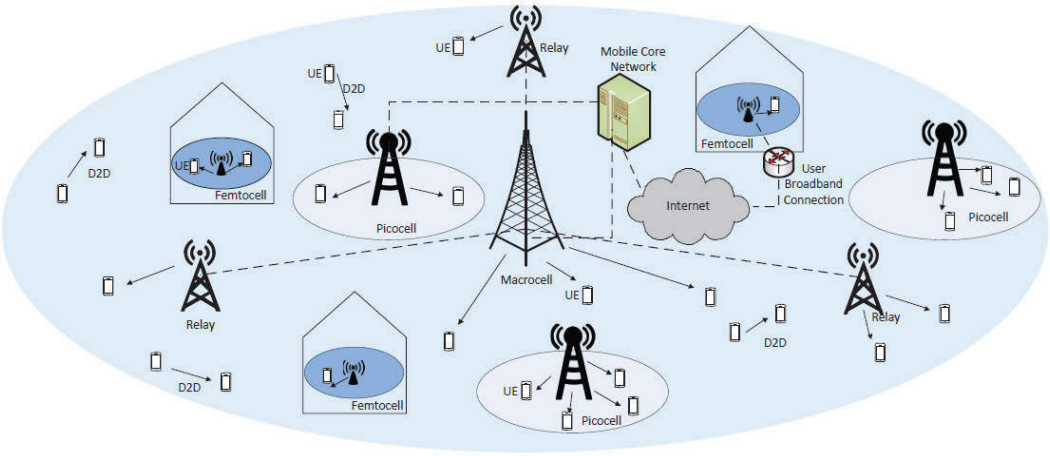

Figure 4.1: D2D communication system in a multi-tier cellular network architecture [10].

It is already proven that D2D communication in a cellular network will improve data rates in many aspects. It can extend coverage considerably by acting as a relay or directly communicating with the device where other devices might be located out of the standard cellular coverage. It can increase network capacity extensively because two devices can exchange data directly instead of using a base station. As they communicate directly, D2D communication can offload the data traffic from the base station so that base station capacity increases and the cellular users can get better network performance. A D2D-enabled network could also improve energy efficiency significantly. Since the network will transmit over a short range, transmitting power should be according to distance, which in turn can reduce the overall power consumption of both the base station and the mobile device.

D2D communication will also open the door for new applications that can make our daily life easier. Paper [11] shows various roles for D2D communication. Figure 4.2 also indicates the different roles of D2D communications.

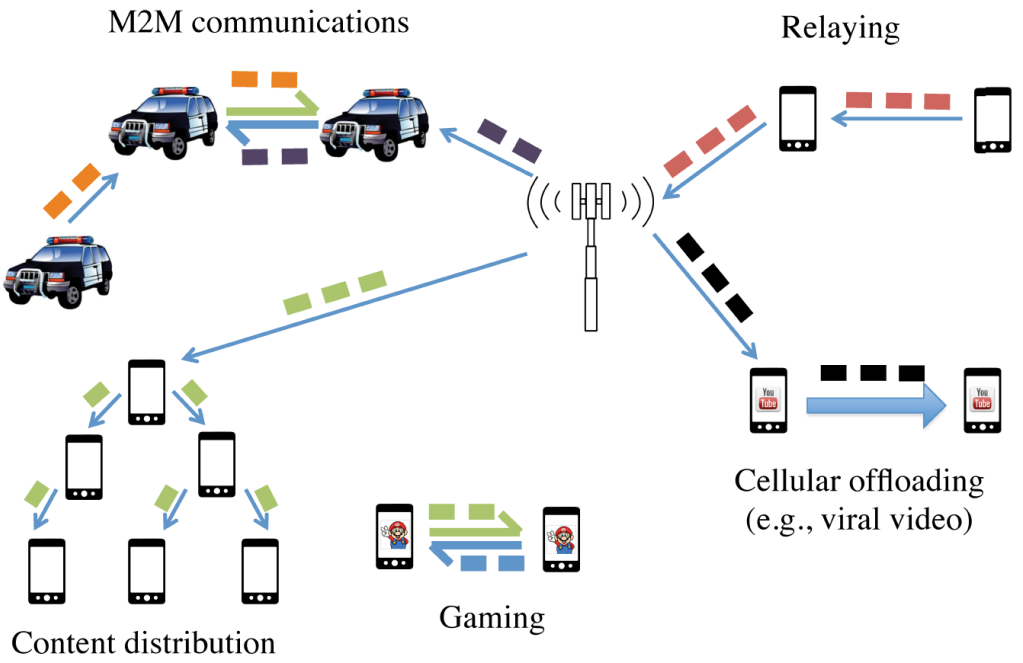

Figure 4.2: Different roles of D2D communication [11].

4.1 Types of D2D Communication

D2D communications can be classified from different perspectives. Figure 4.3 shows the basic categories of D2D communication.

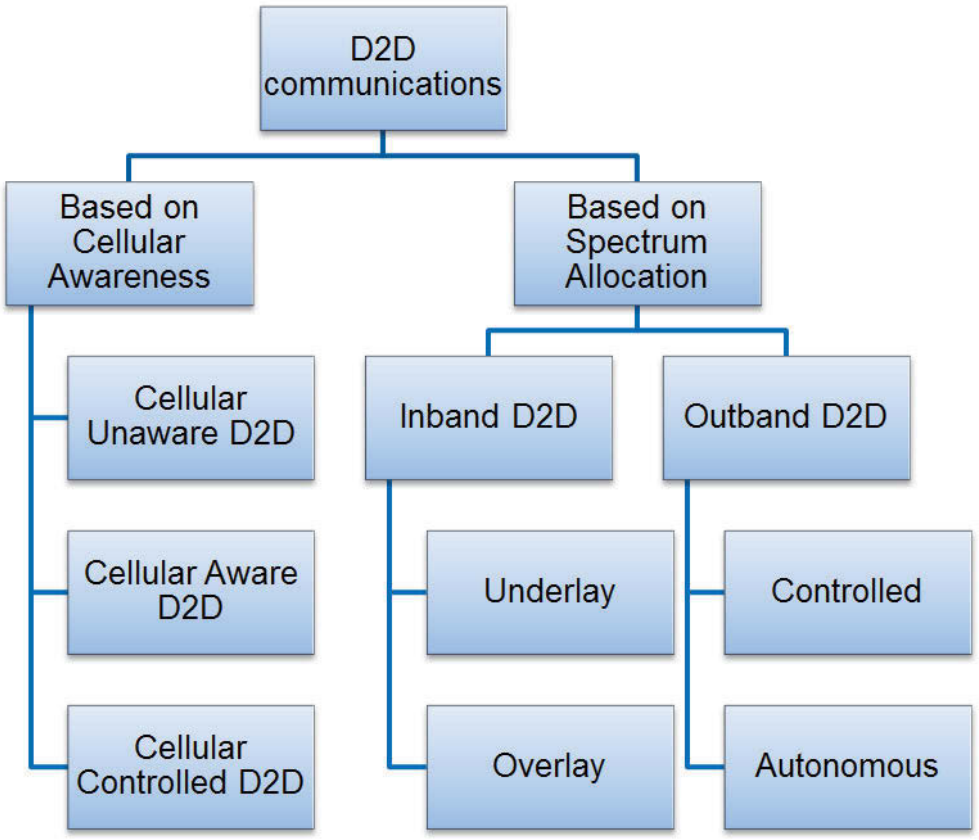

Figure 4.3: Overall classification of D2D communication.

4.1.1 Based on Cellular Awareness

In this category, a D2D communication system can be classified into three different types.

- Cellular Unaware D2D
- Cellular Aware D2D, and
- Cellular Controlled D2D

4.1.1.1 Cellular Unaware D2D

Cellular unaware D2D communication takes place when the cellular network is not aware of D2D communication. Multiple RATS, e.g., cellular and WiFi can be used in that type as there is no cooperation between them.

4.1.1.2 Cellular Aware D2D

In this type, a cellular network is aware of the existence of D2D communication but does not control. Multiple RATS, like LTE and WiFi, can still be used. Cooperation between cellular and D2D exists in this type of communication.

4.1.1.3 Cellular Controlled D2D

When D2D communication is an integral part of cellular communication, and base stations take all the responsibility of D2D communication, it is called Cellular Controlled D2D. Only single RAT, e.g., LTE-A can be used in that case.

4.1.2 Based on Spectrum Allocation

Spectrum management in D2D communication is the most critical and challenging part. Figure 4.4 shows the types of spectrum allocation of different types of D2D communications [11]. The spectrum allocation of D2D communication can be divided mainly into two part:

- Outband D2D, and
- Inband D2D

4.1.2.1 Outband D2D

Cellular users in outband D2D use licensed cellular spectrum, and D2D users use available unlicensed spectrum. Outband D2D communication is less challenging and considerably easy to plan because there is no interference issue between cellular and D2D links.

Advantages of outband D2D communication:

- There is no interference issue with the cellular link.
- Users with D2D communication can have cellular transmission simultaneously.

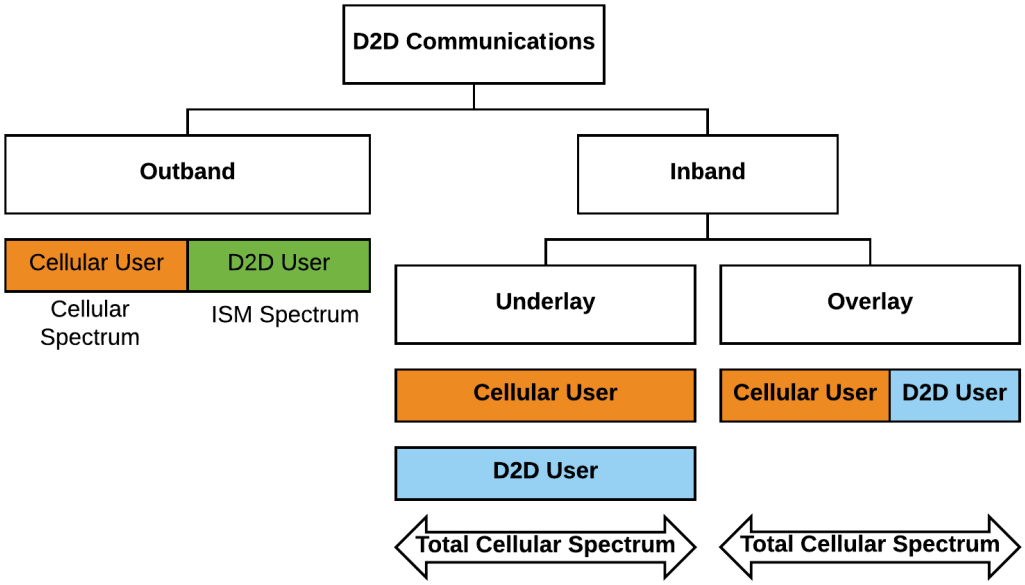

Figure 4.4: Classification of D2D communication based on spectrum allocation [11].

- Easy to plan and flexible to deploy

Disadvantages of outband D2D communications:

- Two wireless modes and interfaces are required, e.g., WiFi and LTE-A.
- Power consumption is high due to an additional interface for ISM band.
- Transmission distance is low because of the free higher frequency spectra, e.g., 2.5GHz, 5GHz.
- Data rates are lower since maximum speed is limited to WiFi technology. It cannot transmit data at more than the WiFi speed.
- It may be affected by the uncontrolled behaviour of unlicensed spectra.
- The operator will have almost no control because of using free spectrum.
- Regulation issues are a major challenge.

Taking the pros and cons of outband D2D into consideration, some papers [63, 64, 65, 66] suggest giving control to the cellular networks which is called controlled outband D2D. In contrast, an other paper [67] proposes control to the D2D communication user, which is called autonomous D2D.

4.1.2.2 Inband D2D

Inband D2D communication proposes the use of licensed spectrum for both cellular and D2D users. It can be divided into two separate types. Figure 4.4 shows the classification of D2D communications based on spectrum allocation. There are two kinds of inband D2D and they are:

- Underlay Inband D2D
- Overlay Inband D2D

In the underlay inband D2D network [68, 69], D2D users and cellular users share the same radio resources. This type of communication is a unique choice for many researchers and scientists because of the advantage of its maximum spectral efficiency. This is because no extra bandwidth is allocated for the D2D users.

When a part of the cellular spectrum is allocated for D2D users, the system is called overlay D2D. Spectrum efficiency of this type is not as high as underlay inband D2D; however, it has less interference since dedicated bandwidth is allocated for D2D users.

Advantages of inband D2D communications:

- The efficiency of the cellular spectrum is greatly increased, especially in the underlay system.
- Transmission distance can be maximised up to the cellular range.
- Any cellular device can use inband D2D communications.
- Managing Quality of Service (QoS) is easy because the cellular base stations control the entire spectrum allocation.
- Higher data rates.

Disdvantages of inband D2D communications:

- Some cellular bandwidths may remain unused, especially in the overlay system, if no D2D communication takes place.
- Interference management is critical, and cellular management is complex and challenging.
- A user cannot have D2D and cellular transmission simultaneously.

- Mobility management is critical.
- Operators might need more spectrum resources, which could impact capital expenses (CAPEx) substantially.

So far, D2D communication is the latest concept in the cellular network. Very few books and publications are available on this topic. Books [70, 71] explain the wireless D2D network strategy in brief. An excellent survey [11] explains almost all the basics of D2D communication in a cellular network. It also highlights the major areas in this regard. Survey papers [68, 69] also describe the overall concepts and research ideas in D2D communication.

4.2 Basics of D2D Communication Procedures

Many papers have already discussed the basics of the D2D communications system. Papers [72, 73, 74, 68, 75] analyse the basic procedures of the D2D commutations. They follow some steps as other communication systems. I summarize some major procedures, as shown in Figure 4.5. A detailed analysis of each step is beyond the scope of this dissertation.

4.2.1 Device discovery

The first step to establish a D2D communication is to discover the device in the proximity. A device must be able to detect the presence of the other device. It could be network assisted, or a device can search other devices by sending beacon messages at regular' time intervals. Papers [76, 77, 78, 79, 80, 81] discuss the different discovery algorithms for the D2D communication system.

4.2.2 Device Association

Once the device is detected, next step is to attach the device to the network. This can be could also be via the assisted device itself, using the relay mode or network assisted.

4.2.3 Device Synchronisation

Device synchronisation takes place immediately after the device association. The synchronisation happens explicitly between the D2D devices and the

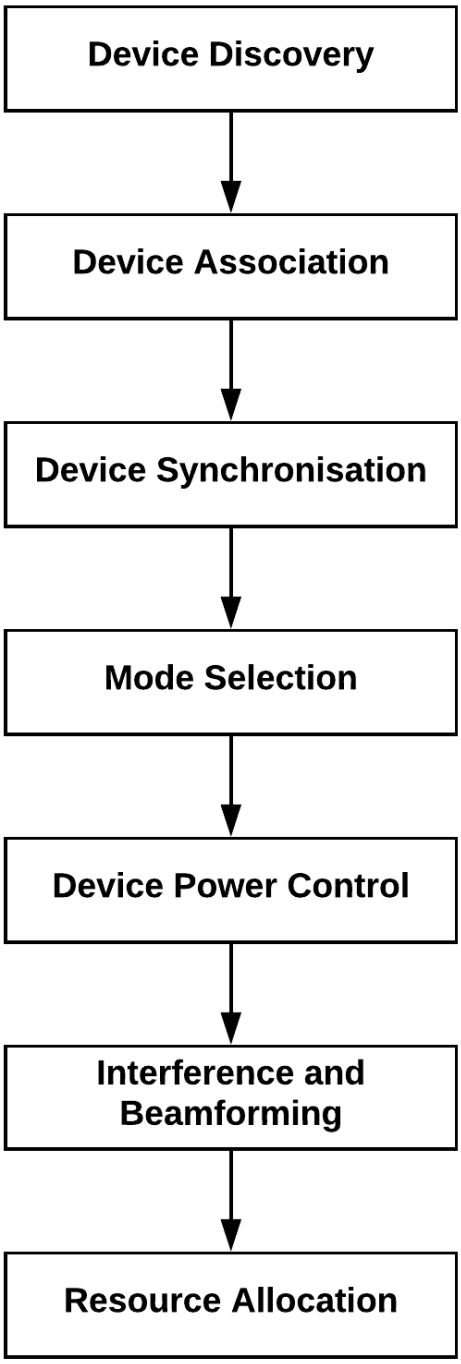

Figure 4.5: Steps of D2D communication procedure.

base station is notified once the synchronization is done so that the base station can decide which mode to select for the particular devices.

4.2.4 Mode Selection

Mode selection is an essential part of D2D communications. Two types of modes can take place while the communication is being established. The cellular mode is a usual mode when devices transmit data through the cellular base station. On the other hand, the D2D mode is when a device sends data directly to the other device. Paper [82] illustrates the queuing models with the application while paper [83] highlights the flexible uplink/downlink TDD mode to select the D2D communications mode.

Some other papers [84, 85, 86, 87] also discuss some particular procedures to choose the mode conveniently. The mode selection process also involves several problems. Some papers from this list have attempted to solve them. Authors also propose optimisation-based approaches and Coalitional Game-based methods to select an appropriate mode.

However, I propose five modes selection in Chapter 6, based on the received signal level from the D2D devices. They are as follows:

- D2D Mode
- Cellular Mode
- Relay Mode
- Call Waiting, and
- Call Drop

4.2.5 Device Power Control

Power control plays a crucial role in quality D2D communication. Proper power control can reduce the interference considerably so that D2D and cellular communication can interfere with each other only within a threshold limit. Paper [88] describes the power allocation technique for uplink subchannel OFDMA-based D2D communication system. Paper [89] proposes a power optimisation system of D2D communication for underlaying cellular communication. Optimum power allocation means proper control of uplink and downlink power, distributed power control and power control using MIMO.

4.2.6 Interference and Beamforming

Interference coordination for D2D communication is closely related to power control of the devices and base stations. It is required to analyse the interference and status and makes an optimum power allocation to avoid interference. Many papers highlight the interference issue and how to mitigate them. Papers [90, 91, 92, 93, 94, 95, 96] propose different techniques to allocate power and reduce interference.

Beamforming techniques are used to locate the D2D users accurately by using DOA estimation techniques. An accurate beamforming technique can reduce interference considerably, as D2D users can transmit a very directional beam to each other or the base station can send to the direction of D2D users only. I propose some beamforming techniques for D2D communication in Chapter 5.

4.2.7 Resource Management

The key challenge part of D2D communication is to allocate the resource in such a way that maximum speed with minimum interference is ensured. As mentioned earlier in this chapter, there are some advantages and disadvantages while allocating the resources in the underlay or overlay inband system. The subcarrier allocation might be centralized or distributed. The operator controls centralised allocation, and the network, i.e., the devices manage distributed allocation. Scheduling is also important in this regard. Time-domain and frequency-domain scheduling are possible. Papers [97, 98] proposed Stackelberg-type game-based scheduling in the time domain while papers [99, 100, 101, 102, 103, 104, 80] discuss some different techniques.

4.3 Challenges of D2D communication

The D2D communications system is still not a mature technology. A lot of research is being carried out to make it feasible in the real network. Some challenges are as follows:

4.3.1 Security for D2D Communications

Security becomes vital as the technologies get updated day by day. Similar to other communication systems, security and privacy for the D2D communications should be considered as a high priority. Security involves cybersecurity for D2D, physical layer security and user privacy. On the other hand, when

a device acts as a relay, it is also essential for the data to be encrypted so that the relay device cant interpret it easily. The data that passes through another device needs to be rigorously protected. Proper signal processing techniques should be applied to make sure that third parties cannot retrieve it. Very few papers [105] discuss the security issues of the D2D cellular network.

4.3.2 Application of D2D communications

Some advantages of using the D2D communication technique have already been mentioned at the beginning of this chapter. D2D communication can also facilitate the vehicular ad-hoc network and enhance both proximity services and mobile social networks. It may also extend the scope of the internet of things (IoT), as the device can facilitate coverage issues to connect any other things located outside the network coverage area. Papers [64, 106, 63, 107] highlight the applications of D2D communications.

4.3.3 Standardisation of D2D Communications

D2D communications techniques have not been fully standardised yet. It is still an immature technology, and a lot of problems need to be solved before implementing it into a real network. The Third Generation Partnership Project (3GPP) is telecommunication body mainly responsible for the standardisation of significant telecommunication technologies. In [108, 109], some standardisation policies have been mentioned based on proximity services.

4.3.4 Mobility Management of D2D Communications

Wireless communication without mobility are hardly acceptable. Mobility management for any wireless communications has been regarded as the high priority issue. We have almost smooth mobility management for the latest telecommunications system like LTE-A. However, mobility for D2D devices is not so easy to compare with the currently available techniques. The aim of this dissertation is to establish an algorithm that will facilitate a smooth mobility system for D2D devices. Chapter 6 will discuss the proposed mobility management system of cellular devices as well as D2D devices.

4.3.5 Location of D2D Users

Knowing the location of a user is very important to establish good communication among the devices and the base stations. This knowledge enables D2D communications and reduces transmission power and interference considerably. It is also a challenge to implement the beamforming techniques in D2D communications. As users can move anywhere at any time, a precise beamforming technique is needed to locate the users and track their changing positions. Finding some state-of-the-art beamforming techniques and comparing them with simulations are also a part of this dissertation. Chapter 5 is dedicated to estimating the Direction of Arrival (DOA) by analysing the channel between the devices and base station.

Part II

Our Proposition and Modeling

Chapter 5

Direction of Arrival (DOA) and Channel Estimation for D2D Communication

This chapter is based on our published book chapter [20] and paper [19]. The detailed chapter is available in the Appendices A and B.

The D2D operation mode mostly depends on the exact location of the users from the base station. Location estimation techniques can play an essential role in this case. Estimating a user's location is going to be an integrated system with the upcoming mobile technology. This chapter shows some techniques for estimating the Direction of Arrival (DOA) with mathematical modeling. Chapter 8 presents the simulation results of this chapter. Estimating the DOA in this chapter is regarded as the purpose of using the Smart Antenna System (SAS). It is possible to calculate the location of a user by considering the uplink transmission system of the mobile communication system. Estimating the channel and actual path delay is also an important task which might be done by using the 1D Uniform Linear Array (ULA) or 2D Uniform Rectangular Array (URA) antenna systems. In this chapter, 1D ULA is considered to utilise some popular techniques. The behaviours of the channel characteristics substantially determine the performance of a communication system between two ends. This behaviour defines signal transformation while propagating through the channel between receivers and transmitters. Accurate channel information is crucial for both the transmitter and receiver ends to provide their best service. The ultimate focus of this chapter is to estimate the channel based on 2D parameter estimation. Uniform Rectangular Array (URA) is used to perform the 2D parameter estimation. It is possible to determine the

Azimuth and Elevation of a source by using a URA model.

During the last few decades, wireless communication technology has improved enormously. However, the technology did not only perform the communication between two ends. The state-of-the-art technologies cannot meet all the requirements demanded by people. The primary interest of recent research is to design a model to estimate efficiently the location, direction, distance and path delay (induced by the fading channel) of a source. A proper channel model plays an important role performing those tasks efficiently. Therefore, the problem of appropriate channel estimation arises in a large variety of important work for the researchers.

To keep going with the demand of increasing data rate, LTE was standardised by the 3GPP. This is one of the most popular technologies because it provides low latency, higher spectrum efficiency, and seamless mobility. The two leading latest technologies i.e., MIMO and OFDM (Orthogonal Frequency Division Multiplexing) have been integrated into LTE system so that it performs better than any earlier technologies. In this chapter, techniques for estimating the direction of arrival(DOA) are investigated. It is expected that angle or direction of arrival will play a vital rule to track the user's location precisely for the upcoming mobile generation like 5G.

To estimate DOA, channel estimation should be measured precisely. Estimation of a channel for a 2D rectangular array is discussed in section 5.2. I have considered only the uplink parameters to estimate the channel. Proper planning for the uplink channel is crucial because the power of the user equipment (UE) is limited. We can calculate the DOA and delay of arrival directly from the estimated channel.

Propagation signals transmitted from arbitrary sources contain a lot of information about the origins that produce them. This information includes the location of the sources, path delays, angular elevation, etc. It is possible to estimate that information by analysing the channel between two ends with the help of smart antenna technology.

The antenna array receives spatial samples of propagating wave field, which are then processed to estimate DOA. A DOA estimation technique performs spatial filtering to separate signals from different spatial locations that have overlapping frequency contents [110, 111] But there are many other

techniques also available, and some of them will be discussed in this chapter.

The need for estimating DOA has been increasing enormously to keep pace with the requirement of advanced technologies like finding the geographical location of the User Equipment (UE). Positioning has many applications, such as emergency services, location-based billing, hostage rescue, etc. For some applications, beam pattern of the antenna array can, therefore, be changed without physically changing the antenna pattern.

I have considered a Uniform Linear Array (ULA) in the receiving antennas where all the antennas are placed in a line, and the distance between two adjacent antennas is the same. There are other array configuration options possible, e.g., Uniform Circular Array (UCA), Uniform Rectangular Array (URA).

The purposes of using smart antenna system in this dissertation are for

- Direction of Arrival (DOA) estimation,
- Path delays estimation, and
- Accurate channel estimation,

This chapter (see Appendices A and B) briefly explains how to estimate them.

In the simulations discussed in Chapter 8, primarily, I considered four receiving antenna arrays and two different sources located in different directions. A uniform linear array antenna geometry has been used according to Figure A.1. For estimating channel, finally, I have considered the eight receiving antenna arrays for the simulations.

5.1 Techniques for Estimating DOA

There are a couple of techniques used to determine the DOA. They are as follows:

- Conventional Beamformer Technique,
- Capon Beamformer Technique,
- Multiple Signal Classification (MUSIC) Method, and

- Estimation of Signal Parameters via Rotational Invariance Technique (ESPRIT)

Detailed mathematical model are beyond the scope of this chapter but they are available in the Appendices A and B.

5.1.1 Conventional Beamformer Technique

Conventional Beamformer Technique is the basic and primary technique used to estimate the DOA. Its sensor spacing is normally half of the wavelength. If the spacing is larger, it results in the performance degradation. The smaller spacing usually reduces the total aperture and then results in a lower spatial resolution that is the ability to distinguish two closely spaced sources. The spatial resolution directly depends on the number of sensors, i.e., if the number of sensors with proper spacing is increased, spatial resolution is also improved.

Some pros and cons of Conventional Beamformer are as follows:

- Spatial resolution determined by the sensors array is not very good If we do not have a good number of array antennas.
- The array has to be fully calibrated in order get an accurate estimation.
- Multipath is not that much problem since signals are not necessarily to be uncorrelated.

5.1.2 Capon Beamformer Technique

Capon Beamformer came with a better performance. It is formulated according to the Minimum Variance Distortionless Response (MVDR) algorithm [115]. It was designed to overcome the limitation (poor resolution problem) of the conventional beamformer.The complexity of this technique is a bit higher than the Conventional Beamformer. However, we can get better resolution performance when two users are located in a closer distance.

5.1.3 Multiple Signal Classification (MUSIC) Method

Multiple Signal Classification (MUSIC) method was first formulated by Schmidt [117], Bienvenue and Kopp [111]. It is one of the most popular subspace-based techniques to estimate DOA. It depends on the spatial covariance matrix of the data. Some considerable facts about the MUSIC are follows:

- The total number of sources has be smaller than the total number of sensors in the array.
- MUSIC shows high-resolution property.
- MUSIC cannot perform well for closely spaced signals and low SNR conditions. [120].
- MUSIC could be computationally expensive because exhaustive search through the field of view (all θ in Appendix) is required.
- MUSIC is very sensitive to antenna position, phase errors, and gain. Therefore, precise calibration is required.
- Since MUSIC is unable to estimate DOAs of the correlated signals correctly, multipath is a significant problem.
- Accuracy is also dependent on the number of snapshots [120].

5.1.4 Estimation of Signal Parameters via Rotational Invariance Technique (ESPRIT)

Estimation of Signal Parameters via Rotational Invariance Technique (ESPRIT) was proposed by Paulraj, Roy, and Kailath [121]. It is a search-free DOA estimation technique based on the shift-invariance property of the ULA steering matrix [117]. ESPRIT is considered as a computationally efficient technique compared with MUSIC. The Unitary 2D ESPRIT (see Appendix B) is the most precise techniques used to estimate the DOA.

5.2 Multipath Channel Estimation using 2D Parameter Estimation Method

In this section, I have considered the Uniform Rectangular Array (URA). We could estimate azimuth and elevation of a source by using URA model. This model poses a similar structure to the channel model, which has been introduced in section A.8. It is possible to estimate the user's location (angle) along with the time delay of an incoming signal to the antenna array sensors with the help of this technique. To estimate this, Unitary 2D ESPRIT method has been considered although elaborating 2D ESPRIT is not the aim of this section. 1D parameter estimation model that has already been discussed in Appendix A is easy to implement. However, it has some drawbacks as well. After formulating unitary ESPRIT [122], 2D

parameter estimation technique has become much popular because of its high-resolution estimation ability and computational efficiency. There are several antenna arrays can be implemented by using the unitary ESPRIT, i.e., URA, Triangular Antenna Array (TAA). Here, only URA antenna configuration has been considered. Nevertheless, this estimation technique can only perform precise result if the array positions are properly spaced with equal distance. A proper signal model is formulated in the Appendix part, and finally, multipath channel model is compared with that signal model for the 2D rectangular channel estimation method (See Appendices A and B). URA model involves complex geometries [12, 122, 123].

Multipath channel estimation using unitary 2D ESPRIT has also been discussed in the book chapter which is also available in the Appendix section A.

As we move forward, next chapter will be dedicated to the mobility management of the D2D communication, proposed algorithm and its derivation.

Chapter 6

Mobility Management of D2D Communication

D2D communication takes place when two devices communicate directly without taking significant help from a base station. For any wireless communication system, mobility management is a big issue. When two devices are active, one or both users might change their location, and when they are in cellular mode, it is not difficult to keep the service uninterrupted. However, when they are in D2D mode, mobility management becomes crucial, since a proper algorithm is yet to be developed that can handle the communication without interruption. In this chapter, I propose a novel approach to handle the mobility of D2D users.

6.1 Mobility and Handover Management for the LTE-A Network

Mobility management for the LTE-A is so far well standardised and already implemented. A mobility model that takes into consideration energy and bandwidth efficiency is proposed in [127] for the LTE-A network. A technical overview of handover and mobility management for the heterogeneous network (4G) in LTE-A is provided in [13]. The authors investigated A3 events that take control of the entire handover parameters. Usually, the mobility of a user is mentioned broadly in three different states, i.e., idle, active, and detached mode.

When UE searches a network with which to register and does not belong to any network yet, it is said to be in detached mode. However, based on the initial request from the UE, Evolved NodeB (eNodeB)

performs a complicated process in association with Mobility Management Entity (MME), Evolved Packet Core (EPC), Serving Gateway (S-GW) and Evolved Packet Core (P-GW). After that, the UE is attached to the network, but there is no packet data transfer during this time, the UE goes to an idle mode which is sometimes called a power conservation mode. In active mode, UE receives or transmits data through the nNodeB. Details are beyond the scope of this chapter.

In the 4G network, for the event A3 (See Appendix C), we could optimise the handover in three ways:

- Modifying the parameters **a3offset** and **hysteresisa3**
- Changing the parameter **timetotriggereventa3**
- Modifying of the parameter **filtercoefficient** and **CellIndividualoffsetEutran**

Parameters are set by following the conditions below:

RSRP(target) > **RSRP**(Serving) + **a3offset** + **hysteresisa3** - **cellindividualoffsetEutran**

where **RSRP** denotes Reference Signal Receive Power.

a3offset is identified as the LTE Event A3 is triggered when a neighbouring cell becomes better than the serving cell by an offset. **a3offeset** is the threshold in dB unit and **hysteresisa3** is the time period. If target cell dB unit is higher than serving cell to **a3offset** for **hysteresisa3** period, UE starts to measure report. The role of **timetoTriggera3** is to avoid a ping-pong effect in Event A3. **CellIndividualoffsetEutran** is applied periodically to each neighbour cell with the purpose of load management. This parameter is used if the neighbour lists have the special broadcast configuration.

Handover takes place when the UE moves from one location to another location. A detailed description of the handover process of a UE for the LTE-A network is also beyond the scope of this chapter. Paper [13] describes the entire handover process which is shown in Figure 6.1 in terms of state line diagram.

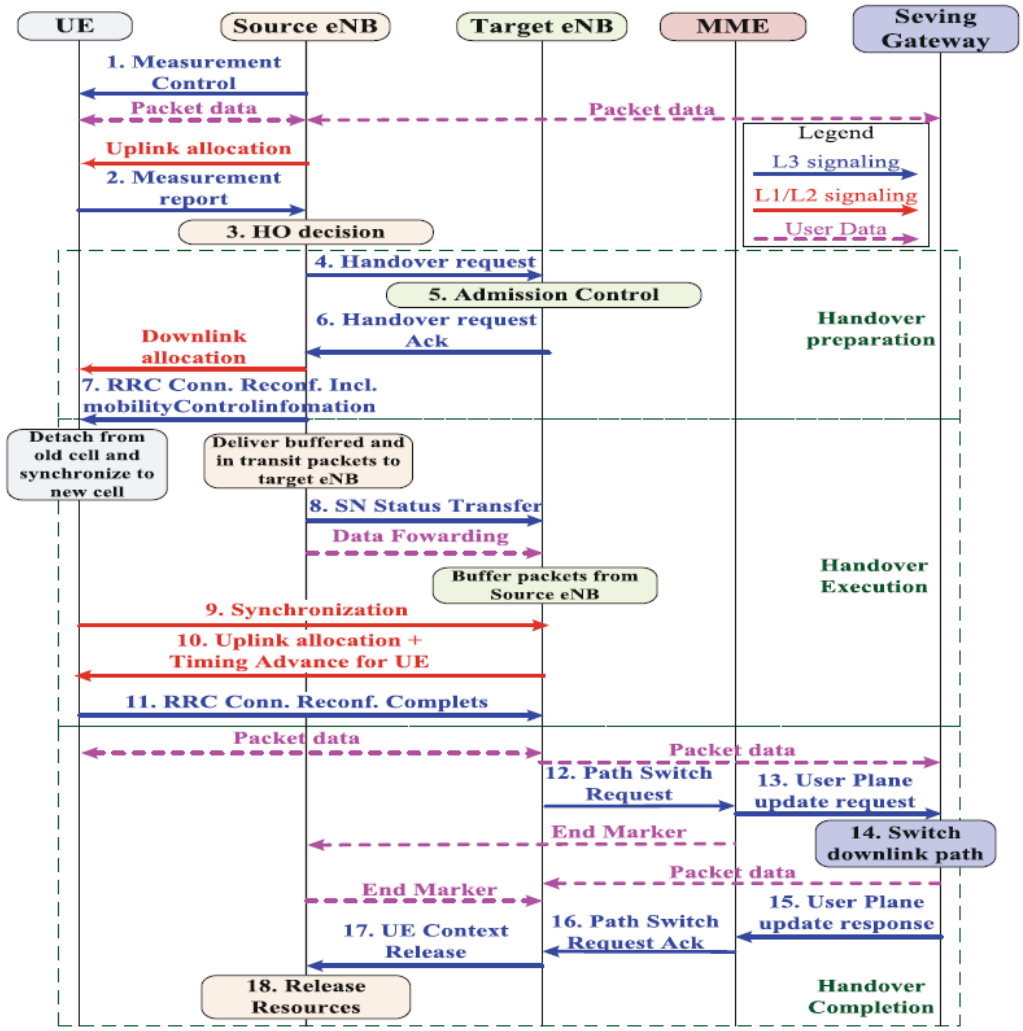

Figure 6.1: Procedure of inter-eNodeB and intra-MME/S-GW. Image source: [13].

6.2 Mobility and Handover Management for the D2D Communication of a 5G Network

Low latency and reliable data communication between two devices, while they are moving is a challenging task that is yet to be developed efficiently. A few papers have discussed this topic so far. When several base stations are involved in making the handover, the latency could be increased because exchanging the controlling signal makes D2D communications unfeasible while they are moving. A low latency, smooth mobility management is very crucial because, besides the human-centric aspect, one of the very important applications of this communication is vehicle-to-vehicle (V2V) communication and a bit longer latency might cause severe damage in this regard. Paper [14] proposes some mobility management solutions that show expected gains under certain assumptions for a small cell network. The authors categorised two smart solutions that could reduce the negative impact:

- D2D-aware handover solution
- D2D-triggered handover solution

6.2.1 D2D-Aware Handover Solution

This solution is proposed to reduce the latency by minimising signaling overhead. Figure 6.2(a) shows the normal communication when two devices are stable. However, a lot of overhead is involved while UE1 is moving from one location to another location that is served by another base station. This is not feasible because of the higher latency. The authors propose a group handover algorithm so that latency is reduced greatly. An A3 event was considered where $RSRP_{target} - RSRP_{source} > offset$. They proposed to control both devices under the same base station and until and unless this condition was satisfied they proposed not to perform the handover for the individual device. Figure 6.3 shows the detailed steps needed to perform this task.

6.2.2 D2D-Triggered Handover Solution

Figure 6.4 shows a signalling flow chart of a D2D-triggered handover process for which a target cell performs the control of the handover of a new D2D user to join the group communication. In this type of solution, the authors intended to cluster the total members of a D2D group within a minimum number of BSs or cells, so that the network signalling overheads caused

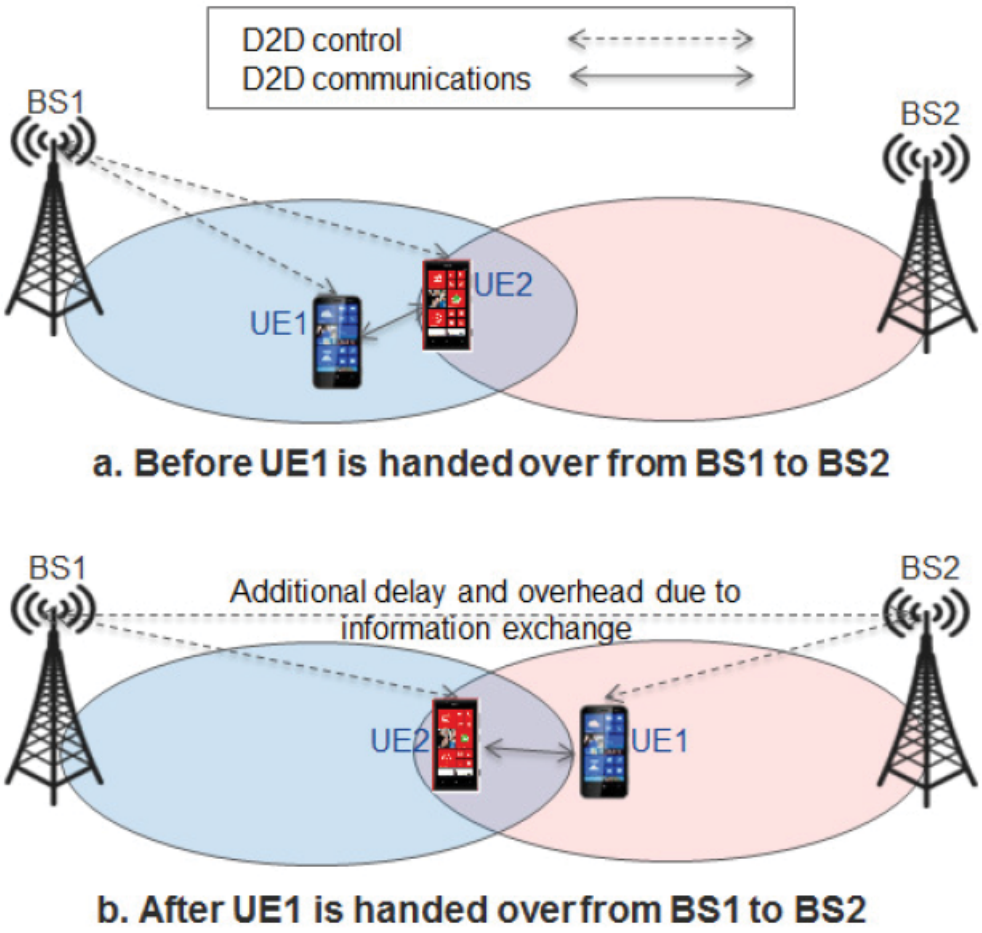

Figure 6.2: D2D communication and control before and after a normal cellular handover execution. Image source: [14].

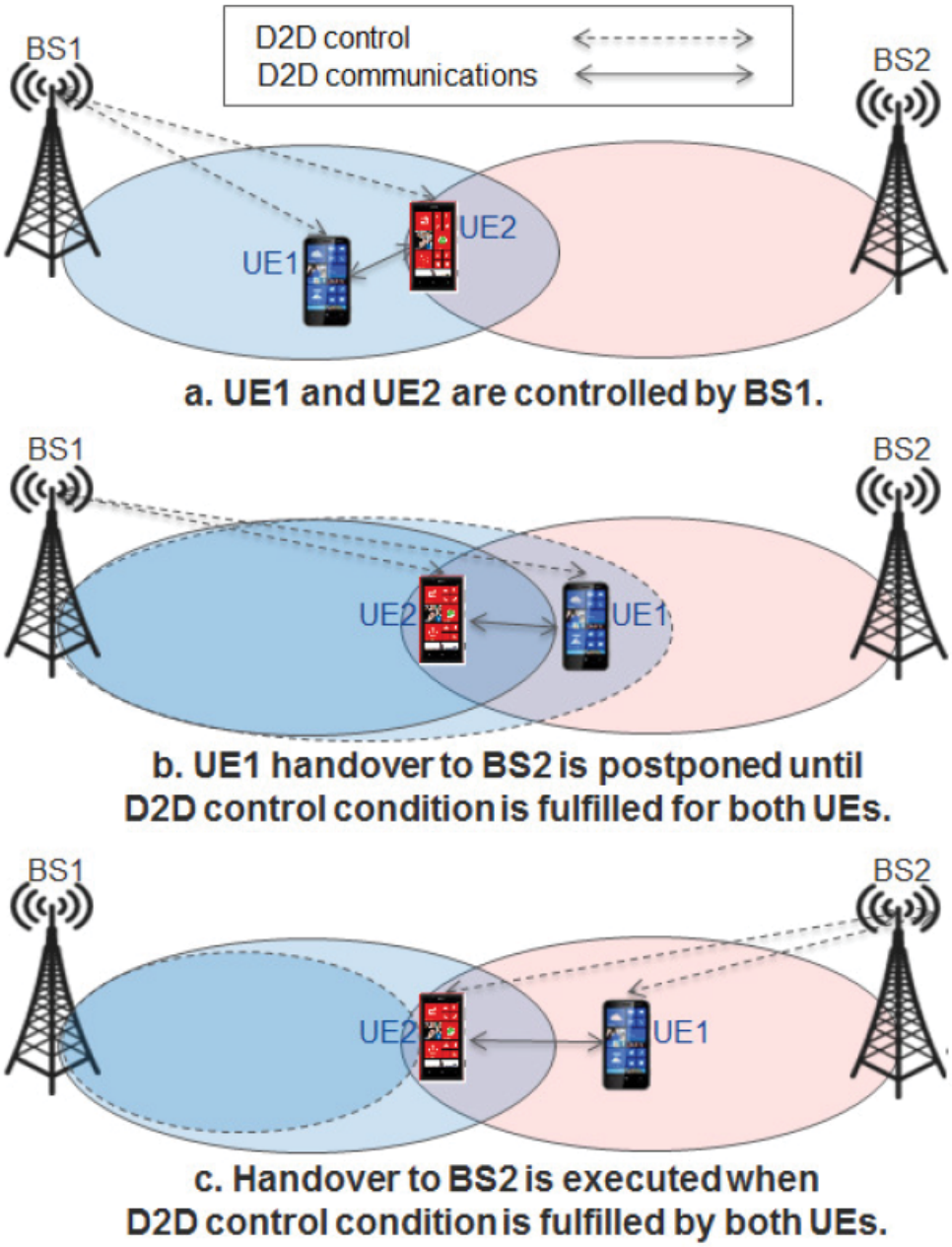

Figure 6.3: D2D-aware handover solution during mobility. Image source: [14].

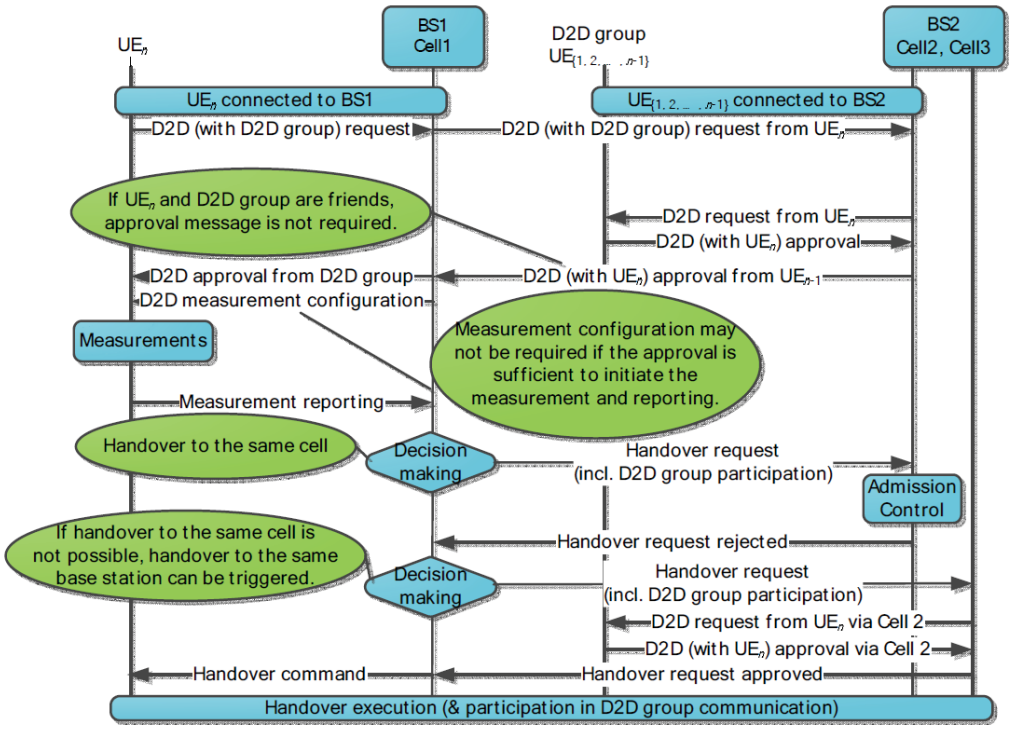

Figure 6.4: A signaling flow-chart of D2D-triggered handover solution during mobility. Image source: [14].

by the inter-BS communication, e.g., D2D radio resource information were reduced.

As I propose only group handover as per Figure 6.3 in my proposal, described in the next section, a detailed analysis of the D2D-Triggered handover solution is beyond the scope of this chapter.

6.3 Proposed Model

In this part, I consider the TDD configuration that is already used for LTE-A. Standard power control mechanism for the TDD will be considered accordingly. For convenience, I assume that DUEs use the uplink resources of a mobile cellular network. The purpose of my proposal is to increase the sum-rate that should remain the same while moving.

Firstly, I consider an area where different users are attached to a cell. Figure 6.5 shows a model that represents different links and channel gains among the mobiles users and the base station. In this scenario, I consider one eNB and three devices, numbered $p = 1, 2, 3, 4$ and $q = 1, 2, 3, 4$ respectively as per the diagram. The link is indicated X_{pq} where p is the position of the first device, and q is the position of the second device of a link. Three possible conditions can be considered, and some gains for the specific links might be ignored as they are negligible compared with others. Cases are as follows:

- Common for both CUEs and DUEs
- for CUEs
- for DUEs

For the first case:

$$X_{pq} = 0 \text{ if } p = 1, 4 \text{ and } q = 4, 1 \text{ respectively} \tag{6.1}$$
$$\text{or } p = 2, 3 \text{ and } q = 3, 2 \text{ respectively} \tag{6.2}$$

For the second case:

$$X_{pq} = 0 \text{ if } p = 2, 4 \text{ and } q = 4, 2 \text{ respectively} \tag{6.3}$$
$$\text{or } p = 3, 4 \text{ and } q = 4, 3 \text{ respectively} \tag{6.4}$$

For the third case:

$$X_{pq} = 0 \text{ if } p = 1, 2 \text{ and } q = 2, 1 \text{ respectively} \tag{6.5}$$
$$\text{or } p = 1, 3 \text{ and } q = 3, 1 \text{ respectively} \tag{6.6}$$

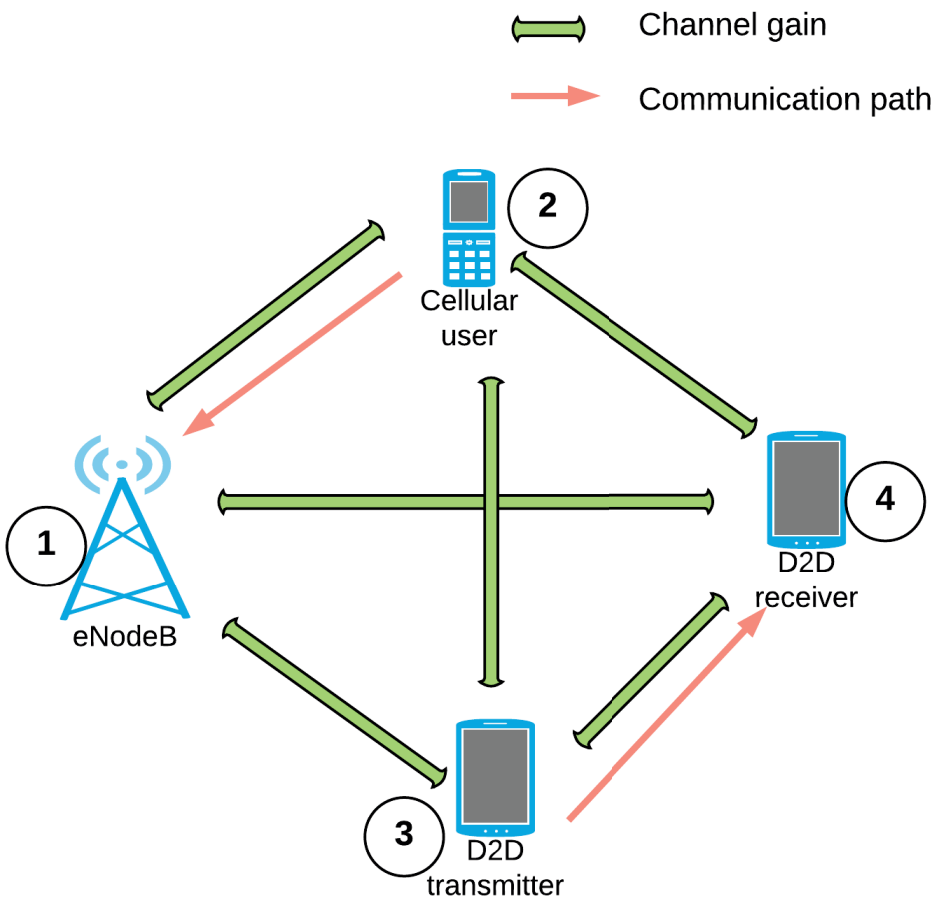

Figure 6.5: Possible channel gains within a cell.

Sum rate for the cellular:

$$r_{\text{Cellular}} = B \log_2 \left(1 + \frac{S_{\text{Cellular}}}{\sum_p \sum_q X_{pq} + N_0} \right) \tag{6.7}$$

Sum rate for the DUEs:

$$r_{\text{D2D}} = B \log_2 \left(1 + \frac{S_{\text{D2D}}}{\sum_p \sum_q X_{pq} + N_0} \right) \tag{6.8}$$

Total sum-rate can be calculated as:

$$R_{\text{Sum}} = r_{\text{Cellular}} + r_{\text{D2D}} \tag{6.9}$$

where B indicates the bandwidth of each sub-channel. S_{D2D} is the signal gain of D2D users and S_{Cellular} is the signal gain of the cellular user. N_0 is the additive noise.

My proposal considers the paper [15] where an operational procedure of an LTE network that supports D2D communications is proposed. Figure 6.6 shows how this proposal works. My algorithm extends this procedure which should support the mobility of DUEs without compromising the quality.

Consider a total number of CUEs and DUEs pair as N_c and N_d respectively. Assuming each pair consists of two D2D users where one is the transmitter, and another is the receiver. To improve the spectrum efficiency, I consider using the same uplink resources for both CUEs and DUEs.

I propose an extended algorithm of this model that enables the mobility functionality of D2D users in a 5G cellular network. Figure 6.7 shows the proposed model, and it shows the mobility direction, relevant channel gain, and communication paths among the cellular users, D2D users, and base station. I ignore some links as they are negligible according to Equations 6.1 to 6.6. This figure also shows the notation of channel gains.

Based on the moving opportunities, I consider four scenarios as follows:

- $DUET_X$ moving towards another eNB. Here, $DUET_X$ is the transmitter of the D2D pair.

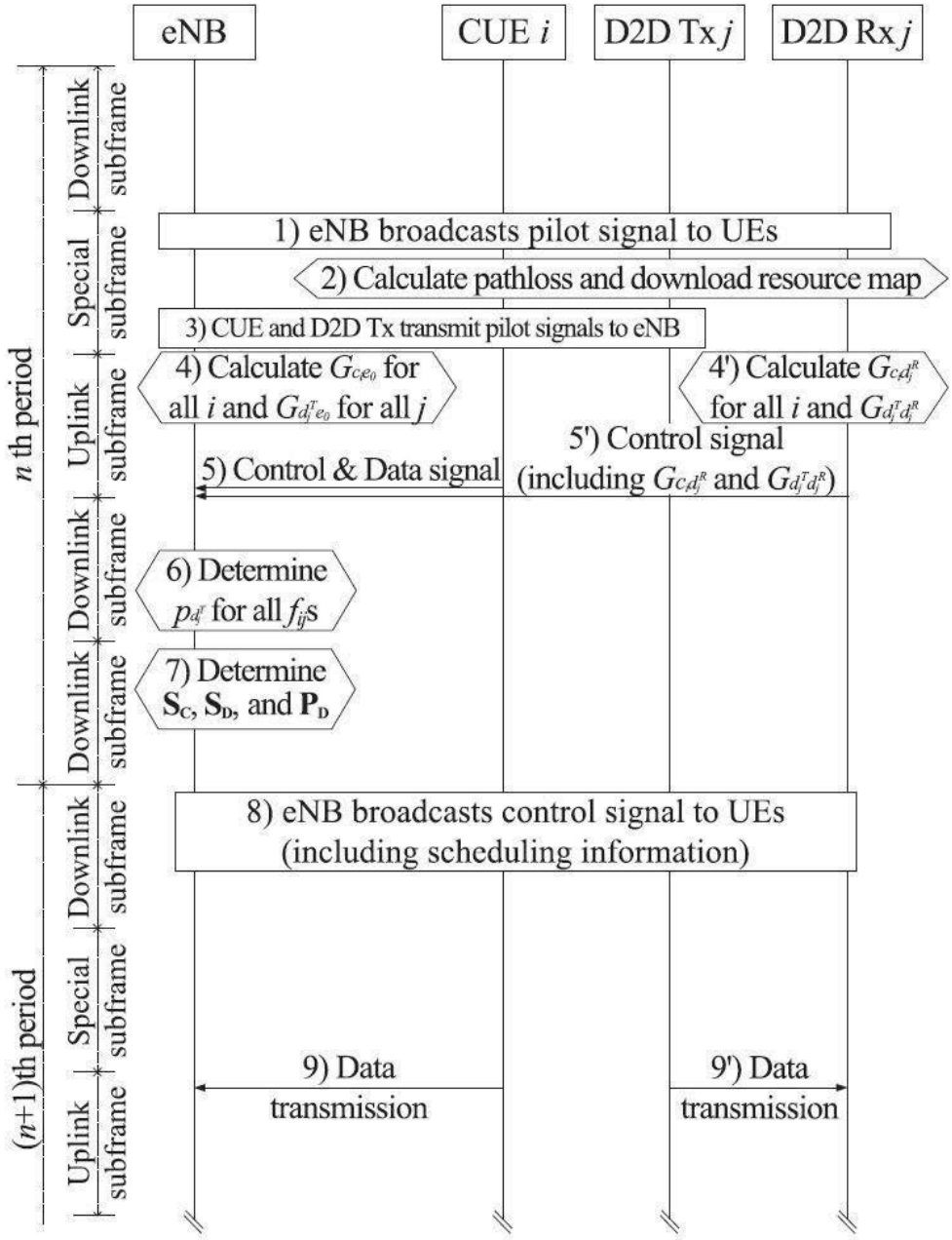

Figure 6.6: A D2D operation model proposed in [15]

- $DUER_X$ moving towards another eNB. Here, $DUER_X$ is the receiver of the D2D pair.
- Both $DUET_X$ and $DUER_X$ are moving into same eNB.
- Both $DUET_X$ and $DUER_X$ are moving apart from each other and exiting the current eNB serving area.

For convenience, I consider only the first condition in this report where a D2D transmitter is moving towards another eNB, as shown in Figure 6.7. The rest of the conditions follow the same strategy.

eNodeB always collects the channel state/gain information and allocates the resources along with transmitting power of CUEs and DUEs. I assume that total $N_c \times N_d$ resource sharing pairs for the current cell and target cell. One resource sharing pair consists of one D2D pair and one CUE within the same cell. Consider f_{ij} where $i \in 1, ..N_c$ and $j \in 1, ..N_d$ composed of CUEs and DUEs. For convenience, to indicate a gain of a link, d_j^R is referred to as the D2D receiver, d_j^T is the D2D transmitter, e_0^T is the cellular user of the target cell, and e_0^S is the cellular user of the source cell. Also, the cellular user is indicated as CUE_i^S for the source cell and CUE_i^T for the target cell. $DUET_{xj}$ is the D2D transmitter, and $DUER_{xj}$ is the receiver of the same cell. The new gain between the D2D users after moving is $\bar{G} d_j^T d_j^R$.

Assuming the same amount of source sharing pair exists after the moving takes place in the target cell, i.e., DUEs moving into the new cell would not change the number of total CUEs and DUEs. So the values of i and j will remain the same before the handover in the source cell and after the HO in the target eNB. Figure 6.8 shows the steps of the handover management during the D2D communication. The handover process is initiated at $(n+2)$th time, whereas previous time is for the usual D2D communications without any mobility scope.

During the data transmission, periodic measurement broadcast signals are sent to all CUEs and DUEs. In these measurement signals, path loss and relevant parameters data are sent and based on this information, D2D users or eNode decide to make the handover. The relevant channel gains are indicated in Figure 6.7 where channel gain between CUE_i^S and $DUET_{xj}$, and eNB and $DUER_{xj}$ are neglected as indicated earlier in equations.

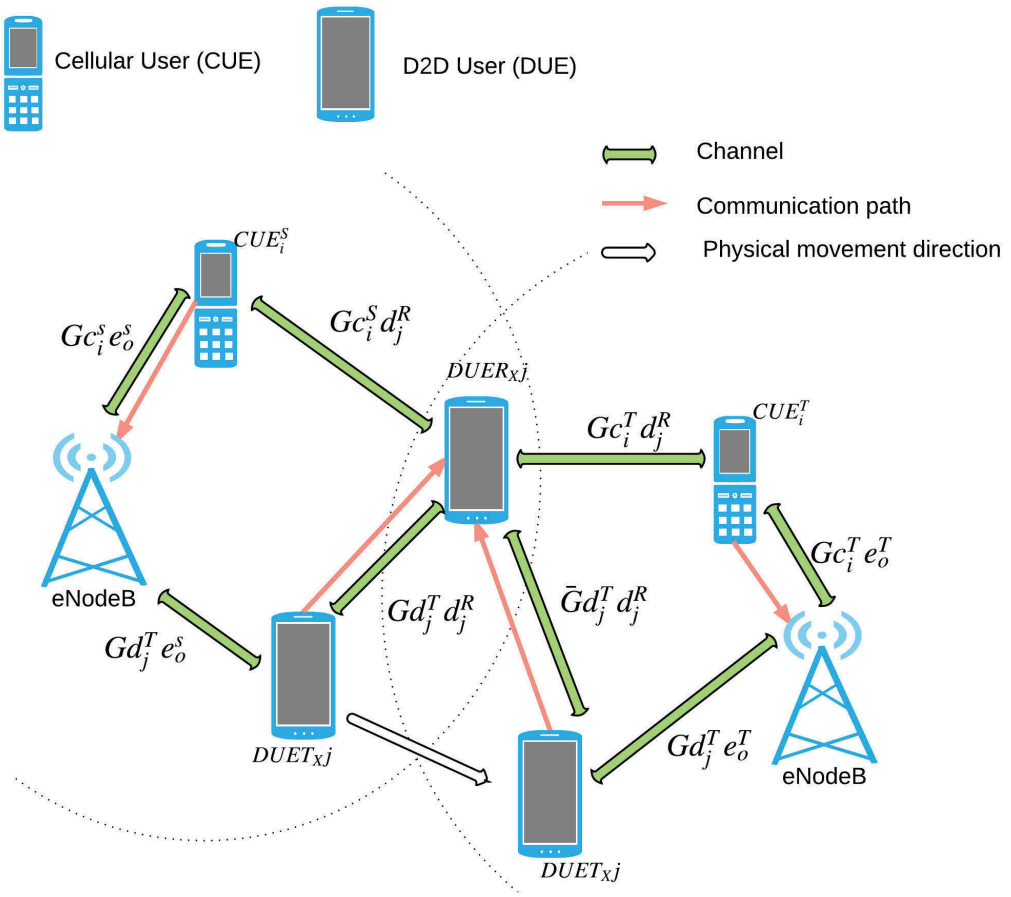

Figure 6.7: Proposed mobility algorithm of D2D users.

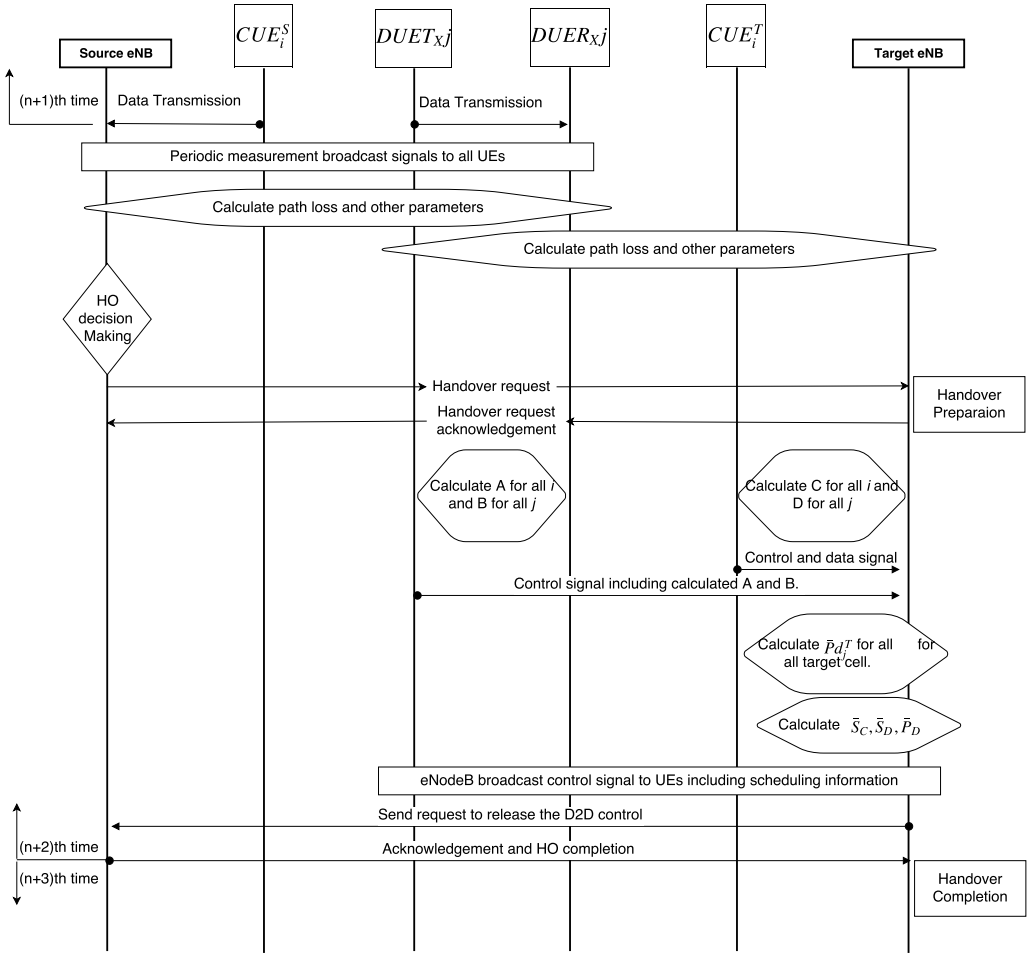

Figure 6.8: Line diagram of proposed model

It is to be noted that when one of the D2D users is moved to a target cell, the procedures for the resource allocations and scheduling are the same as with the source cells. Target eNB determines the transmission power $\bar{P}d_j^T$ for the D2D users. Based on the power allocation, eNB calculates the matrix $\bar{\mathbf{S}}_C$ and $\bar{\mathbf{S}}_D$ for assigning the subchannel to the cellular users and D2D users. Finally, eNB constructs the matrix $\bar{\mathbf{P}}_D = \bar{\mathbf{S}}_C\bar{\mathbf{P}}_F$ for all the users within the cell, where, $\bar{\mathbf{P}}_F$ is the matrix consisting of the values $\bar{p}d_j^T$ for each f_{ij}. Based on the calculations in paper [15], final transmission power for D2D users on each subchannel is calculated by the equation,

$$\mathbf{P}_D = \mathbf{S}_D \circ \bar{\mathbf{P}}_\mathbf{D} \tag{6.10}$$

where $\circ$ is a Hadamard operator.

6.3.1 Mode Selection

Mode selection should take place when a cellular network system enables the D2D communication. It is essential to select the proper mode to have an uninterrupted communication between the devices and the base station or between the two D2D users. Usually, we know two modes are available for the D2D communications enabled network. These are Cellular mode and D2D mode. However, I propose five different operation modes in my dissertation. They are as follows:

- D2D Mode
- Cellular Mode
- Relay mode
- Call Waiting, and
- Call Drop

6.3.1.1 D2D Mode

D2D mode is the most wanted mode for the D2D communications system. In this mode, two D2D users communicate directly with each other without using the base station. The base station monitors and can control this operation. The data rate and spectral efficiency are maximum when the D2D mode is in action.

6.3.1.2 Cellular Mode

When the D2D mode fails, cellular mode takes place, and this is the standard mode of operation for a D2D-disabled network. In this mode, two devices communicate with each other via the base station irrespective of their locations. The handover process follows the A3 algorithm and the base station controls the mechanism.

6.3.1.3 Relay mode

Relay mode is another form of D2D communication when one user acts as a relay and conveys the message from another device to the base station. In this mode, one device can extend the coverage to its proximity areas where another device is out of the base station but still reachable via the relay device. Figure 7.1 shows the relay mode operation where the relay device extended the coverage.

6.3.1.4 Call Waiting Mode

The call waiting mode takes place only when the base station monitors the movement of the users, and it is for too short time. A group handover has been proposed in this thesis, and before taking the group handover, the base station measures the receive level to make a decision which should be a D2D mode or cellular mode or relay mode and finally in the worst case, drop the call.

6.3.1.5 Call Drop

When one or both devices are moving out of the base station coverage area, and no communication is possible by the received level, the base station terminates the call. Once this mode is selected, it is not possible to go back to any other modes.

6.3.2 Mode Selection Algorithm

I propose a mode selection algorithm controlled by the base station. This algorithm considers the data from the source and target base station as this algorithm is applicable when the D2D users are moving or about to make a handover between two base stations. In that case, a modified version of an A3 handover event is also proposed that fits with two devices for the D2D communications. This event happens when a neighbour cell becomes higher than the serving cell by an offset. However, the A3 handover triggers

for both devices as a group handover. If another device's received signal level to the target cell is not enough to get the D2D communication, mode selection takes place. A selection criterion is set regarding which mode to operate according to the received levels of both devices.

Flowchart 6.9 shows the detailed algorithm of how the mode selection process should work. Algorithm 1 also shows the simplified simulation model of how modes are selected. The selection of modes depends on mainly the threshold value that is set and the total path loss from the moving device to the base station.

The next part of this dissertation is to validate and simulation results of the proposed techniques. A Markov Chain model has been used to validate the proposed movements.

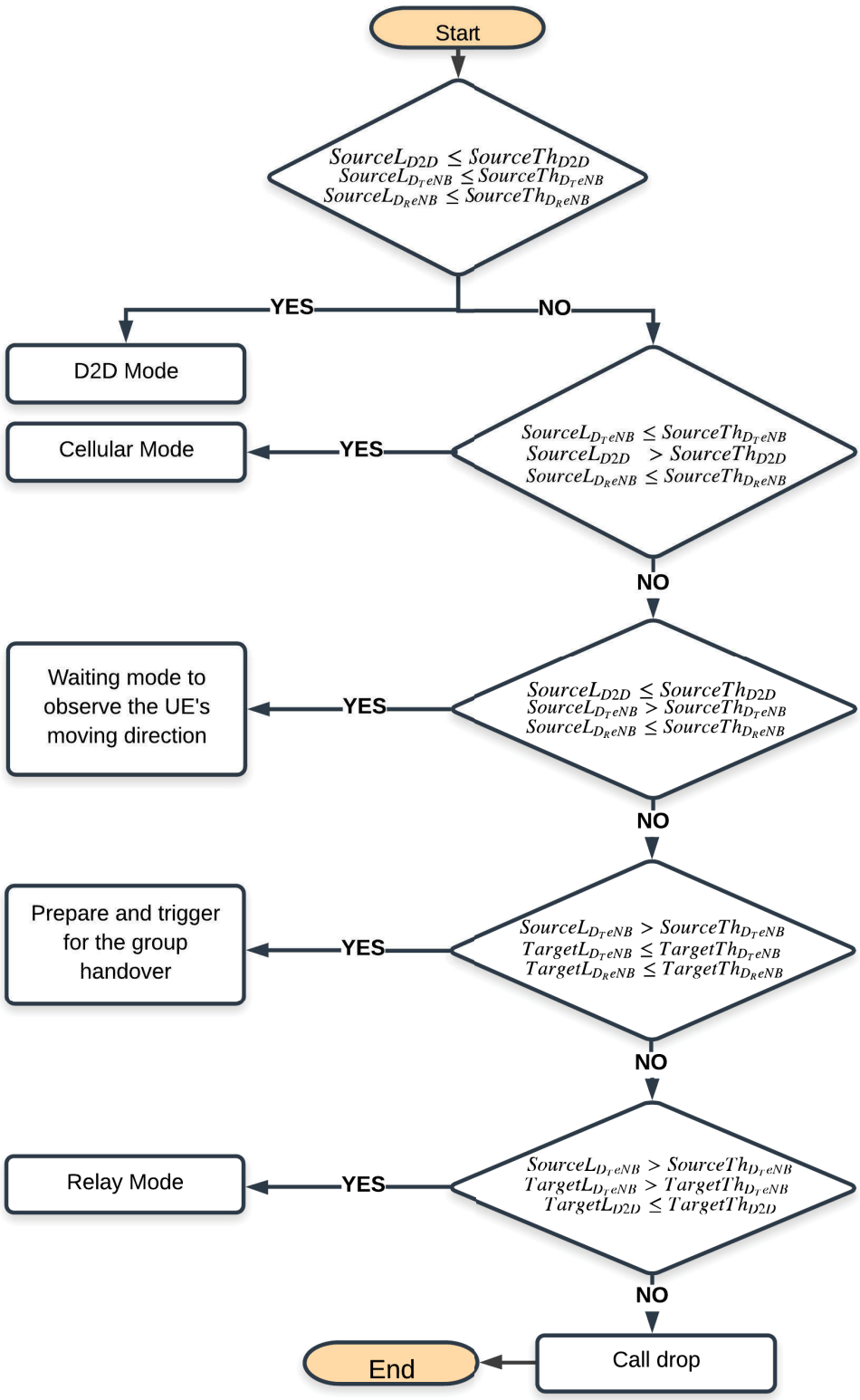

Figure 6.9: Flowchart diagram of the proposed mode selection model.

Data: **Source eNodeB:** Total loss between D2D pairs = $SourceL_{D2D}$, Threshold between D2D pair = $SourceTh_{D2D}$, Total loss between D2D transmitter and eNodeB = $SourceL_{D_TeNB}$, Threshold between D2D transmitter and eNodeB = $SourceTh_{D_TeNB}$, Total loss between D2D receiver and eNodeB = $SourceL_{D_ReNB}$, Threshold between D2D receiver and eNodeB = $SourceTh_{D_ReNB}$. **Target eNodeB:** Total loss between D2D pairs = $TargetL_{D2D}$, Threshold between D2D pair = $TargetTh_{D2D}$, Total loss between D2D transmitter and eNodeB = $TargetL_{D_TeNB}$, Threshold between D2D transmitter and eNodeB = $TargetTh_{D_TeNB}$, Total loss between D2D receiver and eNodeB = $TargetL_{D_ReNB}$, Threshold between D2D receiver and eNodeB = $TargetTh_{D_ReNB}$,

if $SourceL_{D2D} \leq SourceTh_{D2D}$ *and* $SourceL_{D_TeNB} \leq SourceTh_{D_TeNB}$ *and* $SourceL_{D_ReNB} \leq SourceTh_{D_ReNB}$ **then**
| Select D2D Mode;
else
| Search for the next possible mode
end
if $SourceL_{D2D} > SourceTh_{D2D}$ *and* $SourceL_{D_TeNB} \leq SourceTh_{D_TeNB}$ *and* $SourceL_{D_ReNB} \leq SourceTh_{D_ReNB}$ **then**
| Select cellular Mode;
else
| Search for the next possible mode
end
if $SourceL_{D2D} \leq SourceTh_{D2D}$ *and* $SourceL_{D_TeNB} > SourceTh_{D_TeNB}$ *and* $SourceL_{D_ReNB} \leq SourceTh_{D_ReNB}$ **then**
| Select waiting mode to observe the UE's moving direction;
else
| Search for the next possible mode
end
if $SourceL_{D_TeNB} > SourceTh_{D_TeNB}$ *and* $TargetL_{D_TeNB} \leq TargetTh_{D_TeNB}$ *and* $TargetL_{D_ReNB} \leq TargetTh_{D_ReNB}$ **then**
| Prepare and trigger for the group handover;
else
| Search for the next possible mode
end
if $SourceL_{D_TeNB} > SourceTh_{D_TeNB}$ *and* $TargetL_{D_TeNB} > TargetTh_{D_TeNB}$ *and* $TargetL_{D_ReNB} < TargetTh_{D_ReNB}$ *and* $TargetL_{D2D} \leq TargetTh_{D2D}$ **then**
| Select Relay Mode;
else
| Call Drop;
end

Algorithm 1: Simulation model of mode selection algorithm.

Part III

Validation and Simulation

Chapter 7

A Markovian Approach to the Mobility Management for the D2D Communication

I have already proposed a unique algorithm of mobility management for the D2D communication system in the previous chapter. In this chapter, I highlight and explain the mobility model mathematically and analytically by taking advantage of the Markovian model. Markov model is essentially a simplified approach to describing a system that occupies a discrete state at any point in time. I also make a bridge between my mobility model and the Markovian model.

7.1 D2D and the Markov Chain Model

D2D communication is a promising technology for the next-generation cellular network system like 5G. It will enhance the data rate, coverage and quality of the network along with spectral efficiency. Figure 7.1 illustrates an overall view of D2D communication in a cellular network.

I propose a mobility model for D2D communication in my papers [21, 22], where a D2D user is considered moving in different directions from the eNodeB and another D2D pair. This algorithm proposes the complete handover model to achieve the maximum sum-rate. In those papers, I simulated the proposed model and reached at optimum time for the D2D operation while data sum-rate was satisfactory. In this chapter, I introduce the Markov Chain model to describe the random mobility of D2D users mathematically and analytically. The Markov Chain model is a great choice to represent discrete space. The movement behaviour of D2D users could be described

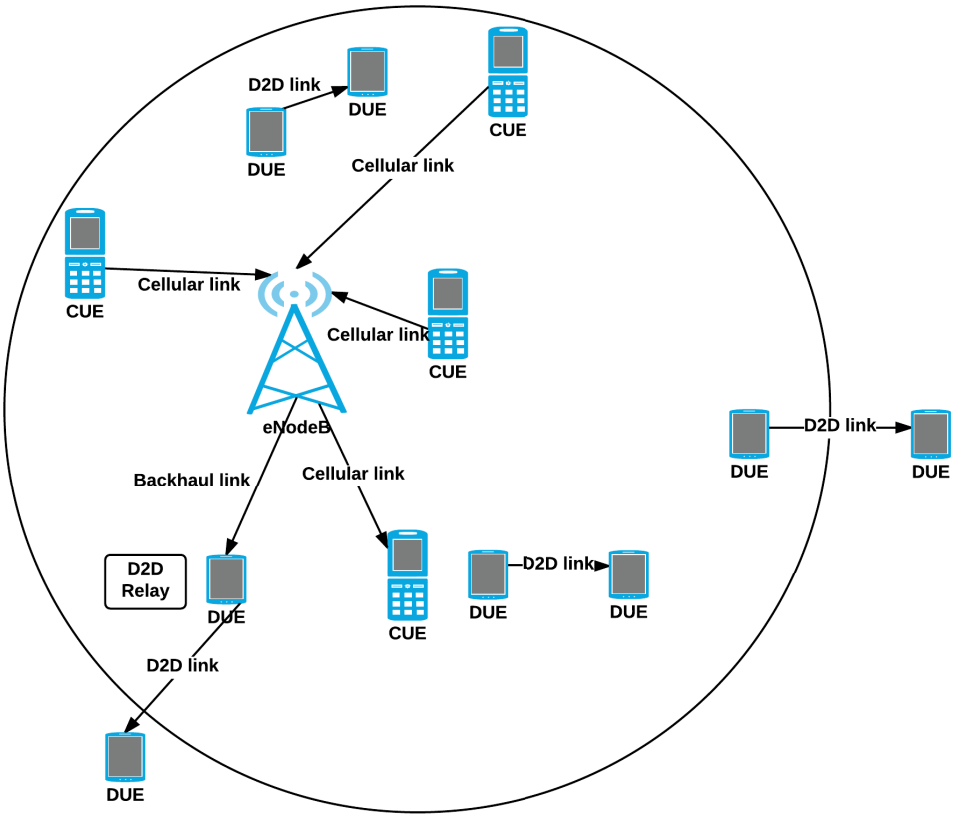

Figure 7.1: A model of D2D communication in a cellular system.

entirely by using the Markov Chain model.

7.2 Markov Chain Analysis on Moving D2D Users

The movement of D2D users is completely unpredictable from the network point of view. Any device from a pair can move in any direction from the other device. Initially, I assume that any device can move towards any direction or remain in the same position.

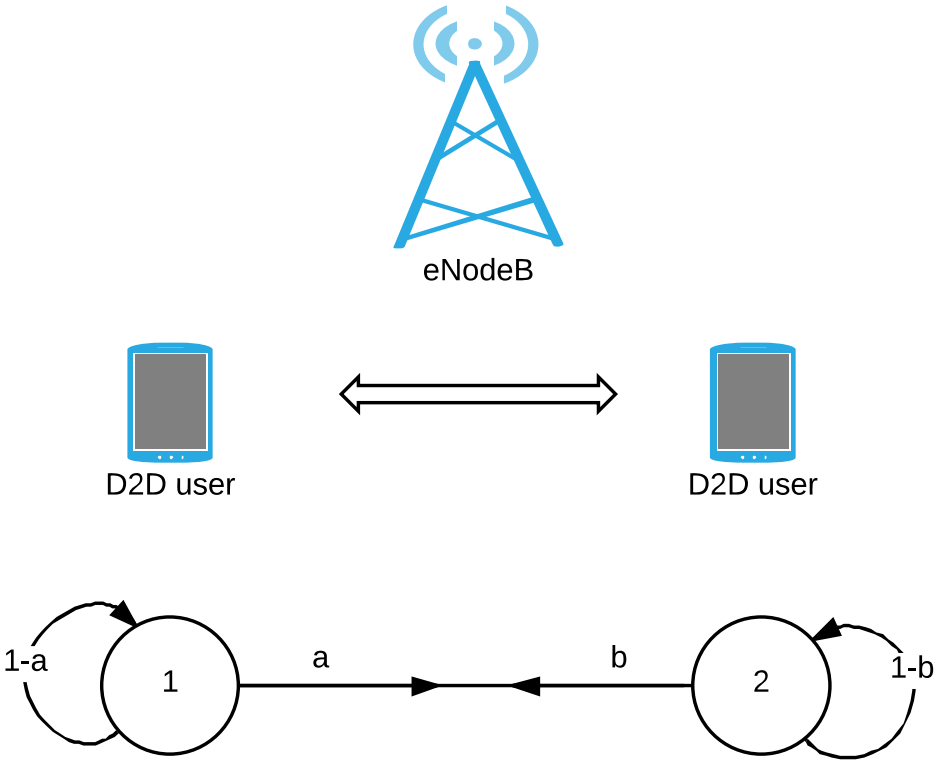

Figure 7.2: Basic Markov state model of D2D communication devices.

I considered a D2D pair located within an area of a cell, as per Figure 7.2. I also considered two different states, numbered 1 and 2. The users can move only between these two states. When a user is located at state 1, the probability of moving from state 1 to 2 is a and the likelihood of it remaining at the same position or state is then $1 - a$. Similarly, another

device from the pair located at position 2 can move towards the position 1 or stay in the same place. The probability of changing the position from 2 to 1 is b and staying at the same location is $1-b$. Referring to the books [128, 129, 130, 131, 132], we can write the transition matrix as:

$$P = \left(\begin{smallmatrix} 1-a & a \\ b & 1-b \end{smallmatrix}\right). \tag{7.1}$$

The eigenvalues of this matrix are 1 and $(1-a-b)$. Then the matrix could be written as:

$$P = U \left(\begin{smallmatrix} 1 & 0 \\ 0 & 1-a-b \end{smallmatrix}\right) U^{-1}. \tag{7.2}$$

For the n number of states, this equation will be

$$P^n = U \left(\begin{smallmatrix} 1 & 0 \\ 0 & (1-a-b)^n \end{smallmatrix}\right) U^{-1}. \tag{7.3}$$

Now, we can write

$$p_{11}^n = A + B(1-a-b)^n \tag{7.4}$$

where p_{11}^n is the first component of the transition matrix P for the n number of states. A and B indicate some values depend on the following equation.

$$A = b/(a+b) \quad \text{and} \quad B = a/(a+b). \tag{7.5}$$

From the equations 7.4 and 7.5,

$$p_{11}^n = P_1(X_n = 1) = \frac{b}{a+b} + \frac{a}{a+b}(1-a-b)^n \tag{7.6}$$

where $(X_n)_{n\geq 0}$ is a Markov Chain. Its initial distribution is λ and transition matrix is P for $i_0, i_1, ..., i_{n+1} \in I$ and all $n \geq 0$. Similarly, we can compute the other components of P^n and finally get transition matrix P for all the states $i \in I$ where i is the state and I is the state space.

$$P^n = \begin{pmatrix} \frac{b}{a+b} + \frac{a}{a+b}(1-a-b)^n & \frac{a}{a+b} - \frac{a}{a+b}(1-a-b)^n \\ \frac{b}{a+b} - \frac{b}{a+b}1-a-b)^n & \frac{a}{a+b} + \frac{b}{a+b}(1-a-b)^n \end{pmatrix}. \tag{7.7}$$

Now, we extend from two positions to seven positions of a D2D user can moves per Figure 7.3. The physical meaning of these seven positions is just the specific position where we measure the receive level signal of a D2D user from the eNodeB. Every state is a possible destination from the previous states as per the moving directions. It is understood that there are much more states possible in the real network. However, to make a model, only

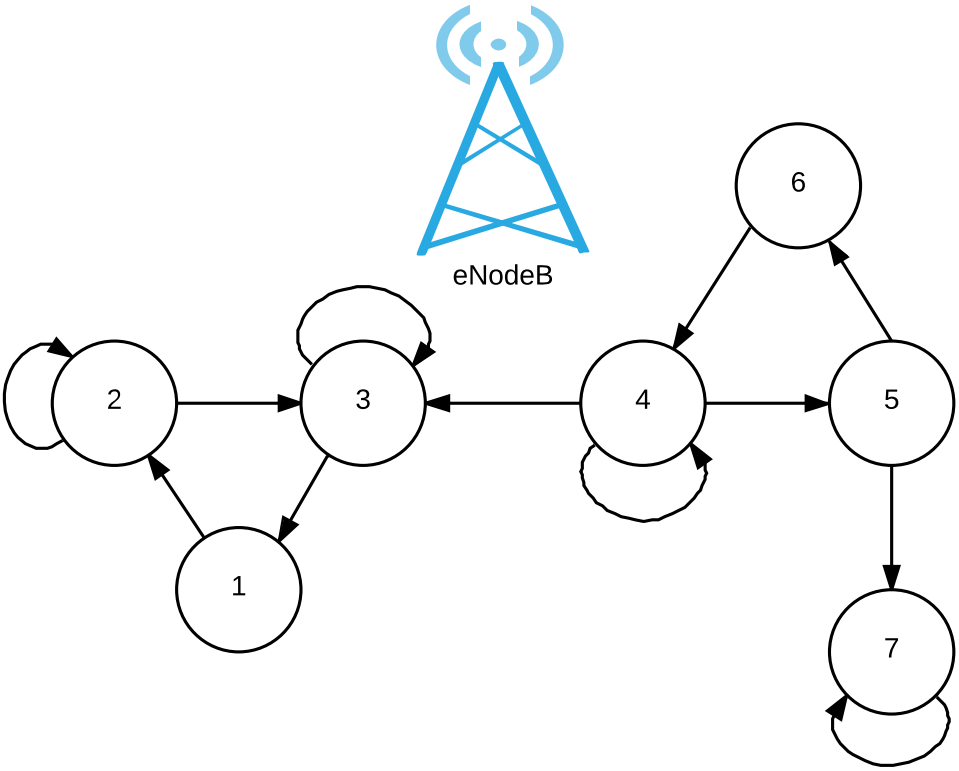

Figure 7.3: Seven position Markov Chain model of D2D communication in a cellular system.

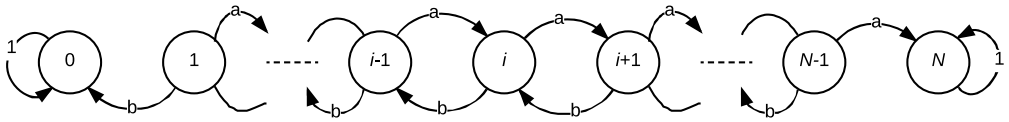

Figure 7.4: N state model.

7 states have been considered. These states may be located within the network coverage area or outside the coverage area where different D2D modes may be operated. To avoid the complexity, we break the model into some smaller positions, each of which is comparatively easy to understand. If i is the initial position and j is the next position to the moving direction where another device is located, we can say that i is leading to j and write $i \to j$ provided the condition is that $P_i(X_n = j \quad \text{for some} \quad n \geq 0) > 0$. If a user communicates with any other users from position i to position j as a part of D2D communication, we write it $i \leftrightarrow j$ if $i \to j$ and $j \to i$ satisfy.

Considering the Markov theorem for the distinct states of i and j, we can write equivalents as $p_{ij}^{(n)} > 0$ for some $n \geq 1$ and $p_{i_0 i_1} p_{i_1 i_2} p_{i_2 i_3} .... p_{i_{n-1} i_n} > 0$ for some states $i_0 i_1 i_2 ... i_n$, where $n \geq 1, i_0 = i$ and $i_n = j$.

We consider another path model as per Figure. 7.4 to calculate the hitting probabilities and estimated mean hitting times. It is an asymmetric random walking model for a D2D user from a location to another location. Here, $0, 1, 2, ..., i-1, i, i+1, ..., N$ are the integers of locations with absorption at 0 and N. We assume that $a + b = 1$.

From the 7.4, let $h_i = P_i(\text{hit } 0)$. Then, $h_0 = 1, h_N = 0$ and $h_i = bh_{i-1} + ah_{i+1}$ for $1 \leq i \leq N-1$. Using the boundary conditions, we get finally,

$$h_i = \frac{(b/a)^i - (b/a)^N}{1 - (b/a)^N}. \tag{7.8}$$

For the symmetric random walk where $a = b$, general solution is $h_i = 1 - 1/N$ and $E_i(\text{Time to hit } \{0, N\}) = i(N-1)$.

Considering Markov Chain $(X_n)_{n \geq 0}$ with transition matrix P, we can calculate hitting time and first passage time on i as

$$H_i = \inf \{n \geq 0 : X_n = i\} \text{ and} \tag{7.9}$$

$$T_i = \inf \{n \geq 1 : X_n = i\}. \tag{7.10}$$

If, $X_0 = i$, H_i and T_i can only differ. Now, we can find the number of visits to i, return probability to i and mean return time to i from the following equations respectively.

$$V_i = \sum_{n=0}^{\infty} 1_{\{X_n=i\}} \tag{7.11}$$

$$f_i = P_i(T_i < \infty) \tag{7.12}$$

$$m_i = E_i(T_i). \tag{7.13}$$

If $P_i(V_i = \infty) = 1$, i is recurrent. It means the device user is keeping come back. And if $P_i(V_i = \infty) = 0$, i is transient. It means user leave forever eventually. For the n-step transition probabilities, we can calculate the equivalence of transience and summability as per the following equations.

$$\sum_{n=0}^{\infty} p_{ii}^{(n)} = \infty \Leftrightarrow f_i = 1 \quad \text{implies that } i \text{ is recurrent,} \tag{7.14}$$

$$\sum_{n=0}^{\infty} p_{ii}^{(n)} < \infty \Leftrightarrow f_i < 1 \quad \text{implies that } i \text{ is transient.} \tag{7.15}$$

7.2.1 Simple Random Walk on One Dimension $\mathbb{Z}$

Consider a random walk model as per Figure 7.5 where $0 < a$, $b < 1$, and $a + b = 1$. Let $h_i = P_i(\text{hit } 0)$ and consider $f_0 = P_0(\text{return to } 0)$.

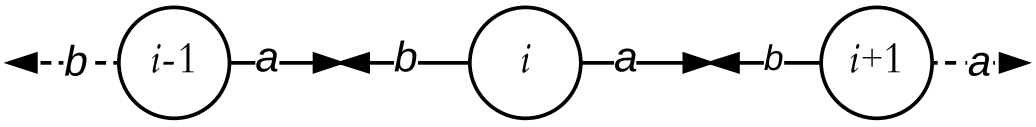

Figure 7.5: Simple random walk model in one dimention.

Using the Markov property $f_1 = b + ah_1^2$, we get

$$f_0 = bh_{-1} + ah_1. \tag{7.16}$$

The smallest solution for h_1 is $\min\{1, b/a\}$. If we consider $a = b = 1/2$, then $h_{-1} = h_1 = 1$ which implies that $f_0 = 1$ and the random walk is recurrent. If $b > a$, then $h_{-1} < 1$ and this is transience. Similarly, if $b < a$, then $h_1 < 1$ that implies $f_0 < 1$ and this implies also transience.

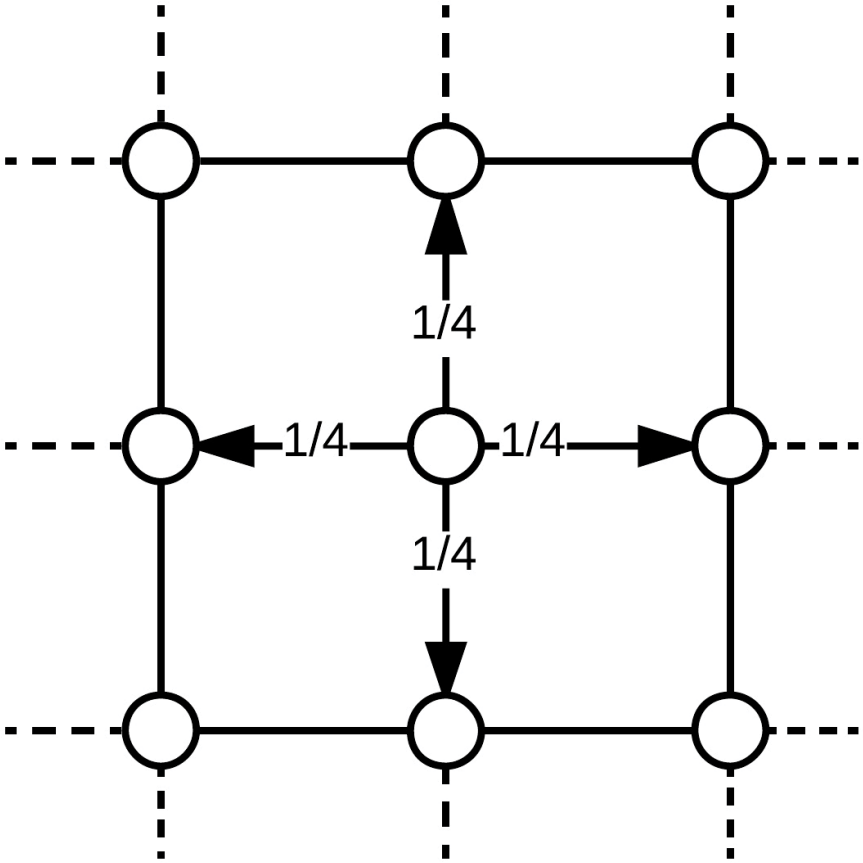

Figure 7.6: Simple random walk model in two dimentions.

7.2.2 Simple Random Walk on Two Dimension $\mathbb{Z}^2$

Using the equation 7.14 and 7.15, we could also analyse the two dimensional $\mathbb{Z}^2$ random walk model as mentioned in Figure 7.6. If we start at 0 position, we cannot come back to the original position after an odd number of steps. Therefore, $p_{00}^{(2n+1)} = 0$ for all n. With the probability of $a^n b^n$, and considering a sequence of steps of length $2n$ from 0, i.e., n steps right and n steps left, we get the equation as

$$p_{00}^{(2n)} = \binom{2n}{n} a^n b^n. \tag{7.17}$$

Using Stirling's approximation,

$$p_{00}^{(2n)} = \frac{(2n)!}{(n!)^2}(ab)^n \sim \frac{(4ab)^n}{A\sqrt{n/2}} \tag{7.18}$$

where $A \in [1, \infty)$ and $n \to \infty$. For the symmetric case, $4ab = 1$ and the equation becomes

$$p_{00}^{(2n)} = \frac{\sqrt{2}}{A\sqrt{n}}. \tag{7.19}$$

So,

$$\sum_{n=N}^{\infty} p_{00}^{(2n)} = \frac{\sqrt{2}}{A} \sum_{n=N}^{\infty} \frac{1}{\sqrt{n}} = \infty \tag{7.20}$$

which can show that the random walk is recurrent. If $a \neq b$, then $4ab = r < 1$, and for some N,

$$\sum_{n=N}^{\infty} p_{00}^{(2n)} \leq \frac{1}{A} \sum_{n=N}^{\infty} n^n < \infty \tag{7.21}$$

and then the random walk is transient.

These equations can help the calculations for the two dimensional simple symmetric random walk on $\mathbb{Z}^2$ as per the Figure 7.6. As this is symmetric, the transition probabilities are as follows.

$$p_{ij} = \begin{cases} 1/4 & \text{if } |i-j| = 1 \\ 0 & \text{otherwise} \end{cases} \tag{7.22}$$

Consider we start at 0. If we call the walk X_n, we can also write independent symmetric random walks X_n^+ and X_n^- for the projection of the walk on the diagonal lines. we can get $X_n = 0$ if and only if $X_n^+ = X_n^- = 0$. Then, if $n \to \infty$, for X_n we can get the equation by Stirling formula

$$p_{00}^{(2n)} = \left(\binom{2n}{n} \left(\frac{1}{2}\right)^{2n} \right)^2 \sim \frac{2}{A^2 n}. \tag{7.23}$$

By comparison with $\sum_{n=0}^{\infty} 1/n$,

$$\sum_{n=0}^{\infty} p_{00}^{(n)} = \infty, \tag{7.24}$$

and the walk is recurrent.

7.2.3 Simple Random Walk on Three Dimension $\mathbb{Z}^3$

Consider the simple three dimensional symmetric random walk model $\mathbb{Z}^3$. In that case, transition probabilities are

$$p_{ij} = \begin{cases} 1/6 & \text{if } |i-j| = 1 \\ 0 & \text{otherwise} \end{cases} \tag{7.25}$$

As the user can move into three different directions with equal probabilities, we can not apply the three independent walks on $\mathbb{Z}$ as we have done above for the two dimensional symmetric random walk model.

We again start at 0. If we want to come back to the starting position, we must complete even number of steps, $2n$. These $2n$ steps must be the combination of i up, i down, j north, j south, k east, k west where $i+j+k=n$ and $i,j,k \geq 0$. We can get the equation by counting the number of ways.

$$p_{00}^{(2n)} = \sum_{\substack{i,j,k\geq 0 \\ i+j+k=n}} \frac{(2n)!}{(i!j!k!)^2} \left(\frac{1}{6}\right)^{2n} \tag{7.26}$$

$$= \binom{2n}{n} \left(\frac{1}{2}\right)^{2n} \sum_{\substack{i,j,k\geq 0 \\ i+j+k=n}} \binom{n}{ijk} \left(\frac{1}{3}\right)^{2n}. \tag{7.27}$$

Here,

$$\sum_{\substack{i,j,k\geq 0 \\ i+j+k=n}} \binom{n}{ijk} \left(\frac{1}{3}\right)^{n} = 1. \tag{7.28}$$

In the case where $n = 3m$, we can calculate for all i,j,k

$$\binom{n}{ijk} = \frac{(n)!}{i!j!k!} \leq \frac{n!}{m!m!m!} = \binom{n}{mmm}. \tag{7.29}$$

As $n \to \infty$, this implies,

$$p_{00}^{(2n)} \leq \binom{2n}{n} \left(\frac{1}{2}\right)^{2n} \binom{n}{mmm} \left(\frac{1}{3}\right)^{n} \sim \frac{1}{2A^3} \left(\frac{6}{n}\right)^{3/2}. \tag{7.30}$$

After the calculation, for all m, we will have

$$\sum_{n=0}^{\infty} p_{00}^{(n)} < \infty, \tag{7.31}$$

and the walk is transient.

Chapter 8

Simulation Setup and Results for the Direction of Arrival

In this chapter, I discuss setting up the MATLAB simulation model to determine the Direction of Arrival. I also analyse the results of the simulation and the effect of changing such parameters as the antenna configuration. A calibration of the receiving antenna array response is needed to experiment correctly with real hardware. However, as I performed it with the MATLAB tool, the calibration process was no longer required although I discuss the calibration system in the first section. Array processing techniques involve some other factors. For example, the properties of the antenna materials that determine the electromagnetic field in the space around them, the dimensions of the antennas and far and near-field effects are essential. I assume the receive antenna array is in the far-field of the transmitters, so the antenna characteristic depends on the distance and RF carrier frequencies are ignored. Further gain offsets and RF carrier phase offsets of the different RF interfaces have to be compensated for explicitly. Other effects, like antenna coupling, were not considered in the experiments. As I used MATLAB as a simulation tool in this dissertation, it is beyond the scope to discuss all of these factors. The results are usually shown either as a plot diagram directly copied from the MATLAB or a table format. The scenarios are measured individually and discussed accordingly.

8.1 Signal Calibration

In reality, estimation accuracy and resolution are severely affected by the errors in the assumed system model or experimental setup. Additive noise in the receiver circuitry also limited the accuracy of the results. For this reason, calibration techniques were used to model these errors and mitigate

them. Under favourable conditions, it is possible to estimate the errors with some of known parameters and auto-calibrating is also possible. Manual calibration is also recommended if the auto-calibration mechanism is not possible. Here, I discuss manual calibration, which is usually done before starting the experiment with real hardware and the result is included in the final estimation. Calibration should be used to correct the array response for errors due to several imperfections. These might be the imbalance between I/Q data, gain or phase errors in the receiving RF circuitry, uncertain sensor locations, etc. For details of calibration techniques, I refer to [133].

A single source as a reference is placed in a position such that it is perfectly perpendicular to the array antenna axis to calibrate the RF interfaces. Under these circumstances, the baseband signals from the different RF interfaces should be identical. However, due to carrier phase offsets and gain offsets at the different RF interfaces, this was not the case in practice. For this reason, the correlation of each interface signal with reference to the first interface should be computed, and the phase and amplitude information used to correct the different interface signals.

If we consider that the signal of antenna l at sample t is $y_l(t)$, then, the calibration factor is computed thus:

$$c_l = \frac{1}{T}\sum_{t=1}^{T} y_1^*(t)y_l(t) \tag{8.1}$$

$$Q_l = c_l/\sqrt{\mid c_1 \mid} \tag{8.2}$$

and the estimated output is

$$\hat{y}_l(t) = y_l(t)/Q_l \tag{8.3}$$

$$\hat{y}_l(t) = y_l(t) * \sqrt{\mid c_1 \mid}/c_l. \tag{8.4}$$

8.2 DOA Estimation Using Common Techniques

I started simulations by first implementing and testing common DOA estimation techniques like Conventional Beamforming, Capon and MUSIC. ESPRIT technique was considered for the 2D beamforming technique to estimate both the delay and direction and two sources and an array consisting of four antennas as sensors. The sources were placed in two

Angle of first source	40° (variable)
Angle of second source	80° (variable)
Angle of third source	120° (variable)
Signal transmitted by first source	Complex exponential
Signal transmitted by second source	Complex exponential
Signal transmitted by third source	Complex exponential
Frequency for first sources	2 MHz (variable)
Frequency for second sources	3 MHz (variable)
Frequency for second sources	4 MHz (variable)
Sampling frequency	40 MHz
Number of sensors	4
Angel resolution for plotting	0.1
Number of sample	1000
RF carrier wavelength	12.34cm
RF carrier frequency	2.432GHz

Table 8.1: Simulation setup for DOA estimation using two/three sources and four sensors.

different directions which could be changed randomly. Near-field effects were not considered. Table 8.1 shows the specifications of the investigated simulation, as source signals were complex exponential signals with their frequencies given in the same table.

I considered three different sources as the mobile devices located in different directions and elevations. For convenience, firstly, I simulated the two sources and then added another source to become more practical. Variable frequencies were considered for different sources, and they were sampled with a 40MHz sampling frequency. The total number of sensors that could be used in a base station were four, and I considered 4x1 MIMO technology in this regard. It is to be noted that the more antenna we could use as sensors, the better the performance we could get in relation to the direction of arrival. The RF carrier frequency was 2.432GHz. The total number of sample and resolution of plotting were 1000 and 0.1 respectively.

The results for my realisation with Conventional, Capon, and MUSIC techniques are stated in Figures 8.1, 8.2, and 8.3 for the two and three sources located in different directions. Here, using ESPRIT, the DOA estimates in simulation realisation were 90.54° and 105.26° for two sources located exactly at 90° and 105° respectively. It is to be noted that the

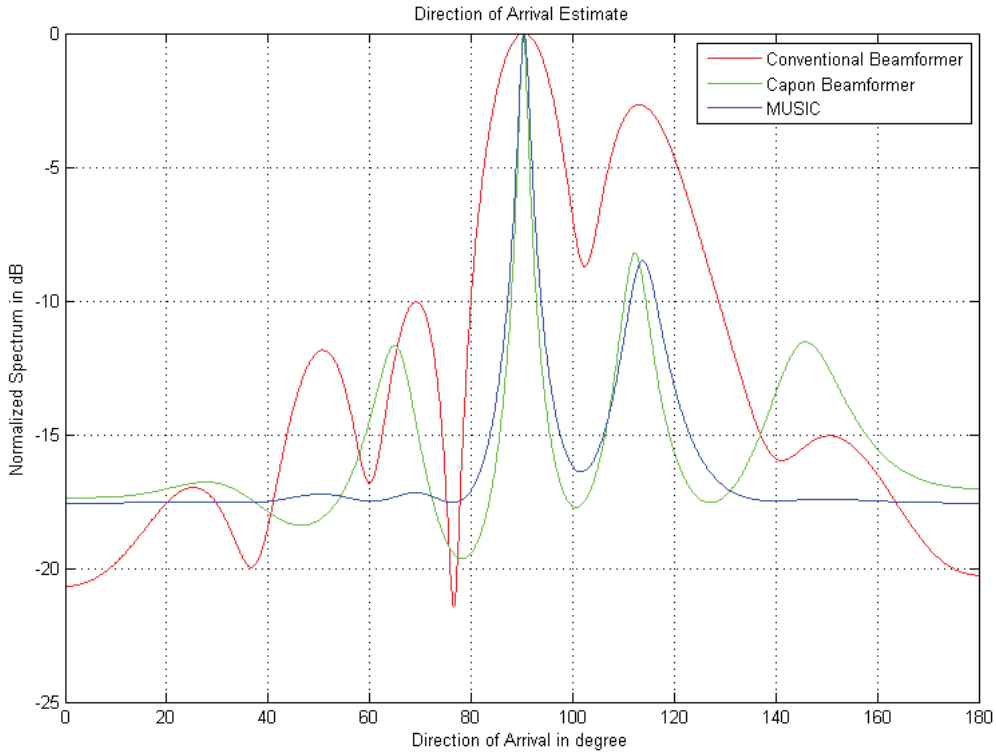

Figure 8.1: Simulation of DOA estimation using Conventional, Capon, and MUSIC techniques for two sources at angles of 90° and 115°.

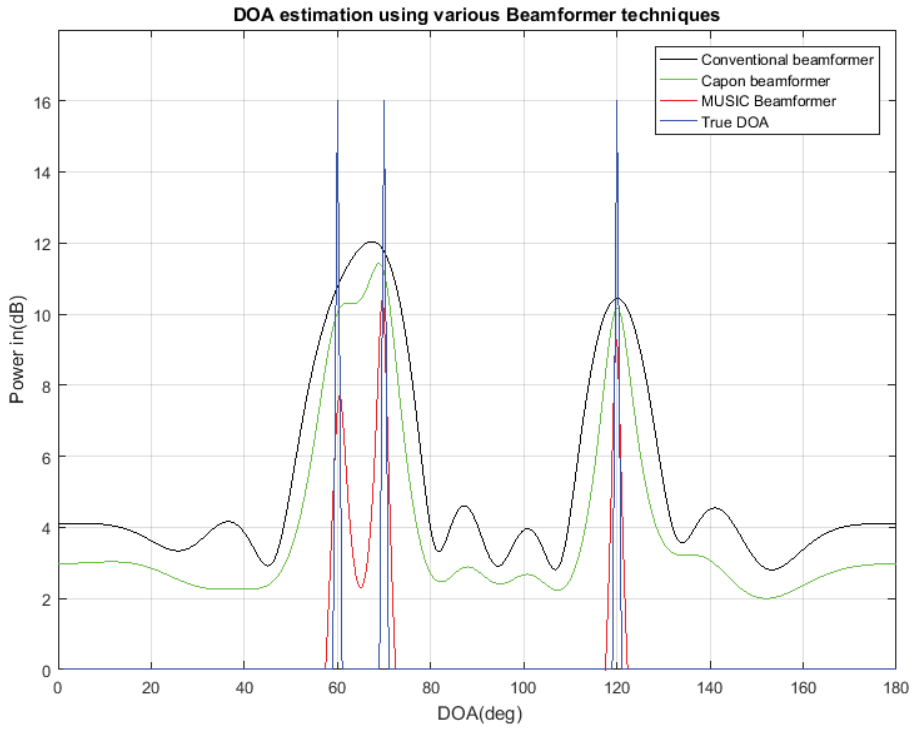

Figure 8.2: Simulation of DOA estimation using Conventional, Capon, and MUSIC techniques for three sources at angles of 60°, 70° and 120°.

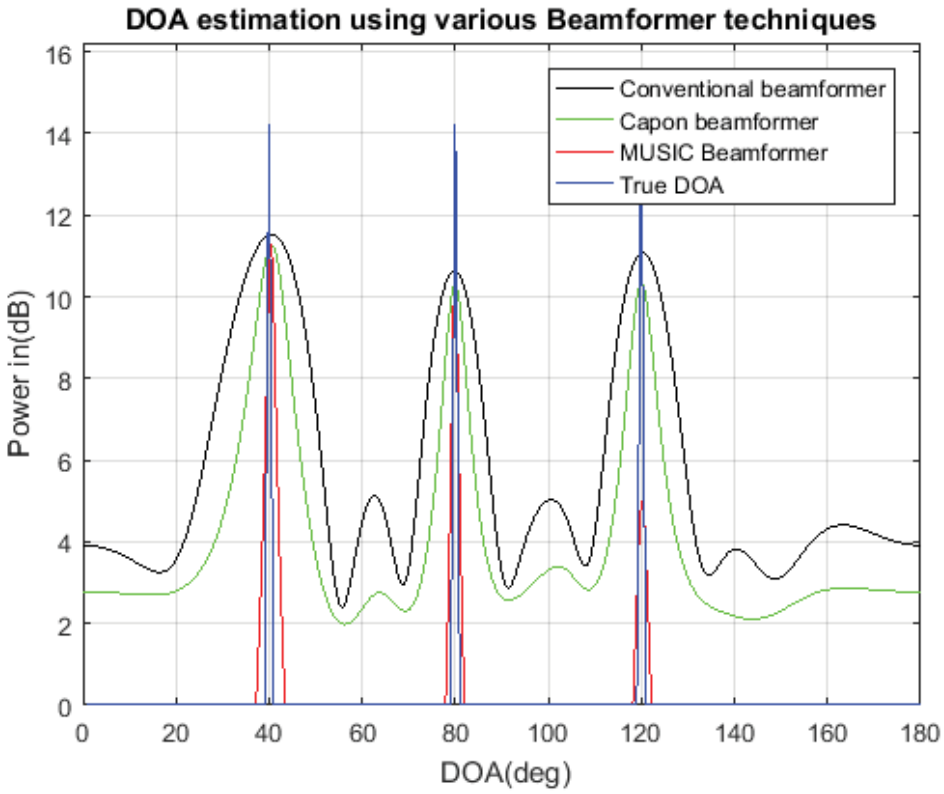

Figure 8.3: Simulation of DOA estimation using Conventional, Capon and MUSIC techniques for three sources at angles of 40°, 80°, and 120°.

simulation result of ESPRIT could not be plotted as it is not a search based technique. The simulation shows that the ESPRIT technique performance is outstanding to get direction pretty close to reality.

It is possible that the peaks for the Capon beamformer are even more accurate than the Conventional beamformer. It was also observed that MUSIC performed the best among Conventional, Capon, and MUSIC in terms of side lobe and sharp peak. However, Conventional Beamformer suffered from poor resolution compared with others since its main lobe was not sharp enough.

Figure 8.2 shows that for a close angle distance, e.g., 60° and 70°, the Conventional beamformer technique could not determine the direction correctly. The Capon beamformer can still determine but not accurately. However, the MUSIC could estimate the direction quite accurately, and a sharp peak was observed compared the other two techniques. However, Figure 8.3 indicates that when angle differences are quite significant, e.g., 40°, 80°, and 120° all techniques can perform well, although MUSIC and ESPRIT are the most recommended.

8.3 DOA Estimation Using Estimated Channel

In this simulation, I applied the channel estimation technique described in Section A.8.1 to estimate delay and direction. To allow an array consisting of eight receiving antennas, I followed the theory as described in Chapter 5. Here, I used unitary 2D ESPRIT technique (see Appendix B) to estimate the DOAs.

Considering the MIMO scenario, I could formulate the channel equation as

$$\mathbf{x} = \mathbf{H}\mathbf{s} + \mathbf{n} \tag{8.5}$$

where $\mathbf{H}$ is the channel matrix, $\mathbf{x}$ and $\mathbf{s}$ are the received and transmitted vectors, respectively, and $\mathbf{n}$ is the noise signal, which is considered negligible. Channel could be estimated as

$$\left[\hat{\mathbf{H}}\right]_{i,i} = \frac{y_i}{x_i} \tag{8.6}$$

where x and y are the received and transmitted signal respectively for the ith time.

Number of sources	1
Number of multipath considered	2
Number of sensors	8
Antenna positions	Different angels from sensors
Reference signals	DMRS
Bandwidth	20 MHz
Number of resource blocks	100
Subcarrier spacing	15 KHz
FFT size	2048 Samples
CP type	Normal
Sampling frequency	30.72MHz
Number of subcarriers	1200

Table 8.2: Experimental setup for estimating channel.

True angles (Degree)	**Estimated angles (Degree)**	**True delay (s)**	**Estimated delay(s)**
90, 110	89.91, 110.66	3.75×10^{-7}	3.70×10^{-7}
90, 130	90.11, 131.99	3.75×10^{-7}	3.65×10^{-7}
65, 125	66.16, 126.98	3.75×10^{-7}	3.19×10^{-7}
110, 125	109.64, 124.49	3.75×10^{-7}	3.47×10^{-7}
60, 100	58.23, 98.89	3.75×10^{-7}	3.31×10^{-7}
30, 70	31.51, 72.36	3.75×10^{-7}	3.55×10^{-7}

Table 8.3: Experimental results for true and estimated DOA and delays.

I considered two paths from the transmitter to the receiver. I modelled multipath environment with two paths by transmitting the same source signal via two transmitters, while the signal at the second transmitter was delayed by a small period. Furthermore, I placed the transmitters in different angular directions to model different DOAs for the two paths. I also used eight receiving antennas in the sensor array. LTE standard Zadoff-Chu sequences were considered for the transmission. The basic parameter setup is depicted in Table 8.2. Table 8.3 shows the simulation results of several different experimental setups.

The result shows that the delays for the different angles, which were very close to the actual delays, were entirely satisfactory. For example, for the angle of 90° and 110°, the estimated directions of arrival were 89.91° and 110.66°, and the delays were estimated as 3.70×10^{-7} for the actual delay

of 3.75×10^{-7}. The simulation for the other directions are also listed in Table 8.3.

8.3.1 Histogram Analysis of the DOA and Delays

I computed the simulation result for 1000 iterations and Figures 8.4, 8.5 and Figures 8.6, 8.7 show the different histogram (number of occurrences) for the different DOAs and delays, respectively. I compared the delays with known values that we set manually.

It can be observed from Figure 8.4 that we have two peaks at the angles 89.42° and 121.8°, i.e., maximum occurring angles for the true angles 90° and 120°, respectively. The percentage of error was approximately one for both cases. The same was true for Figure 8.5. We can also observe from the Figure 8.6 and 8.7 that the estimated path delays were always lower than the true delays and varied significantly if we varied the time sample and delay manually.

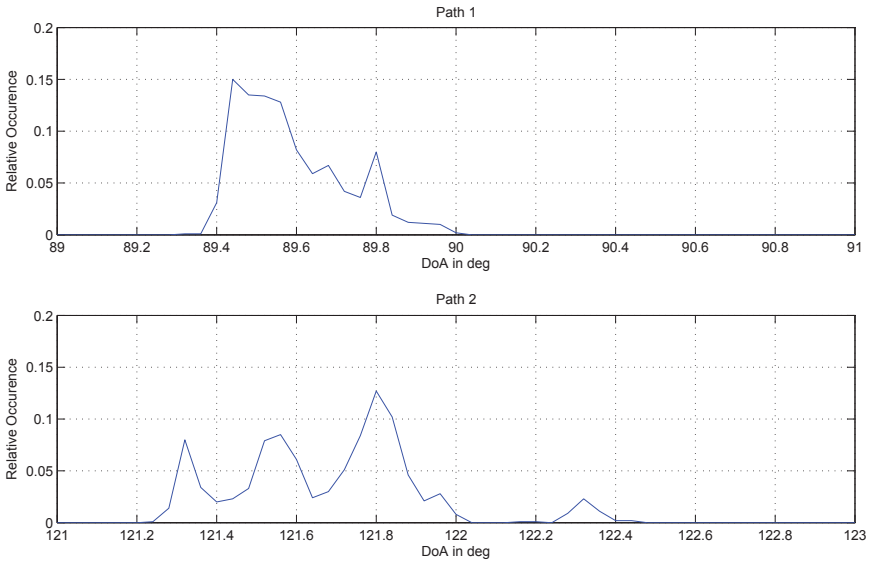

Figure 8.4: Histogram for the estimation angles of 90° and 120°.

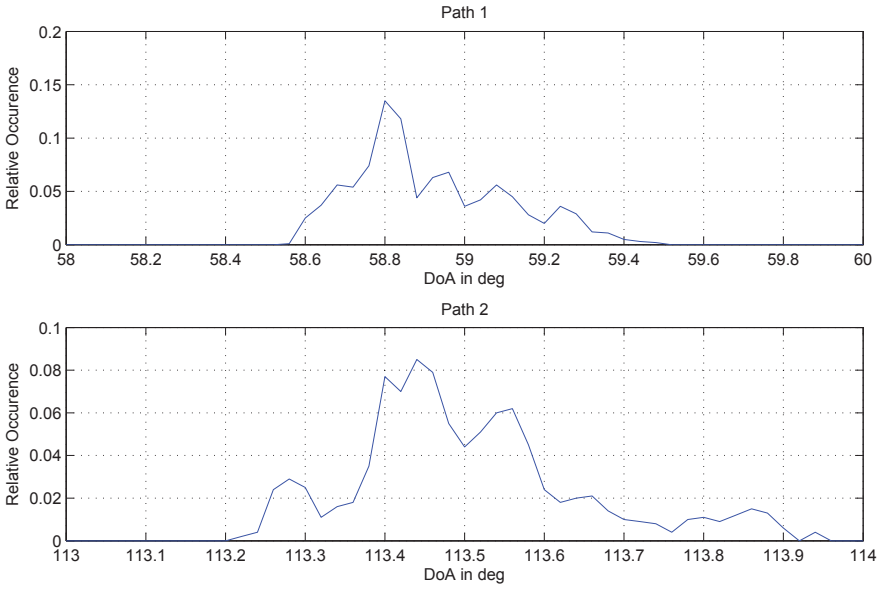

Figure 8.5: Histogram for the estimation angles of 58° and 113°.

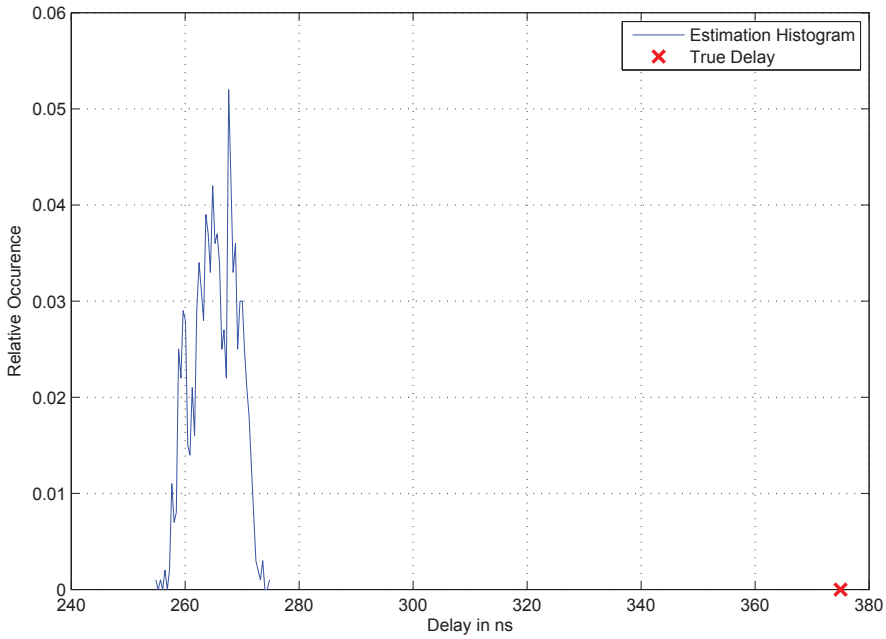

Figure 8.6: Histogram for the experimental delay and true delay for 15 time samples.

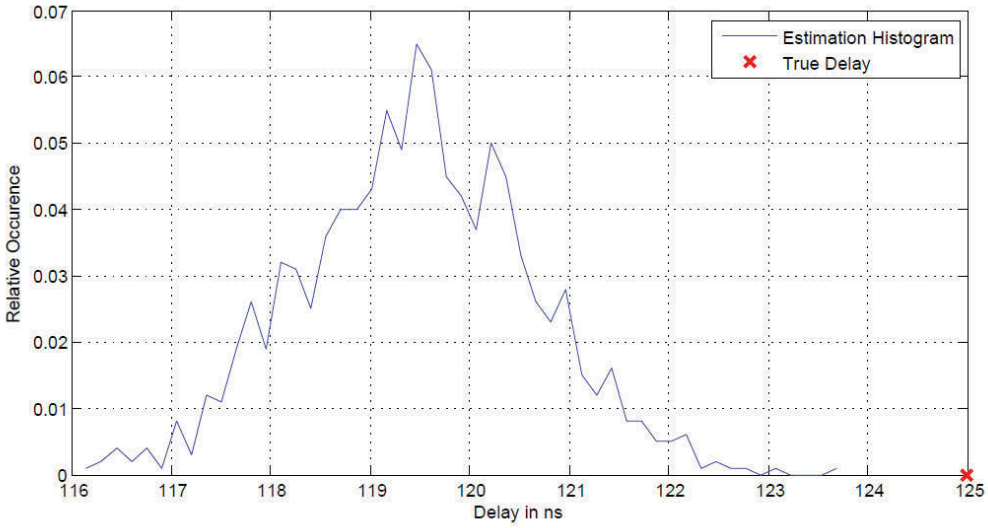

Figure 8.7: Histogram for the experimental delay and true delay for five time samples.

Chapter 9

Simulation Setup and Results for the Mobility Management

In this chapter, I discuss setting up the MATLAB simulation model for the mobility management of D2D communications. I analyse the results of the simulation. This chapter also mentions some relevant equations that contain the essential parameters. The detailed theory was discussed in Chapter 6. Firstly, I set up an animation model in MATLAB to have a better understanding of the mobility, and then I simulated the probable mode selection based on the distances and directions among the cellular device, the D2D devices, the source base station and the target base station. The mode selection is one of the most critical tasks for the base station.

9.1 Simulation Parameters and Results

In Chapter 6, four possible moving directions has been proposed. Although, only one direction has been considered for the mathematical model, as per Figure 6.7, for simulaiton, all possible directions have been considered. Based on the power allocation as stated in [21], I simulated the possible handover attempts done by the mobile station, as only the theory of the D2D-aware handover solution had been investigated.

It is also considered that none of the devices was out of the network area at the beginning and if a device moves towards an out-of-network coverage area but still in proximity to another D2D pair, it may act as a relay.

In order to select the best mode, as per Section 6.3.1, five possible operational conditions has been proposed that could have occurred. These were the Cellular mode, D2D mode, Relay mode, Waiting mode and Drop

mode. The algorithm for the proposed simulation model to select the best operational mode is depicted in Figure 6.9 and Algorithm 1.

For the high signal-to-noise ratio (SNR) and full load, I applied the following equation [134]:

$$\text{RSRP (dBm)} = \text{RSSI (dBm)} - 10 * log_{10}(12 * N). \tag{9.1}$$

Here, RSRP is the Reference Signal Receive Power and RSSI indicates Received Signal Strength Indicator, which can be calculated by the equation:

$$\text{RSSI} = \text{wideband power} = \text{noise} + \text{serving cell power} + \text{interference power} \tag{9.2}$$

Reference Signal Received Quality (RSRQ) is determined by the following equation:

$$\text{RSRQ} = N * \frac{\text{RSRP}}{\text{RSSI}}, \tag{9.3}$$

where N is the number of Physical Resource Blocks (PRBs).

Total path loss is calculated according to paper [15].

$$\text{Pathloss(PL)} = \alpha.PL_{LOS} + (1 - \alpha).PL_{NLOS}, \tag{9.4}$$

where, α is the average ratio of D2D users in Line of Sight (LOS) and non line of sight (NLOS) regions. PL_{LOS} and PL_{NLOS} are the path loss for the line of sight and non line of sight distance respectively and calculated by

$$PL_{LOS/NLOS} = K_1 + K_2.\log_{10}.d. \tag{9.5}$$

Here, K_1 and K_2 are the path loss coefficients and calculated from the receiving and transmitting antennas and frequency used. The pair K_1 and K_2 are different for LOS and NLOS paths. d is the distance between the D2D users.

Total calculated shadowing loss is as follows:

$$L(r) = R(\Delta r).L(r - \Delta r) + \sqrt{1 - (R(\Delta r))^2}.\sigma.X, \tag{9.6}$$

where X is a Gaussian random variable with unit variance and zero-mean. σ is standard deviation. The calculation of $R(\Delta r)$ is referred to paper [15] which depends on the decorrelation distance of shadow fading and distance between the locations.

According to [15], multi-path fading is calculated by the equation:

$$ML = 10\log_{10}(-\log_{10}Y), \tag{9.7}$$

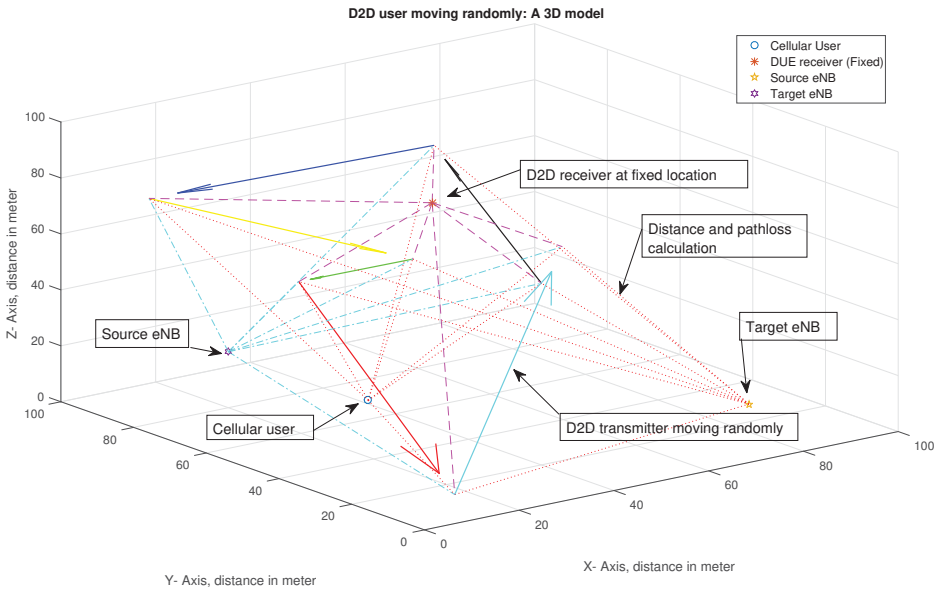

Figure 9.1: MATLAB animation of proposed model

where, Y is a random variable with uniform distribution.

I have designed a MATLAB(R2016a) simulation model based on the proposed algorithm with the help of LTE System Toolbox. In some cases, I also use Simulink. Figure 9.1 shows the MATLAB model where random moving directions are observed as an animation. In this figure, I consider a D2D pair and a cellular user. One of the D2D users who mainly transmits is moving randomly. I set two base stations within the area and they are placed at different heights. This figure also demonstrates the location of the different users and base stations. The arrow indicates the moving location and direction from one to another place. Other lines depict the distances and directions from the origin point to other users and base stations. The path loss is measured based on the distances.

The parameters used for the simulations are in Table 9.1. In most of the cases, I considered standard LTE parameters. Other parameters like resource and D2D types, SINR, different types of transmitting power, handover threshold, resource blocks and constant settings are listed in the same table.

Figure 9.2 shows the simulations results, and it indicates clearly the superiority of the D2D mode, which is the primary target of our model. The next available mode is the cellular mode that should take place when

it doesn't satisfy the requirements of the D2D mode. The relay mode comes next and in the simulation result it is followed by the call waiting mode, which is when the base station waits for a while to observe the motive of the users. If the users do not satisfy any condition to keep the connection active, it drops the connection or call; this was around three percent according to the simulation results.

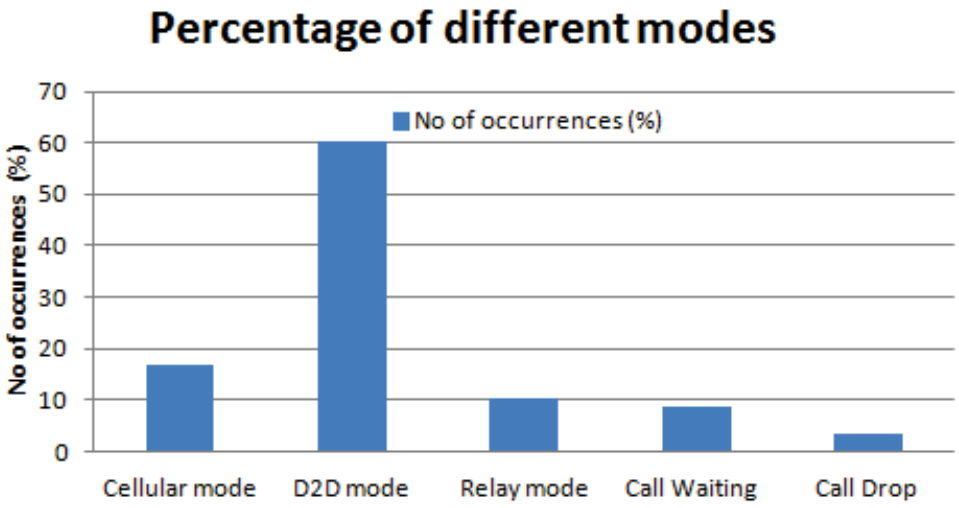

Figure 9.2: Plot for the occurrences (percentage)

Figure 9.3 shows the sum-rate trend while handover is taking place. It shows that handover takes place without any major degradation of data throughput. When the distance from the source base station increases, the data sum-rate decreases slightly. However, it rises again as soon as the target base station becomes closer after the handover is triggered. During the handover, a degradation of the sum-rate observed has almost no or little effect on the overall sum-rate.

Figure 9.4 shows the trend of path loss over distance. It shows that path loss increases when the D2D transmitter is moving further away from the source base station. The handover threshold point is also mentioned there. This threshold is a variable parameter. It should be set based on the requirements of network quality and performance.

Table 9.1: Simulation parameters.

Simulation Parameters	**Values**
Duplexing	TDD
Walking model	Random
Total loss	path loss + shadow fading + multi-path [15]
Cellular User's location	[15 35 25]
D2D User's location	[40 50 60]
Source Base station's location	(80, 15, 10)
Target Base station's location	(20, 80, 20)
Carrier Frequency	2 GHz
Handover Threshold	114dBm
Handover trigger	D2D aware
Handover type	Group handover
Resource used	Uplink
Types of D2D	Underlay Inband
Temperature	290K
SINR	-20dB
Maximum UE transmit power	21 dBm
Transmit power or eNodeB	39 dBm
Network Layout	2 Sites and no grid maintained
Total number CUEs per cell	1
K_1	17.5 dB (NLOS) and 38.8dB (LOS)
K_2	43.3 dB (NLOS) and 16.9dB (LOS)
Total number DUEs pair per cell	2
σ	3dB (LOS and NLOS)
MATLAB version	2016a
Number of resource blocks	100 resource block/20KHz (Full)
Total simulation performed	500

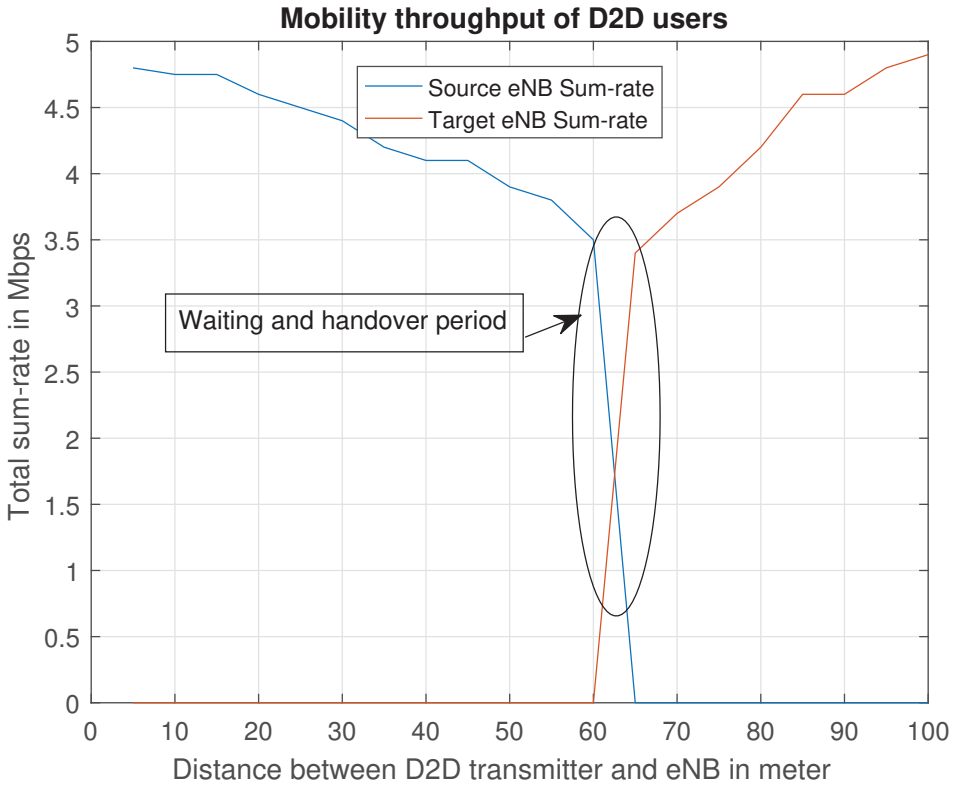

Figure 9.3: Mobility throughput of D2D users

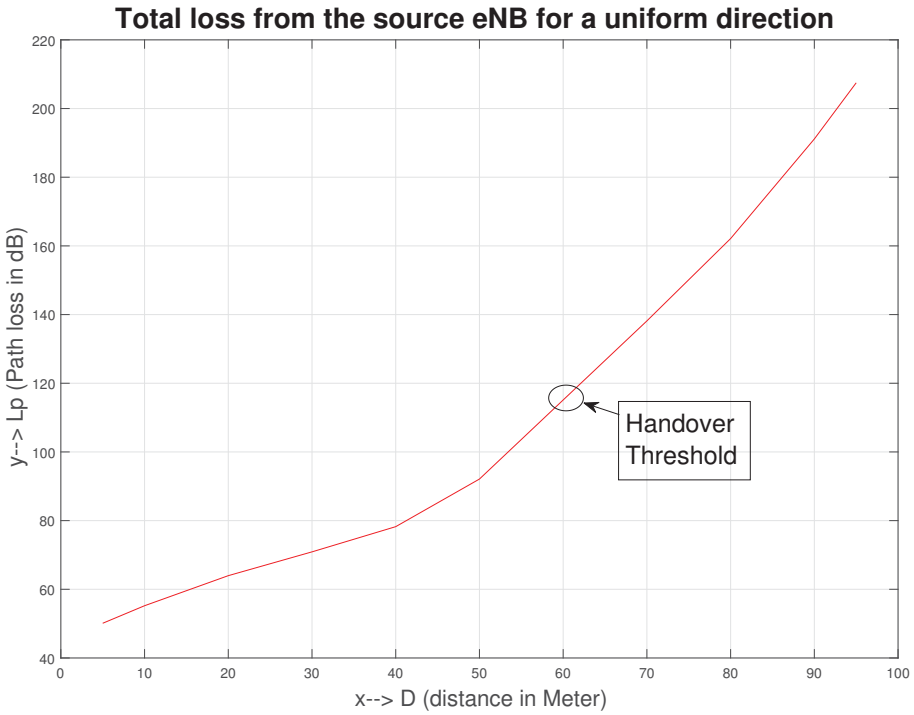

Figure 9.4: Plot for path loss

Chapter 10

Simulation Setup and Results for the Markov Chain Model

In this chapter, a simulation model for the Markov Chain is demonstrated. I have analysed the Markov chain model in Chapter 7, and I analytically make this model for the device-to-device communications of the next generation mobile cellular network. I design some simulation models that reflect different random or planned walking models. I discuss setting up the MATLAB model to simulate the Markov Chain Model for D2D users. The outcomes of the simulation and the effect of changing location are also discussed in this chapter.

10.1 Simulation Parameters and Results

For the simulations, firstly, I assumed a simple Markov chain with two states. I considered the total number of steps to be 50. The speed of the movement was not considered. Consider $a = 0.8$ and $b = 0.7$ from Figure 7.2 and Equation 7.1. The simulation result of the chain was plotted in Figure 10.1 where the total number of state 1 found was 21 and state 2 was 29 for the 50 steps with an initial state of 1.

10.1.1 Case 1

Next, I considered a six stages Markov chain model at different locations within the base station. Figure 10.2 depicts the model. I computed the eigendecomposition and derived the symbolic stationary distribution of a trivial Markov Chain. As the number of transitions or steps increase, the stationary distribution represents the time-independent, limiting, distribu-

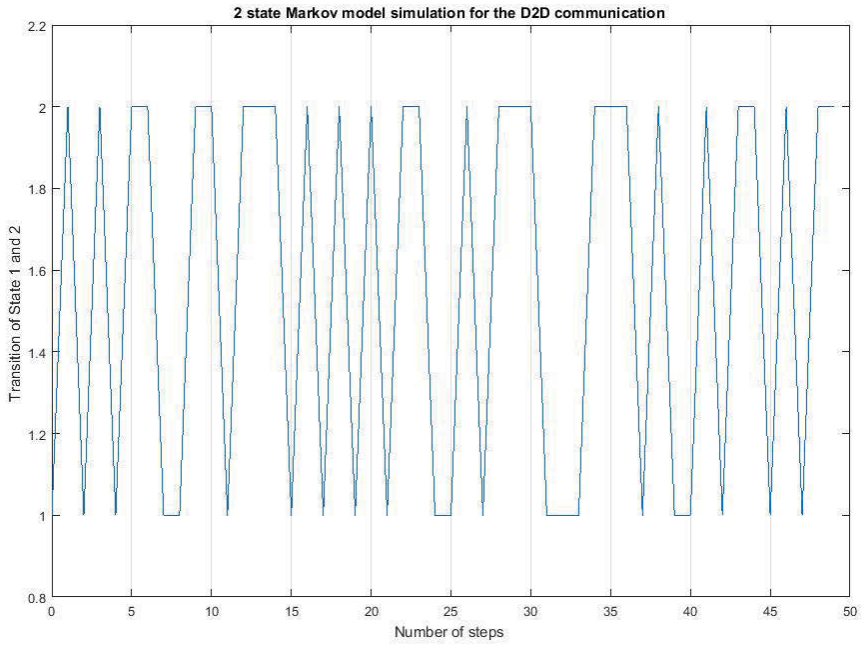

Figure 10.1: Simulation results of the 2 state Markov Chain model.

tion of the states for a Markov process. After calculating the transition matrix, I computed all possible analytical stationary distributions for the states. While extracting eigenvectors with corresponding eigenvalues that could be equal to one for some values of the transition probabilities, this sometimes created a problem, and the simulation stopped with an error message. It was because of some ambiguity in determining this condition for any eigenvalue. In this way, we must be sure that it is reliable when the step is successful.

Figure 10.3 shows the MATLAB simulation output of transition matrix P, the analytical eigenvectors V and the probability matrix. The probability of the steady state being A or B in the first eigenvector case is a function of the transition probabilities a and b, and they are clearly zero. The probability of the steady state being C is a function of the transition probabilities d, and this is clearly one. The probability of the steady state being D is also is a function of c of the transition probabilities, and it is again zero. The probability of the steady state being E or F in the first eigenvector case is a function of the transition probabilities e and f. Figure 10.4 shows the simulation result of the probability of states E and F.

It is seen from the stationary distribution probability that the first, second,

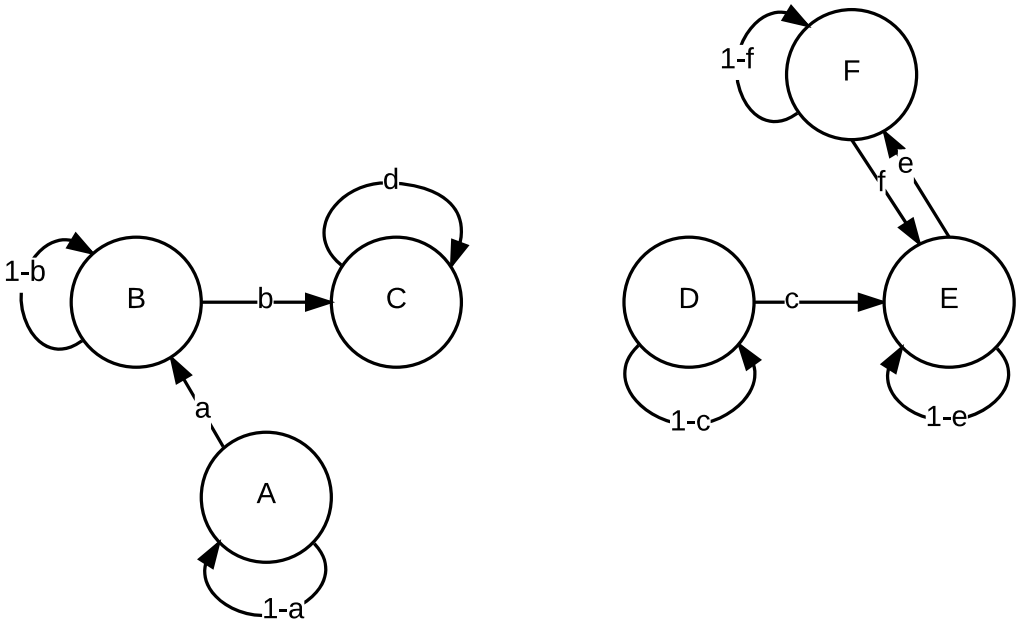

Figure 10.2: Simulation setup for the 6 state Markov Chain model (Case 1).

and fourth rows are entirely zero. Therefore, states A, B and D are never reached and are therefore transient. The rest of the groups (C) and (E, F) do not communicate to each other, and they are recurrent.

```
P =

[ 1 - a,     a, 0,     0,     0,     0]
[     0, 1 - b, b,     0,     0,     0]
[     0,     0, d,     0,     0,     0]
[     0,     0, 0, 1 - c,     c,     0]
[     0,     0, 0,     0, 1 - f,     f]
[     0,     0, 0,     0,     e, 1 - e]

V =

[   0, 0, ((a - b)*(a + d - 1))/(a*b),              0,              0,  0]
[   0, 0,              -(a + d - 1)/b, -(b + d - 1)/b,              0,  0]
[   0, 1,                           1,              1,              0,  0]
[   0, 0,                           0,              0, -(e - c + f)/f,  0]
[ e/f, 0,                           0,              0,     -(c - e)/f, -1]
[   1, 0,                           0,              0,              1,  1]

Probability =

[                   0, 0]
[                   0, 0]
[                   0, 1]
[                   0, 0]
[ e/(e^2 + f^2)^(1/2), 0]
[ f/(e^2 + f^2)^(1/2), 0]
```

Figure 10.3: MATLAB simulation output of transition matrix P, analytical eigenvectors V and Probability matrix for Case 1.

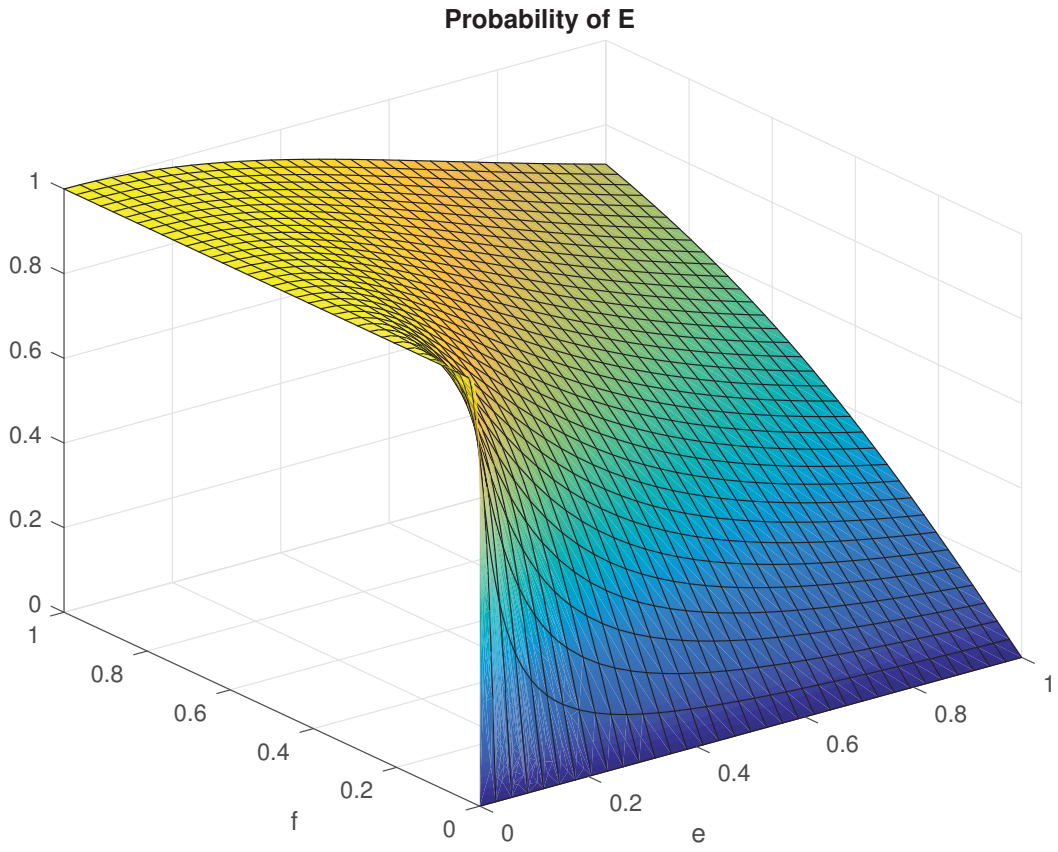

Figure 10.4: Probability of each step.

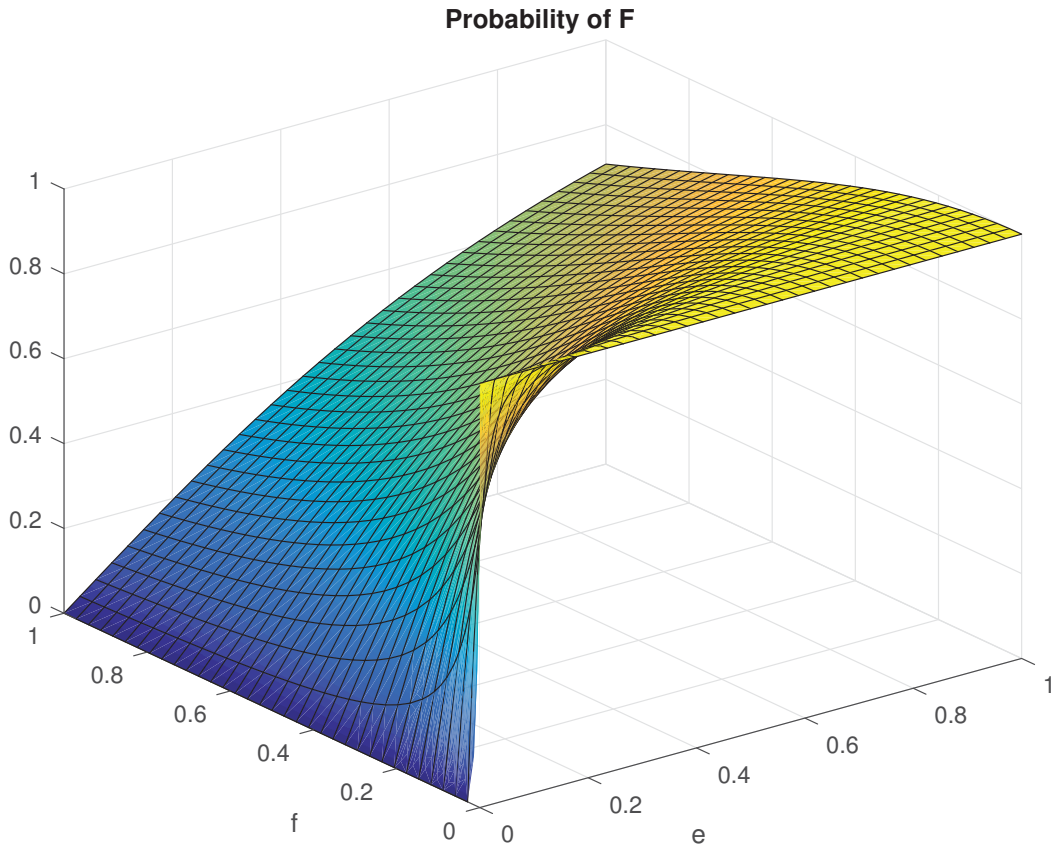

Figure 10.5: Probability of each step.

10.1.2 Case 2

I considered different types of steps for the simulation of the second case. Figure 10.6 shows the model. Here, the steps start from A but once state C is reached, it never comes back to location A. Figure 10.7 shows the MATLAB simulation output of transition matrix P, the analytical eigenvectors V and the probability matrix. It is clear from the probability matrix that state A and state E are never reached and therefore transient, i.e., the first and fifth rows are entirely zero. The rest of the states form two groups (B, C) and (D, F) that are recurrent and do not communicate with each other. Figures 10.8 to 10.13 show the simulation plot of the probability where Figures 10.8 and 10.12 depict that they are transient and never reached.

A couple of cases have been considered where moving directions are different from each other. However, from the simulation results, we can see that not all of the states were recurrent. If a state is recurrent, it has impact behaviour of the mobile users and apparently, eNodeB can predict the user behaviour beforehand using Markov Chain model.

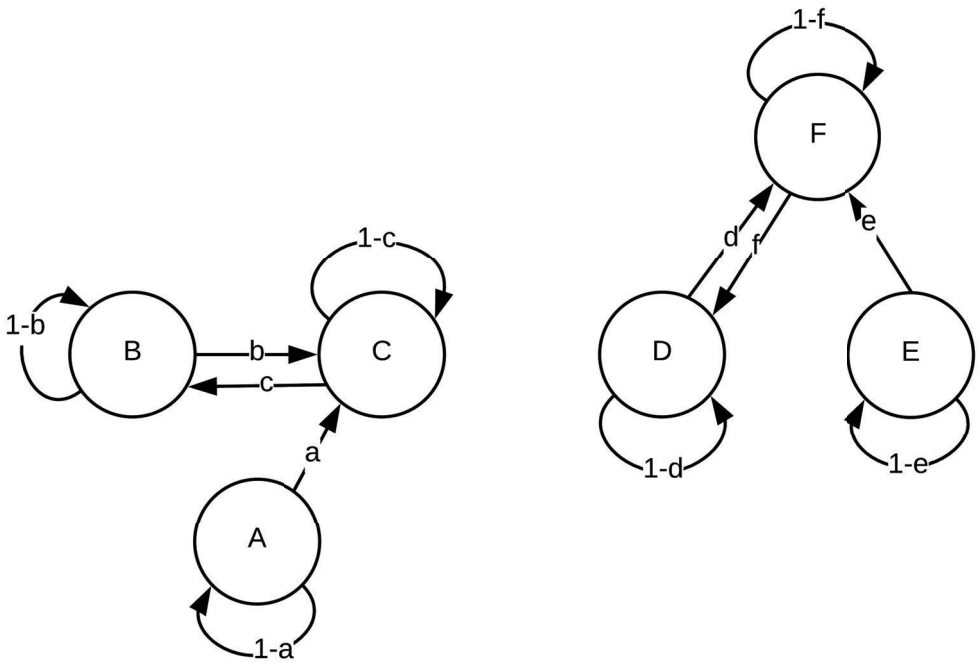

Figure 10.6: Simulation setup for the 6 state Markov Chain model (Case 2).

```
P =

[ 1 - a,     0,     a,     0,     0,     0]
[     0, 1 - b,     b,     0,     0,     0]
[     0,     c, 1 - c,     0,     0,     0]
[     0,     0,     0, 1 - d,     0,     d]
[     0,     0,     0,     0, 1 - e,     e]
[     0,     0,     0,     f,     0, 1 - f]

V =

[   0,   0, (b - a + c)/(a - b),                    0,  0,  0]
[ c/b,   0,          -c/(a - b),                    0, -1,  0]
[   1,   0,                   1,                    0,  1,  0]
[   0, f/d,                   0,           f/(d - e),  0, -1]
[   0,   0,                   0, -(d - e + f)/(d - e),  0,  0]
[   0,   1,                   0,                    1,  0,  1]

Probability =

[                   0,                   0]
[ c/(b^2 + c^2)^(1/2),                   0]
[ b/(b^2 + c^2)^(1/2),                   0]
[                   0, f/(d^2 + f^2)^(1/2)]
[                   0,                   0]
[                   0, d/(d^2 + f^2)^(1/2)]
```

Figure 10.7: MATLAB simulation output of transition matrix P, analytical eigenvectors V and Probability matrix for Case 2 .

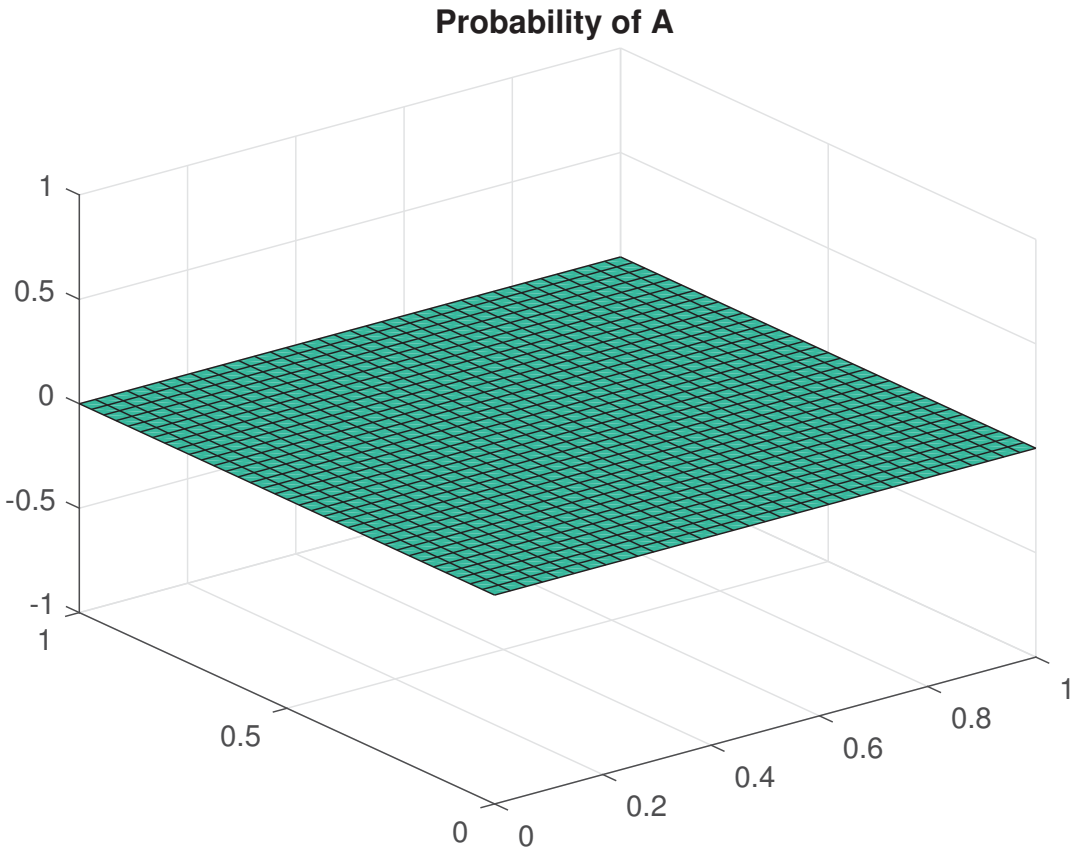

Figure 10.8: Probability of step A.

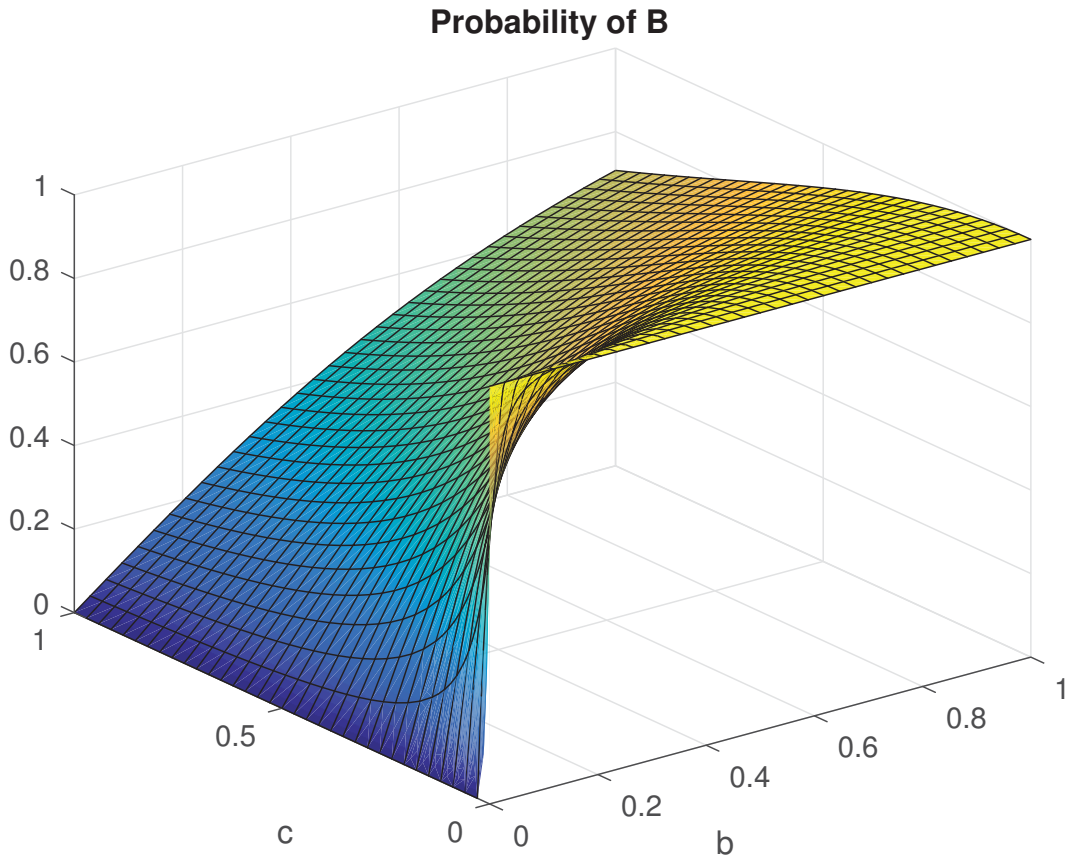

Figure 10.9: Probability of step B.

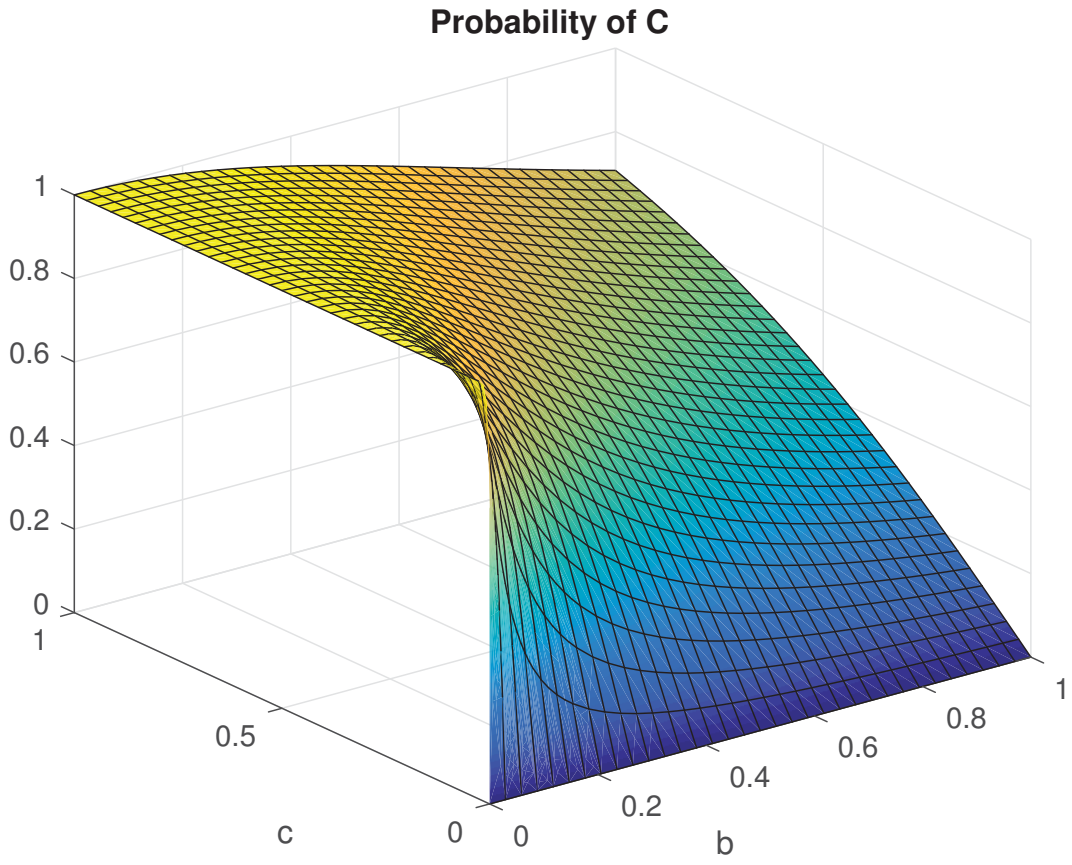

Figure 10.10: Probability of step C.

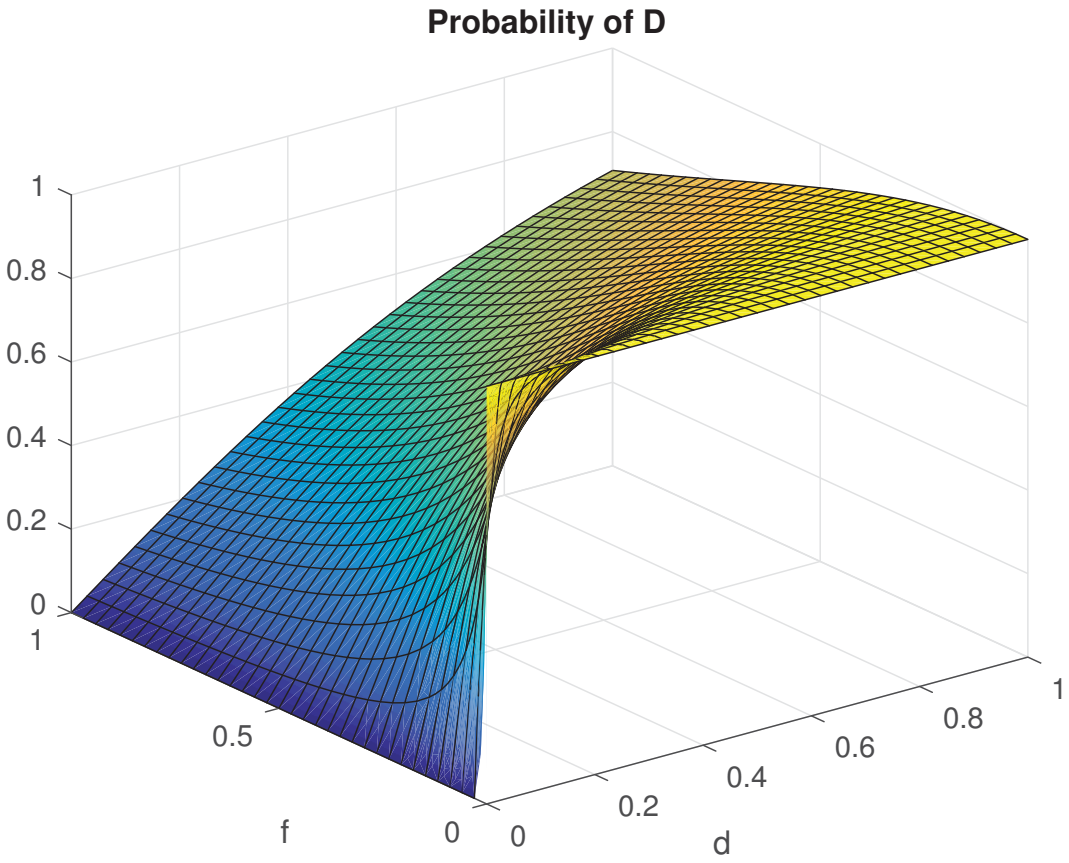

Figure 10.11: Probability of step D.

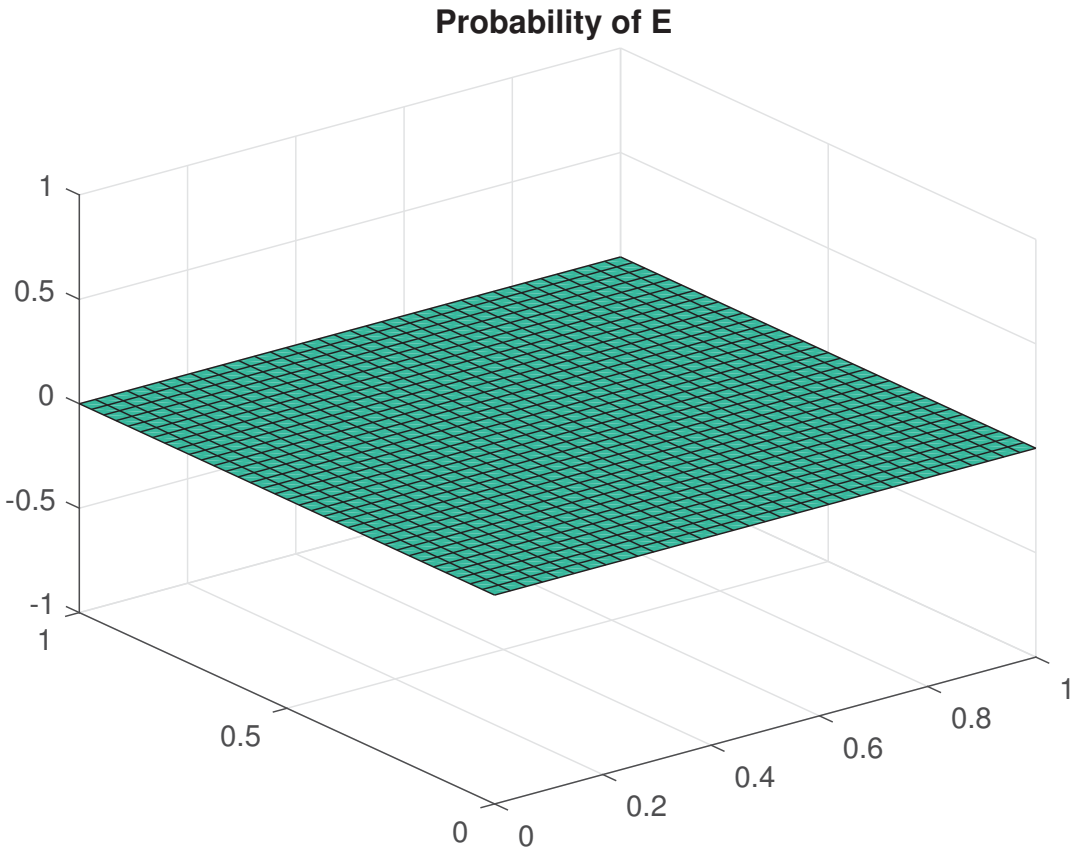

Figure 10.12: Probability of step E.

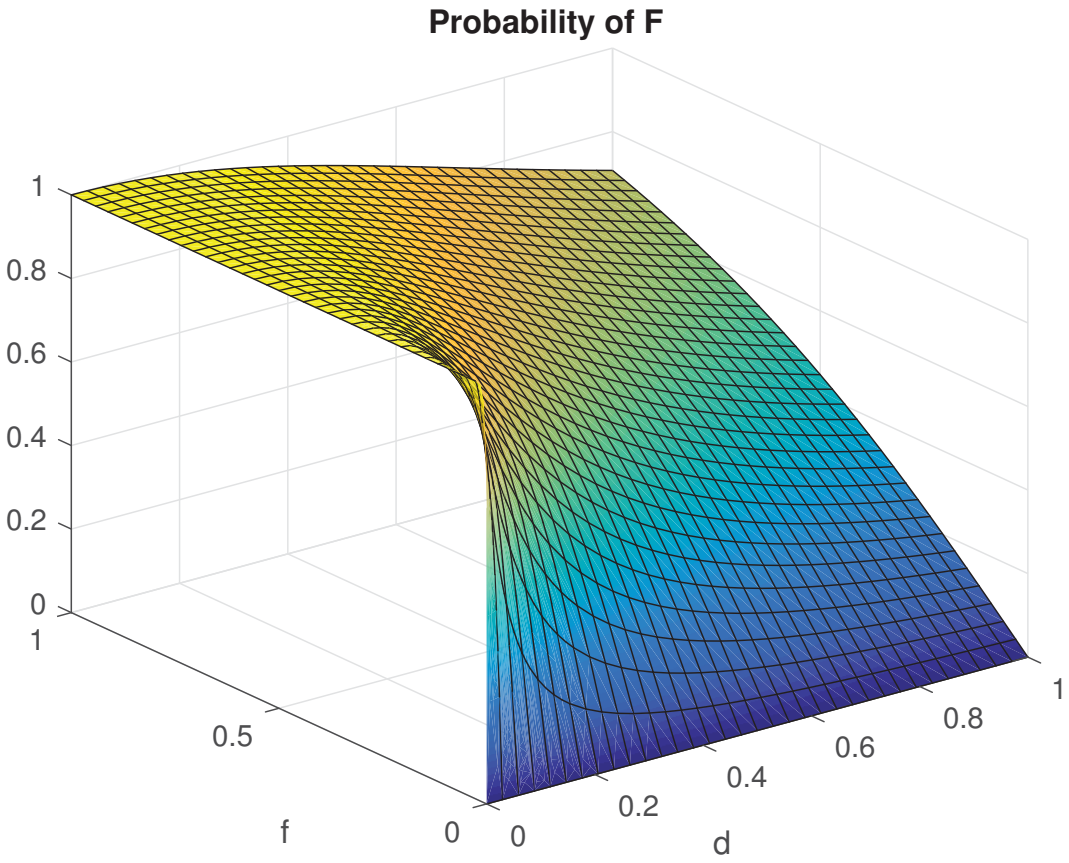

Figure 10.13: Probability of step F.

Part IV

Conclusion and Appendices

Chapter 11

Conclusion and Future Work

This chapter concludes the entire dissertation and suggests possible future research. The first part of this chapter provides a summary of this dissertation including the research contribution and discussion of findings. The second part lists possible future research. Last but not least, this chapter lists some limitations of this dissertation.

11.1 Summary of the Dissertation

There is no doubt that 5G is going to change our lifestyle massively. This dissertation focused the mobility problem of D2D communication which is assumed to be part and parcel of the 5G cellular network. I started this dissertation from the beginnings of the mobile network system and then covered almost all the significant changes and updates from the very first 1G technology in the 1980s to prospective 5G technologies in the 2020s. I also explained extensively the potential technologies for the 5G cellular network.

Chapter 3 described the major prospective technologies for the 5G cellular network system. It highlighted mainly massive MIMO, mmWave, cloud RAN, cognitive radio, multi-RAT, D2D communications and some other enhancements. It also highlighted the design issues of 5G.

The basics of D2D communication were broadly described in Chapter 4. This chapter mentioned the classification of D2D communications from the different perspectives. Advantages of different types of D2D communications was also described. A D2D communication procedure and some challenges were described in this chapter.

As the estimation of users' location is crucial to obtaining the best connection between two devices, the most up-to-date direction of arrival estimation techniques for D2D users was also discussed in Chapter 5.

Chapter 6 was dedicated only to mobility management of D2D communication. In this chapter, I then devised a unique solution to manage the mobility of D2D users. This proposed model may be a part of the next generation mobile network. The algorithm and simulation results were also discussed, and it was proved that D2D communications could ensure maximum sum-rate while the devices are moving.

In Chapter 7, I considered the Markov Chain model to understand the probable movement directions of users. I also simulated the Markov Chain model to validate users' movement directions that could be used to identify user movement trends in a real network. This chapter described the theory with the mathematical model and simulation results were mentioned in Chapter 10.

Finally, I performed the simulations using MATLAB tools to estimate and justify the DOA in Chapter 8 and proposed an algorithm for mobility management with simulation in Chapter 9. It proved that D2D communications could ensure maximum sum-rate while the devices are moving using the proposed model.

The maximum sum-rate comes from using the proposed algorithm where the selection of different modes efficiently plays an important role. We have reduced the latency and proposed the group handover to make sure that minimum signaling overheads are required. Figure 9.2 and 9.3 show that D2D communications take place for most of the cases and during the handover period, the speed doesn't fall down so much which ensures that we get the maximum sum rate.

11.2 Future Works

Firstly, this is a proposed algorithm, and all the simulations were performed on the MATLAB tool. The MATLab code could be customised by preparing MATLab GUI, so that the full feature will be more user friendly. There are other simulation tools available. However, most of them are not compatible with a D2D communication system. A unique simulation platform could be

developed by writing codes from scratch. Moreover, this algorithm could be implemented by using real hardware. However, it would need sponsorship and support from relevant technology companies.

This algorithm could also be extended in different ways. I considered one cellular user and two D2D users per cell, and this remained the same after the handover took place. However, this model could consider more users per cell, and it would need a more mathematical model that could increase the complexity accordingly.

I also considered only one device was moving and other device is in a fixed location. This work could be extended to have both devices moving at the same time. However, this also increases the complexity.

For my algorithm and simulation, I considered only the uplink resources to be used for the D2D communication; further experimentation could also use downlink frequencies. I also considered inband underlay D2D communication for my algorithm and model to get the maximum spectrum efficiency. The same model could be used to examine outbound or inband underlay D2D communications.

I strongly believe that it is possible to explore the new era of communication systems by extending the work that has already been done in this dissertation.

11.3 Limitations of the Dissertation

D2D communications is a very new technology and it has not been standardised for any previous mobile network generations. Moreover, I found few papers that discussed the issues of mobility management of D2D communications. This dissertation is limited by some other practical issues. For example, it was not possible to obtain a result using the real network or hardware. Nor could the latest simulation tools design a D2D communication system straightaway. Instead, this is a generalised algorithm with simulation results and many more simulation are possible by using the same and or a modified algorithm.

I have tried my best to get the most realistic simulation considering the real network parameters.

Appendix A

Direction of Arrival (DOA) and Channel Estimation

A.1 Signal Model

I consider a ULA consisting of L elements which are placed with uniform distance d between two adjacent ones as shown in Figure A.1. We also assume the total number of sources to be P. The wavefront of the far-field signal (at an angle θ) impinges first on the leftmost antenna element of the receiving antenna array. Then, each antenna receives the signal with an amount of phase shift, and that could be calculated with the help of geometry of the uniform linear array. The fact is that wavefront of the source signal takes extra time to reach each antenna elements relative to the first element.

The Figure A.2 exactly shows the geometry of how the signal wavefront arrives. After arriving at the first antenna, the same signal plane then comes at the second antenna elements traveling an additional path Δl. Now using basic trigonometric formula,

$$\Delta l \quad = \quad -d\cos\theta \tag{A.1}$$

the delay becomes,

$$\tau = -d\cos\theta/c \tag{A.2}$$

where c is the speed of light, $3 \times 10^8 l/s$.

The path difference leads to a phase shift of μ between the signals arriving at the two adjacent antennas. Therefore, the propagation phase

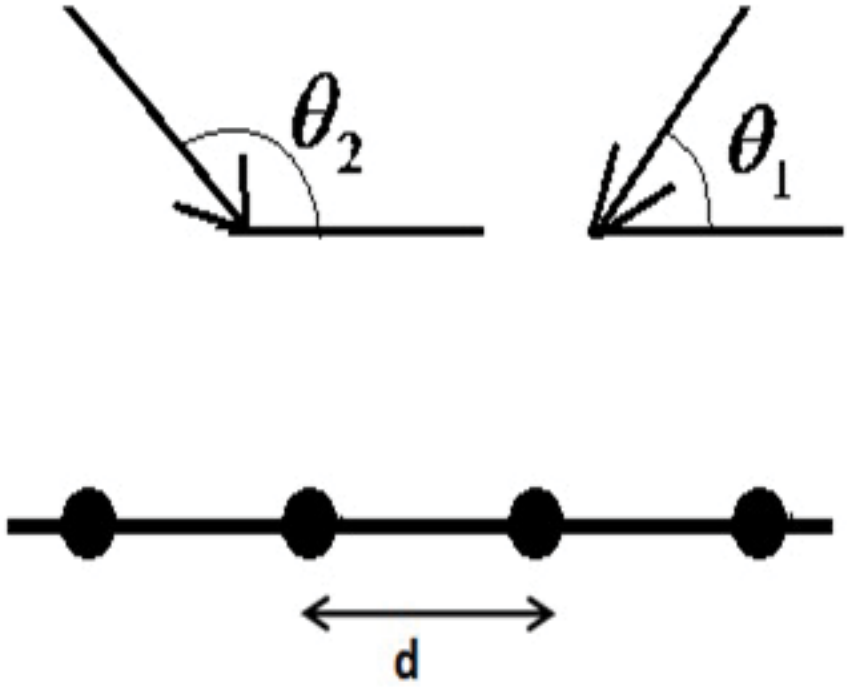

Figure A.1: Concept of basic beamforming technique.

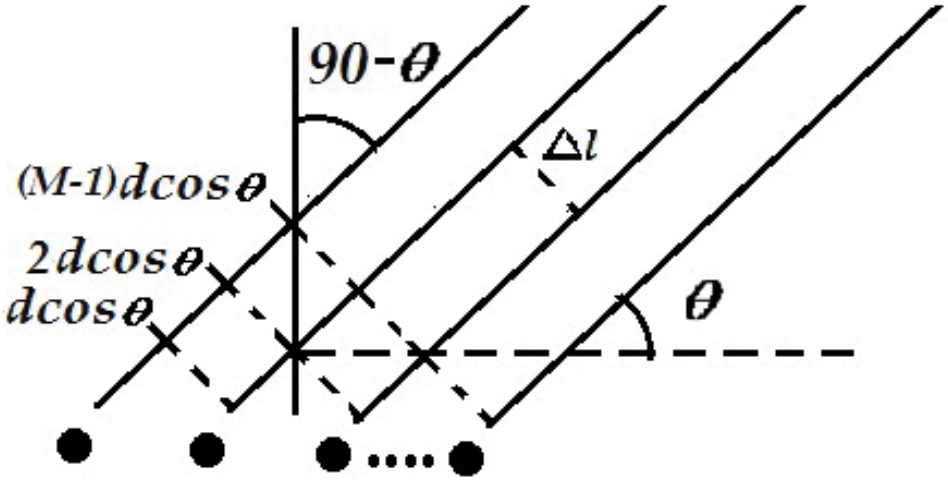

Figure A.2: Uniform Linear Array (ULA) geometry.

shift μ between any consecutive two elements is

$$\mu = \left(\frac{2\pi}{\lambda}\right) \times \Delta l \tag{A.3}$$

where λ is the wavelength of the signal.

Using equation (A.1),

$$\mu = -\left(\frac{2\pi}{\lambda}\right) \times d\cos\theta. \tag{A.4}$$

Now, for L-th element in a ULA consisting of L elements, the phase shift shown in Figure A.2 becomes [112],

$$\mu = -(L-1) \times \frac{2\pi d\cos\theta}{\lambda}. \tag{A.5}$$

Using equation (A.4), DOA can be calculated easily as

$$\theta = -\cos^{-1}(\mu/2\pi d) \times \lambda. \tag{A.6}$$

The signal is assumed to be narrowband, but for simplicity in practice, I consider a sinusoidal signal which could be represented in a complex form as $e^{j\omega_0 t}$ where $\omega_0 = 2\pi f_0$ and t represents time index. The array antenna elements receive this signal. For channel estimation, I use another sequence of the reference signal which is called Zadoff-Chu (ZC) sequence. ZC sequence is used as a reference signal in the LTE standard specified by the 3GPP. The detail description of ZC is out of the scope of this chapter.
Now, the signal received by the first antenna is

$$s_1(t) = e^{j2\pi f_0 t}. \tag{A.7}$$

According to the Figure A.2, the second antenna will receive the signal after additional plane wave traveling the distance Δl which is the delayed version of the signal received by the first antenna. According to the equation (A.2), the delayed time is τ. Therefore, the received signal by the second antenna is

$$\begin{aligned} s_2(t) &= s_1(t-\tau) && \text{(A.8)} \\ &= e^{j2\pi f_0 t} \times e^{-(j2\pi f_0 \tau)} && \text{(A.9)} \\ &= e^{j2\pi f_0 t} \times e^{-(j2\pi f_0 d\cos\theta/c)} && \text{(A.10)} \\ &= e^{j2\pi f_0 t} \times e^{-(j2\pi d\cos\theta/\lambda)}. && \text{(A.11)} \end{aligned}$$

Using equation (A.4),

$$s_2(t) \;=\; s_1(t)e^{j\mu}. \tag{A.12}$$

Since noise is added by the system, first antenna will receive the noise in addition to the signal. I can write as

$$x_1(t) = s_1(t) + n_1(t) \tag{A.13}$$

where x_1 is the total signal received by the first antenna.

Second antenna will receive

$$x_2(t) = s_1(t-\tau) + n_2(t). \tag{A.14}$$

If I continue and represent it in matrix form, then

$$\begin{bmatrix} x_1(t) \\ x_2(t) \\ x_3(t) \\ \vdots \\ x_L(t) \end{bmatrix} = s_1(t) \begin{bmatrix} 1 \\ e^{j\mu} \\ e^{2j\mu} \\ \vdots \\ e^{j(L-1)\mu} \end{bmatrix} + \begin{bmatrix} n_1(t) \\ n_2(t) \\ n_3(t) \\ \vdots \\ n_L(t) \end{bmatrix} \tag{A.15}$$

where

$$\mathbf{a}(\mu) = \begin{bmatrix} 1 \\ e^{j\mu} \\ e^{2j\mu} \\ \vdots \\ e^{j(L-1)\mu} \end{bmatrix}$$

is called array steering vector.

Considering superposition of all the signals generated by P sources, $s_i, 1 \leq i \leq P$ and L antenna noises, the output received by the lth array element at time t can be formulated as

$$x_l(t) = s_i(t) \sum_{i=1}^{P} e^{j(l-1)\mu_i} + n_l(t) \tag{A.16}$$

for $l = 1, 2, ...L$.

In general, I can write this equation as

$$\mathbf{x}(t) = \begin{bmatrix} \mathbf{a}(\mu_1) & \mathbf{a}(\mu_2) & \mathbf{a}(\mu_3) & \cdots & \mathbf{a}(\mu_P) \end{bmatrix} \begin{bmatrix} s_1(t) \\ s_2(t) \\ s_3(t) \\ \vdots \\ s_P(t) \end{bmatrix} + \mathbf{n}(t) \tag{A.17}$$

where

$\mathbf{x}(t) = [x_1(t)\, x_2(t) \cdots x_L(t)]^T$ is the data column vector received by the L array receiving antennas, and

$$\mathbf{a}(\mu_i) = \begin{bmatrix} 1 \\ e^{j\mu_i} \\ e^{j2\mu_i} \\ \vdots \\ e^{j(L-1)\mu_i} \end{bmatrix} \tag{A.18}$$

is called array steering column vector.

Finally, I can write the equation as follows:

$$\mathbf{x}(t) = \mathbf{A}(\theta)\mathbf{s}(t) + \mathbf{n}(t) \tag{A.19}$$

where

$\mathbf{s}(t) = [s_1(t)\, s_2(t) \cdots s_P(t)]^T$ is the signal column vector generated by the P sources.

$\mathbf{n}(t) = [n_1(t)\, n_2(t) \cdots n_L(t)]^T$ is a zero mean spatially uncorrelated additive noise.

$\mathbf{A}(\theta) = [a(\mu_1) \cdots a(\mu_i) \cdots a(\mu_P)]$ is called the $(L \times P)$ steering matrix.

Referring to the equation (A.18), we can write $\mathbf{A}(\theta)$ as

$$\mathbf{A}(\theta) = \begin{bmatrix} 1 & \cdots & 1 & \cdots & 1 \\ e^{j\mu_1} & \cdots & e^{j\mu_i} & \cdots & e^{j\mu_P} \\ \vdots & \vdots & \vdots & \vdots & \vdots \\ e^{j(L-1)\mu_1} & \cdots & e^{j(L-1)\mu_i} & \cdots & e^{j(L-1)\mu_P} \end{bmatrix} \tag{A.20}$$

where

$$\mu_i = -\frac{2\pi}{\lambda} d \cos\theta_i \tag{A.21}$$

is called the spatial frequency for the ith source that generates the signal of the incident angle θ_i [113].

According to the Figure A.3, I can easily design a weight vector $\mathbf{w}$ to linearly combine the data received by the array elements to form a single output signal $y(t)$[114]

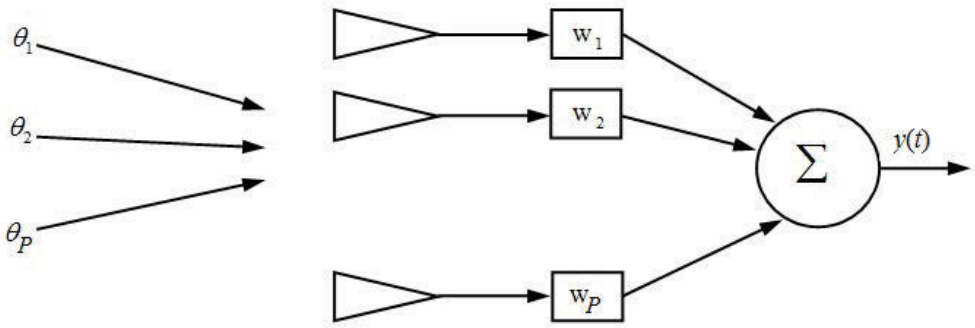

Figure A.3: Adding the weight vector to the received signal at each antenna.

$$y(t) = \sum_{i=1}^{P} w_i^* x_i(t) \tag{A.22}$$

$$= \mathbf{w}^H \mathbf{x}(t). \tag{A.23}$$

Total averaged power at the output of the array using $y(1), y(2), ..., y(T)$ data samples can be expressed as [114],

$$\bar{P}(\mathbf{w}) = \frac{1}{T} \sum_{t=1}^{T} |y(t)|^2 \tag{A.24}$$

$$= \frac{1}{T} \sum_{t=1}^{T} \mathbf{w}^H \mathbf{x}(t) \mathbf{x}^H(t) \mathbf{w} \tag{A.25}$$

$$= \mathbf{w}^H \hat{\mathbf{R}}_{XX} \mathbf{w} \tag{A.26}$$

where $\hat{\mathbf{R}}_{XX}$ is a covariance matrix that can be defined as

$$\hat{\mathbf{R}}_{XX} = \frac{1}{T} \sum_{t=1}^{T} \mathbf{x}(t) \mathbf{x}^H(t). \tag{A.27}$$

A.2 Conventional Beamformer Technique

The conventional beamformer is also known as Delay and Sum method, Fourier method or Bartlett method. It is one of the most straightforward methods of estimating DOA. It is computationally attractive and less costly compared with other techniques. It is also robust against array imperfection. When the source signal is computed with interference and noise, this algorithm is still able to give a reasonable estimation of the DOA [112].

In this type of technique, the array is steered electronically (by changing the phase delays) in one direction at a time, and the output power is measured. The DOA is estimated for the incident sources by the directions that give the maximum output power.

Maximizing the output power can be calculated as

$$\bar{P}_{BF}(\theta) = \max_{\mathbf{w}} \quad E\{y(t)\}^2 \tag{A.28}$$

Referring to the equation (A.23),

$$\bar{P}_{BF}(\theta) = \max_{\mathbf{w}} \quad E\left\{\mathbf{w}^H \mathbf{x}(t)\, \mathbf{x}^H(t)\, \mathbf{w}\right\} \tag{A.29}$$

$$= \max_{\mathbf{w}} \quad \mathbf{w}^H E\left\{\mathbf{x}(t)\, \mathbf{x}^H(t)\right\} \mathbf{w}. \tag{A.30}$$

Using equation (A.19),

$$\bar{P}_{BF}(\theta) = \max_{\mathbf{w}} \quad \left\{E|\mathbf{s}(t)|^2 |\mathbf{w}^H \mathbf{A}(\theta)|^2 + \sigma^2 |\mathbf{w}|^2\right\} \tag{A.31}$$

here, maximization is determined as $\max_{\mathbf{w}} \ |\mathbf{w}^H \mathbf{A}(\theta)|^2$ subject to $\mathbf{w}^H \mathbf{w} = 1$ which imply that

$$\|\mathbf{w}^H \mathbf{A}(\theta)\|^2 \leq \|\mathbf{w}\|^2 \|\mathbf{A}(\theta)\|^2 \tag{A.32}$$

$$= \|\mathbf{A}(\theta)\|^2. \tag{A.33}$$

According to [114], the resulting solution can be formulated as

$$\mathbf{w}_{BF} = \frac{\mathbf{A}(\theta)}{\sqrt{\mathbf{A}^H(\theta)\, \mathbf{A}(\theta)}}. \tag{A.34}$$

Substituting this into equation (A.26)

$$\bar{P}_{BF}(\theta) = \frac{\mathbf{A}^H(\theta)\, \hat{\mathbf{R}}_{XX} \mathbf{A}(\theta)}{\mathbf{A}^H(\theta)\, \mathbf{A}(\theta)} \tag{A.35}$$

where θ is from 0 to 180°.

A.3 Capon Beamformer Technique

Capon beamformer proposes to minimize the contribution of undesired signals and noises by minimizing the total output power while maintaining the gain along to the look direction constant [116].

Therefore, equation (A.26) can be written as

$$\min_{\mathbf{w}} \ \bar{P}(\mathbf{w}) = \min \ \left(\mathbf{w}^H \hat{\mathbf{R}}_{XX} \mathbf{w}\right), \text{subject to } |\mathbf{w}^H \mathbf{A}(\theta)| = 1. \quad \text{(A.36)}$$

The weight factor $\mathbf{w}_{Cap}$ can be found using the technique by Lagrange multipliers that results as

$$\mathbf{w}_{Cap} = \frac{\hat{\mathbf{R}}_{XX}^{-1} \mathbf{A}(\theta)}{\mathbf{A}^H(\theta) \hat{\mathbf{R}}_{XX}^{-1} \mathbf{A}(\theta)}. \quad \text{(A.37)}$$

Substituting this weight vector to the equation (A.26) leads to

$$\bar{P}_{Cap}(\theta) = \frac{1}{\mathbf{A}^H(\theta) \hat{\mathbf{R}}_{XX}^{-1} \mathbf{A}(\theta)}. \quad \text{(A.38)}$$

A.4 Multiple Signal Classification (MUSIC) Method

We assume that noise is spatially and temporarily white and they are uncorrelated [118]. Therefore the spatial correlation $\mathbf{R}_{XX}$ for a single user can be written as

$$\begin{aligned} \mathbf{R}_{XX} &= E\left\{\mathbf{x}(t)\mathbf{x}^H(t)\right\} && \text{(A.39)} \\ &= \mathbf{A}(\theta) E\left\{\mathbf{s}(t)\mathbf{s}^H(t)\right\} \mathbf{A}^H(\theta) + E\left\{\mathbf{n}(t)\mathbf{n}^H(t)\right\} && \text{(A.40)} \end{aligned}$$

where $E\{.\}$ denotes statistical expectation.

I assume that $\mathbf{R}_s = E\left\{\mathbf{s}(t)\mathbf{s}^H(t)\right\}$ is the source covariance matrix and $E\left\{\mathbf{n}(t)\mathbf{n}^H(t)\right\} = \sigma^2\mathbf{I}$ is the noise covariance matrix. Now I can write

$$\begin{aligned} \mathbf{R}_{XX} &= \mathbf{A}(\theta)\mathbf{R}_s\mathbf{A}^H(\theta) + \sigma^2\mathbf{I} && \text{(A.41)} \\ &= \mathbf{Q}\mathbf{\Lambda}\mathbf{Q}^H && \text{(A.42)} \end{aligned}$$

where $\mathbf{Q}$ is a unitary matrix and $\mathbf{\Lambda}$ is a diagonal matrix of real eigenvalues such that $\lambda_1 \geq \lambda_2 \geq \lambda_3 \geq \cdots \geq \lambda_L$.

Any vector that is orthogonal to $\mathbf{a}$ is an eigenvector of $\hat{\mathbf{R}}_{XX}$ with the eigenvalue σ^2. It is clear that there are $(L-P)$ such vectors, which are linearly independent. The rest of the eigenvalues are larger than σ^2. So the eigenvalues (and corresponds their eigenvectors) of $\hat{\mathbf{R}}_{XX}$ can be divided into two groups:

$$\text{signal eigenvalues} : \lambda_i > \sigma^2, i = 1, 2, 3, ..., P$$

$$\text{noise eigenvalues} : \lambda_i = \sigma^2, i = P+1, P+2, P+3, ..., L.$$

.
I can write the equation (A.42)

$$\mathbf{R}_{XX} = \mathbf{E}_S \mathbf{\Lambda}_S \mathbf{E}_S^H + \mathbf{E}_N \mathbf{\Lambda}_N \mathbf{E}_N^H \tag{A.43}$$

where

$\mathbf{\Lambda}_N$ contains the diagonal noise eigenvalues.

$\mathbf{\Lambda}_S$ contains the diagonal signal eigenvalues.

$\mathbf{E}_N$ contains eigenvectors associated with the noise eigenvalues (noise subspace matrix).

$\mathbf{E}_S$ contains eigenvectors associated with the signal eigenvalues (signal subspace matrix).

Since array steering vectors are orthogonal to the noise subspace eigenvectors at the angles $\theta_1, \theta_2, \theta_3, \cdots, \theta_P$, i.e., $\mathbf{a}^H(\theta)\mathbf{E}_N = 0$, I can show that Euclidean distance $\mathbf{a}^H(\theta)\mathbf{E}_N\mathbf{E}_N^H\mathbf{a}(\theta) = 0$ for each and every arrival angle $\theta_1, \theta_2, \theta_3 \cdots \theta_P$.

In practice, we can get a sharp peak at the angle of arrival by placing this Euclidean distance in the denominator. Therefore, the DOAs can now be estimated from the P peaks of the following MUSIC function [119]

$$\bar{P}_{MUSIC}(\theta) = \frac{1}{\mathbf{A}^H(\theta)\hat{\mathbf{E}}_N\hat{\mathbf{E}}_N^H\mathbf{A}(\theta)}. \tag{A.44}$$

A.5 Estimation of Signal Parameters via Rotational Invariance Technique (ESPRIT)

Recall the equation (A.20) for the steering matrix and let $\bar{\mathbf{A}}$ and $\underline{\mathbf{A}}$ be the matrices with eliminated first and last row respectively as shown in Figure

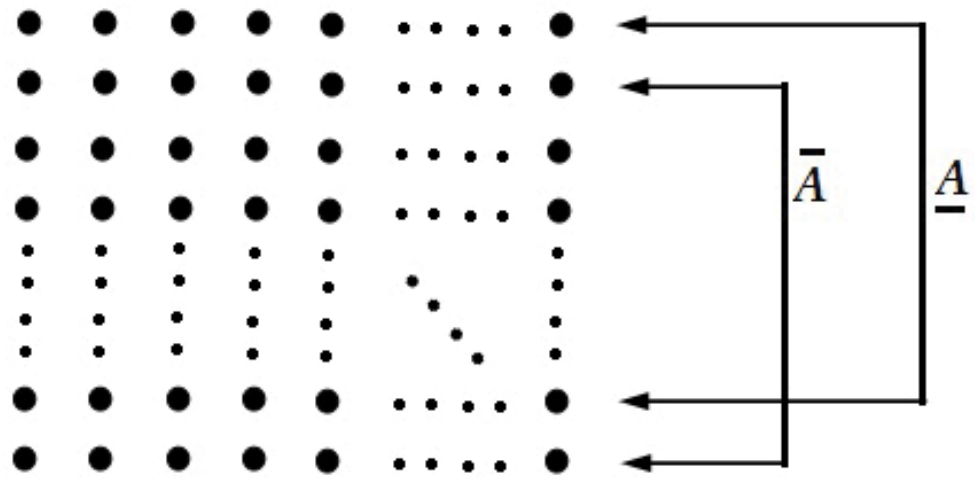

Figure A.4: Formation of $\bar{\mathbf{A}}$ and $\underline{\mathbf{A}}$ from $\mathbf{A}$ steering matrix.

A.4. Therefore, we can write,

$$\bar{\mathbf{A}}\mathbf{D} = \underline{\mathbf{A}} \tag{A.45}$$

where

$$\mathbf{D} = \begin{bmatrix} Z_1 & 0 & 0 & \cdots & 0 \\ 0 & Z_2 & 0 & \cdots & 0 \\ \vdots & \vdots & \vdots & \ddots & \vdots \\ 0 & 0 & 0 & \cdots & Z_L \end{bmatrix} \tag{A.46}$$

Here, $Z_i = e^{j\mu_i}$.

Now compute the eigendecomposition of sample covariance matrix $\mathbf{R}_{XX}$ and obtain the signal subspace $\mathbf{E}_s$.

Let $\bar{\mathbf{E}}_s$ and $\underline{\mathbf{E}}_s$ are formed from the signal eigen vector matrix $\mathbf{E}_s$ in the same way as $\bar{\mathbf{A}}$ and $\underline{\mathbf{A}}$ from $\mathbf{A}$. A full rank $P \times P$ matrix $\mathbf{C}$ existed because $\mathbf{E}_s$ and $\mathbf{A}$ span the same subspace, namely signal subspace.

Therefore,

$$\mathbf{E}_s = \mathbf{A}\mathbf{C}$$

$$\underline{\mathbf{E}}_s = \underline{\mathbf{A}}\mathbf{C} = \bar{\mathbf{A}}\mathbf{D}\mathbf{C}$$

$$\bar{\mathbf{E}}_s = \bar{\mathbf{A}}\mathbf{C}.$$

So,

$$\underline{\mathbf{E}}_s\mathbf{C}^{-1}\mathbf{D}^{-1}\mathbf{C} = \bar{\mathbf{A}}\mathbf{D}\mathbf{C}\mathbf{C}^{-1}\mathbf{D}^{-1}\mathbf{C} = \bar{\mathbf{A}}\mathbf{C} = \bar{\mathbf{E}}_s. \tag{A.47}$$

Using equation (A.47), we get

$$\underline{\mathbf{E}}_s = \bar{\mathbf{E}}_s\mathbf{C}^{-1}\mathbf{D}\mathbf{C} \tag{A.48}$$

$$\Rightarrow \underline{\mathbf{E}}_s = \bar{\mathbf{E}}_s\boldsymbol{\Psi} \tag{A.49}$$

where

$$\boldsymbol{\Psi} = \mathbf{C}^{-1}\mathbf{D}\mathbf{C} \tag{A.50}$$

here, $\mathbf{C}$ and $\mathbf{D}$ are unknown.

Equation (A.50) implies that $\mathbf{D}$ is a diagonal matrix of eigenvalues of $\boldsymbol{\Psi}$.

Computing the solution for $\boldsymbol{\Psi}$ from equation (A.49),

$$\boldsymbol{\Psi} = \left(\bar{\mathbf{E}}_s^H\bar{\mathbf{E}}_s\right)^{-1}\bar{\mathbf{E}}_s^H\underline{\mathbf{E}}_s. \tag{A.51}$$

From (A.46), it is clear that the eigenvalues of $\boldsymbol{\Psi}$ (contained in $\mathbf{D}$) can be written as

$$g_l = -\frac{2\pi}{\lambda}d\cos\theta_l. \tag{A.52}$$

In practice, the sample covariance matrix $\hat{\mathbf{R}}$ is used. Then, after computing the signal subspace estimation $\hat{\bar{E}}_s$, the DOAs can be estimated from

$$\hat{\theta}_l = \cos^{-1}\left(\frac{-\hat{g}_l \times \lambda}{2\pi d}\right) \tag{A.53}$$

where $\hat{g}_l$ for $l = 1, 2, 3, ..., P$ are the eigenvalues of

$$\hat{\boldsymbol{\Psi}} = \left(\hat{\bar{\mathbf{E}}}_s^H\hat{\bar{\mathbf{E}}}_s\right)^{-1}\hat{\bar{\mathbf{E}}}_s^H\hat{\underline{\mathbf{E}}}_s. \tag{A.54}$$

A.6 Signal Model for URA

After exploring the signal model for ULA, now I would like to move on to model signal for the URA that involves a bit complex geometries

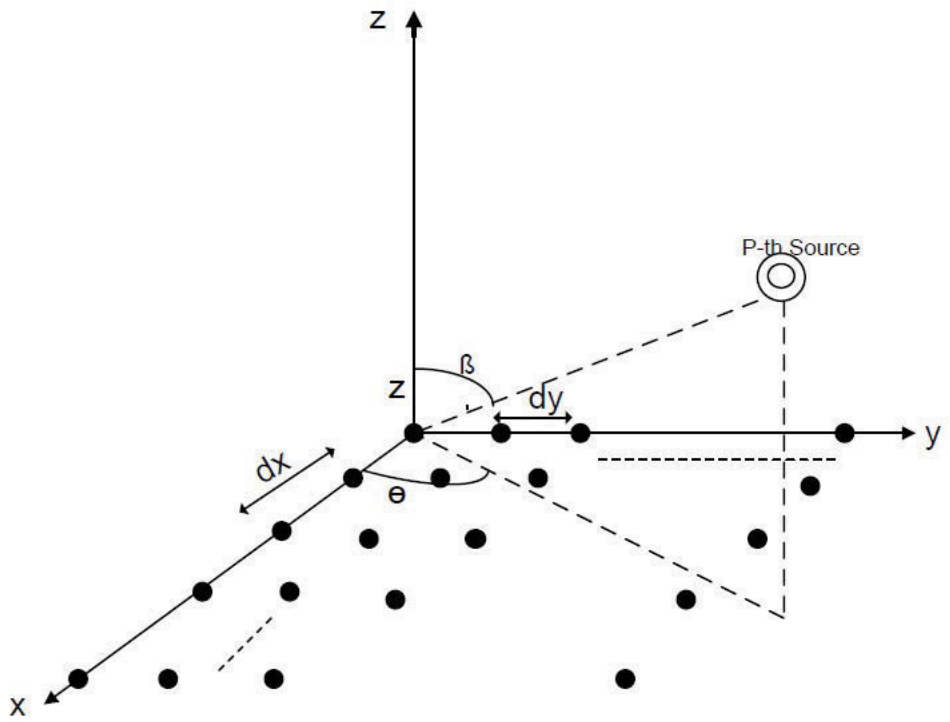

Figure A.5: Array geometry of the URA. Image source: [12].

[12, 122, 123].

Figure A.5 shows a simple model for the URA, where we consider K and L identical omni-directional sensors along with x- and y-axis, respectively.

Consider the distance between two adjacent sensors dx along with x-axis and dy along with y-axis. I also consider $dx = dy = \lambda/2$. Assuming that P narrowband coherent radiating sources located in the far field region with wavelength λ impinge on the URA at azimuth angel θ_p and elevation φ_p for $p = 1, 2, 3, ..., P$.

The received signal at (i, j)th sensor (for $i = 1, 2, ..., K$ and $j = 1, 2, ..., L$) can be written by using analytical signal representation [124]

$$\mathbf{x}(t) = \mathbf{A}\mathbf{s}(t) + \mathbf{n}(t) \tag{A.55}$$

where

$$\mathbf{x}(t) = [x_{1,1}(t), x_{2,1}(t), \cdots, x_{k-1,L}(t), \cdots, x_{K,L}(t)]^T$$

and

$$\mathbf{n}(t) = [n_{1,1}(t), n_{2,1}(t), \cdots, n_{k-1,L}(t), \cdots, n_{K,L}(t)]^T$$

for $t = 1, 2, ..., T$ times snapshot. Here, $[.]^T$ represents the transpose of a matrix.

Equation (A.55) has a similar structure to the channel model of equation (A.88), which is discussed in Section A.8. In equation (A.55), $\mathbf{s}(t)$ represents $P \times 1$ baseband signal vector.

$$\mathbf{s}(t) = [s_1(t), s_2(t), ..., s_P(t)]^T$$

and $\mathbf{A}$ is a $KL \times P$ steering matrix whose columns have the form as $\mathbf{vec}(\mathbf{a}_K(\mu)\,\mathbf{a}_L^T(\nu))$ for

$$\mu = \mu_1, \mu_2, \mu_3, ..., \mu_P$$

$$\nu = \nu_1, \nu_2, \nu_3, ..., \nu_P$$

for $p = 1, 2, ..., P$, where, μ_p and ν_p are DOA parameters corresponding to the p-th source along with x-direction and y-direction, respectively, i.e.,

$$\mu \triangleq \sin(\theta)\cos(\varphi) \tag{A.56}$$

$$\nu \triangleq \sin(\theta)\sin(\varphi) \tag{A.57}$$

for $\theta = \theta_1, \theta_2, ..., \theta_P$ and $\varphi = \varphi_1, \varphi_2, ..., \varphi_P$.

Here, $\mathbf{a}_K(\mu)$ and $\mathbf{a}_L(\nu)$ denote steering vectors for URA defines as [12]

$$\mathbf{a}_K(\mu) = [e^{-j(K/2)\frac{2\pi}{\lambda}d_x\mu}, \ldots, e^{-j(1/2)\frac{2\pi}{\lambda}d_x\mu}, e^{j(1/2)\frac{2\pi}{\lambda}d_x\mu}, \ldots, e^{j(K/2)\frac{2\pi}{\lambda}d_x\mu}]^T \tag{A.58}$$

if K is even, or

$$\mathbf{a}_K(\mu) = [e^{-j(K-1/2)\frac{2\pi}{\lambda}d_x\mu}, \ldots, e^{-j\frac{2\pi}{\lambda}d_x\mu}, 1, e^{j\frac{2\pi}{\lambda}d_x\mu}, \ldots, e^{j(K-1/2)\frac{2\pi}{\lambda}d_x\mu}]^T \tag{A.59}$$

if K is odd, and similarly

$$\mathbf{a}_L(\nu) = [e^{-j(L/2)\frac{2\pi}{\lambda}d_y\nu}, \ldots, e^{-j(1/2)\frac{2\pi}{\lambda}d_y\nu}, e^{j(1/2)\frac{2\pi}{\lambda}d_y\nu} \ldots, e^{j(L/2)\frac{2\pi}{\lambda}d_y\nu}]^T \tag{A.60}$$

if L is even, or

$$\mathbf{a}_L(\nu) = [e^{-j(L-1/2)\frac{2\pi}{\lambda}d_y\nu}, \ldots, e^{-j\frac{2\pi}{\lambda}d_y\nu}, 1, e^{j\frac{2\pi}{\lambda}d_y\nu}, \ldots, e^{j(L-1/2)\frac{2\pi}{\lambda}d_y\nu}]^T \tag{A.61}$$

if L is odd.

The defined steering vectors hold the conjugate centro-symmetric property, and it can be expressed mathematically as

$$\mathbf{\Pi}_K\mathbf{A}_K = \mathbf{A}_K^* \tag{A.62}$$

where $\mathbf{\Pi}_K$ is $K \times K$ exchange matrix with ones on its anti-diagonal and zeros elsewhere.

$$\mathbf{\Pi}_K = \begin{bmatrix} 0 & \cdots & 0 & 0 & 1 \\ 0 & \cdots & 0 & 1 & 0 \\ 0 & \cdots & 1 & 0 & 0 \\ \vdots & & \vdots & \vdots & \vdots \\ 1 & \cdots & 0 & 0 & 0 \end{bmatrix}_{K \times K} \tag{A.63}$$

From the matrix algebra, $\mathbf{\Pi}_K^2 = \mathbf{I}_K$, where

$$\mathbf{I}_K = \begin{bmatrix} 1 & & & & \\ & 1 & & & \\ & & 1 & & \\ & & & \ddots & \\ & & & & 1 \end{bmatrix}. \tag{A.64}$$

Using this property in equation (A.62), we can write as

$$\mathbf{\Pi}_K \mathbf{a}_\mu = \mathbf{a}_\mu^*. \tag{A.65}$$

A conjugate centro symmetric vector can be calculated from a simple matrix as in [12] [123] [125]. If $K = 2\upsilon$ is even, then

$$\mathbf{Q}_K = \frac{1}{\sqrt{2}} \begin{bmatrix} \mathbf{I}_K & j\mathbf{I}_K \\ \mathbf{\Pi}_K & -j\mathbf{\Pi}_K \end{bmatrix} \tag{A.66}$$

and if $K = 2\upsilon + 1$ is odd, then

$$\mathbf{Q}_K = \frac{1}{\sqrt{2}} \begin{bmatrix} \mathbf{I}_K & 0 & j\mathbf{I}_K \\ 0^T & \sqrt{2} & 0^T \\ \mathbf{\Pi}_K & 0 & -j\mathbf{\Pi}_K \end{bmatrix} \tag{A.67}$$

A vector $\mathbf{d}_K(\mu)$ can be defined as [12]

$$\mathbf{d}_K(\mu) \triangleq \mathbf{Q}_K^H \mathbf{a}_K(\mu) \tag{A.68}$$

Now, it is seen that $\mathbf{a}_K(\mu)$ is transformed into real-valued steering vector $\mathbf{d}_K(\mu)$. The same procedure for steering vector $\mathbf{a}_L(\mu)$ will transfer the vector into a form of real valued vector $\mathbf{d}_L(\mu)$

$$\mathbf{d}_L(\mu) \triangleq \mathbf{Q}_L^H \mathbf{a}_L(\mu) \tag{A.69}$$

A.7 Covariance Matrix

Covariance matrix for the array output signal $\mathbf{x}(t)$ can be defined as

$$\mathbf{R}_{XX} \triangleq \mathbf{A}\mathbf{R}_S\mathbf{A}^T + \sigma^2\mathbf{I} \tag{A.70}$$

where $\mathbf{R}_S = E\left\{\mathbf{s}\left(t\right)\mathbf{s}^H\left(t\right)\right\}$.

$\mathbf{R}_{XX}$ is assumed to be full rank, i.e., rank$\{\mathbf{R}\}$ = P. In (A.70), $KL \times KL$ matrix $\mathbf{A}\mathbf{R}_s\mathbf{A}^T$ is of rank $P(< N)$, and, therefore, rank-deficient. In the presence of noise, this low-rank property is exploited to form two subspaces (will be explained shortly), i.e., the signal subspace and noise subspace, respectively.

It should be noticed from (A.70), that $\mathbf{R}_{XX}$ has $KL - P$ eigenvalues equal to the noise power σ^2. In order to obtain the signal and noise subspaces, eigen-decomposition is applied to covariance matrix $\mathbf{R}_{XX}$. Defining λ_m as the m-th largest values

$$\lambda_1 \geq \lambda_2 \geq \ldots \lambda_P \geq \lambda_{P+1} = \ldots = \lambda_{KL} = \sigma^2. \tag{A.71}$$

The P largest eigenvalues ($\lambda_1 \geq \lambda_2 \geq \ldots \lambda_P$) are called signal eigenvalues and the $KL - P$ smallest eigenvalues ($\lambda_{P+1} = \ldots = \lambda_{KL}$) are called noise eigenvalues, therefore we can write

$$\mathbf{R}_{XX} = \mathbf{E}_S\mathbf{\Lambda}_S\mathbf{E}_S^H + \mathbf{E}_N\mathbf{\Lambda}_N\mathbf{E}_N^H, \tag{A.72}$$

where $KL \times P$ matrix $\mathbf{E}_S$ contain the eigenvectors corresponding to the signal eigenvalues and $KL \times (KL - P)$ matrix $\mathbf{E}_N$ contain the eigenvectors corresponding to the noise eigenvalues. In (A.72), $P \times P$ diagonal matrix $\mathbf{\Lambda}_S$ and $(KL-P) \times (KL-P)$ diagonal matrix $\mathbf{\Lambda}_N$ contain signal and noise eigenvalues, respectively, i.e.,

$$\mathbf{\Lambda}_S = \text{diag}\{\lambda_1, \lambda_2, \ldots, \lambda_\text{P}\} \tag{A.73}$$

$$\mathbf{\Lambda}_N = \sigma^2\mathbf{I} \tag{A.74}$$

In practice, the true array covariance matrix is unknown. Assuming we have $t = 1, \ldots, T$ snapshots of data. Using these snapshots we can form a large sample covariance matrix as

$$\hat{\mathbf{R}}_{XX} = \frac{1}{T}\sum_{t=1}^{T}\mathbf{x}(t)\mathbf{x}^H(t) \tag{A.75}$$

In order to obtain the signal subspace and the noise subspace, it is assumed that the number of T snapshots are greater than the number of array

antenna elements.

The signal and noise subspaces can be obtained by applying eigen-decomposition to sample covariance matrix $\hat{\mathbf{R}}_{XX}$. Defining $\hat{\lambda}_m$ as the m-th largest values

$$\hat{\lambda}_1 \geq \hat{\lambda}_2 \geq \ldots \hat{\lambda}_P \geq \hat{\lambda}_{P+1} \geq \ldots \geq \hat{\lambda}_M, \tag{A.76}$$

The P largest eigenvalues $\hat{\lambda}_1 \geq \hat{\lambda}_2 \geq \ldots \hat{\lambda}_P$ are called signal eigenvalues and the $KL - P$ smallest values $\hat{\lambda}_{P+1} \geq \ldots \geq \hat{\lambda}_K L$ are called noise eigenvalues, therefore we can write

$$\hat{\mathbf{R}}_{XX} = \hat{\mathbf{E}}_S \hat{\mathbf{\Lambda}}_S \hat{\mathbf{E}}_S^H + \hat{\mathbf{E}}_N \hat{\mathbf{\Lambda}}_N \hat{\mathbf{E}}_N^H, \tag{A.77}$$

where $KL \times P$ matrix $\hat{\mathbf{E}}_S$ contain the eigenvectors corresponding to the signal eigenvalues and $KL \times (KL - P)$ matrix $\hat{\mathbf{E}}_N$ contain the eigenvectors corresponding to the noise eigenvalues. In (A.77), $P \times P$ diagonal matrix $\hat{\mathbf{\Lambda}}_S$ and $(KL - P) \times (KL - P)$ diagonal matrix $\hat{\mathbf{\Lambda}}_N$ contain signal and noise eigenvalues, respectively, i.e.,

$$\hat{\mathbf{\Lambda}}_S = \text{diag}\{\hat{\lambda}_1, \hat{\lambda}_2, \ldots, \hat{\lambda}_\text{P}\} \tag{A.78}$$

$$\hat{\mathbf{\Lambda}}_N = \text{diag}\{\hat{\lambda}_{\text{P}+1}, \hat{\lambda}_{\text{P}+2}, \ldots, \hat{\lambda}_\text{KL}\} \tag{A.79}$$

A.8 Multipath Channel Estimation

Multipath channel estimation is the final goal of this chapter. Two main channel parameters are DOAs and delays. To formulate the signal model, I first consider 4D parameter estimation [126] and then finally I reach to the final model by considering only 2D. Afterward, I demonstrate that channel model becomes similar to the array processing signal model which has already been discussed in the previous sections in this chapter. Using this signal model, we can implement array processing algorithm to estimate the channel parameters. However, in this chapter, I will introduce a channel model formulated as a multidimensional harmonic retrieval problem for a single user in multipath environment [126].

A.8.1 Signal Model

Consider a MIMO system in which the signal is assumed to travel from the transmitter to the receiver. We also consider a multipath environment where P discrete propagation paths existed. Assume that each path is involved with different parameters like DOA (θ), propagation delay (τ_p).

To fit with standard data transmission, first, perform band-limiting by transmitting the data through a low pass filter and after that sampling is done at sampling period T_s.

In order to make it simple, consider only 2D case in detailed. Therefore, one source and array receive antennas are only considered. Now, parameters of interest are propagation delays τ_p and DOA θ_p for $p = 1, 2, ..., P$. The goal is to estimate P pairs of exponential (a_p, b_p) which can be seen as a 2D harmonic problem [126]

Considering $k = 1, \ldots, K$ is the frequency subcarrier index along one dimension of the array output data and $l = 1, \ldots, L$ denotes the antenna element index along the other dimension of the array output data as in Figure A.5.

Now, from [126], we can formulate the equation for 2D as

$$y_{k,l}(i) = \sum_{p=1}^{P} z_p(i)\, a_p^k b_p^l + n_{k,l}(i) \tag{A.80}$$

where

$$a_p = e^{-j(2\pi/K)\tau_p} \tag{A.81}$$

and

$$b_p = e^{-j(2\pi d_R/\lambda)\cos\theta_p} \tag{A.82}$$

Our two parameters of interest are now a_p and b_p. Now, K and L are the sample support along the a and b axis, respectively [126]. d_R represents the elemental spacing of the receive side.

Let us define steering vector $\mathbf{a}_p$ for p-th path

$$\mathbf{a}_p = [a_p^1, a_p^2, \ldots, a_p^K]^T, \tag{A.83}$$

and vector $\mathbf{b}_p$ for p-th path

$$\mathbf{b}_p = [b_p^1, b_p^2, \ldots, b_p^L]^T. \tag{A.84}$$

Steering vectors $\mathbf{a}_p$ form the column of a $K \times P$ matrix $\mathbf{A}$ defined as

$$\mathbf{A} = [\mathbf{a}_1, \mathbf{a}_2, \ldots, \mathbf{a}_P]. \tag{A.85}$$

It should be emphasized, although I use the same notation for the array steering matrix, namely $\mathbf{A}$, the definition of $\mathbf{A}$ in Section A.6 is slightly

differ from the equation (A.85) although its structure is identical.

Vectors $\mathbf{b}_p$ form the column of a $L \times P$ matrix $\mathbf{B}$ defined as

$$\mathbf{B} = [\mathbf{b}_1, \mathbf{b}_2, \ldots, \mathbf{b}_P] \tag{A.86}$$

Introducing Khatri-Rao product between $\mathbf{B}$ and $\mathbf{A}$, the equation becomes as

$$\mathbf{B} \circ \mathbf{A} = [\mathbf{b}_1 \otimes \mathbf{a}_1, \mathbf{b}_2 \otimes \mathbf{a}_2, \mathbf{b}_3 \otimes \mathbf{a}_3, ..., \mathbf{b}_P \otimes \mathbf{a}_P]\,. \tag{A.87}$$

Introducing a new vector

$$\mathbf{\Omega} = [(a_1, b_1)\,, ..., (a_P, b_P)]$$

containing the parameters of interest and defines the matrix $\mathbf{A} \in \mathbb{C}^{K \times P}$ and $\mathbf{B} \in \mathbb{C}^{L \times P}$. Finally, we could state the 2D harmonic retrieval problem as vector [126]

$$\mathbf{y}\,(i) = \ \mathbf{H}\,(\mathbf{\Omega})\,\mathbf{z}\,(i) + \mathbf{n}\,(i) \tag{A.88}$$

where, $\mathbf{y}\,(i)$ denotes the measurement vector and it can be written as

$$\mathbf{y}\,(i) = [y_{1,1}\,(i)\,, y_{2,1}\,(i)\,, ..., y_{K-1,L}\,(i)\,, y_{K,L}\,(i)]^T \in \mathbb{C}^{KL \times 1}.$$

2D Signal matrix $\mathbf{H}\,(\mathbf{\Omega})$ is calculated by the Khatri-Rao product of matrices $\mathbf{B}$ and $\mathbf{A}$,

$$\mathbf{H}\,(\mathbf{\Omega}) = \mathbf{B} \circ \mathbf{A} \in \mathbb{C}^{KL \times P}. \tag{A.89}$$

In equation (A.88), $\mathbf{z}\,(i) = [z_1, z_2, ..., z_P]^K \in \mathbb{C}^{KL \times P}$ is the complex envelop of the harmonics, which is treated as a nuisance parameter and $\mathbf{n}\,(i)$ is a vector stands for additive zero mean complex Gaussian noise with covariance matrix $\sigma^2 \mathbf{I}_{KL}$.

This is to be noted that equation (A.88) has the same structure as the signal model introduced in Section A.6. Matrix $\mathbf{H}$ has the parameters of interest as in structure $\mathbf{A}$ in equation (A.55). $\mathbf{z}\,(i)$ has the similar structure as complex vector $\mathbf{s}(t)$ in equation (A.55). Therefore, we can finally apply unitary 2D ESPRIT to estimate the DOA and path delays of channel from data vector $\mathbf{y}(i)$ in equation (A.88). Here, $\mathbf{H}\,(\mathbf{\Omega})$ corresponds to the channel in frequency domain.

Appendix B

Unitary 2D ESPRIT

The ESPRIT algorithm was first proposed for 1D DOA estimation in the ULAs, as stated in Chapter 5. Later on the 1D ESPRIT technique was generalised into 2D- and multi-dimensional (MD) ESPRIT, in [122] and [125] for the URAs.

Here, we describe the mathematical formulation of ESPRIT based on the description of [12]. We consider two selection matrices $\mathbf{J}_{K1}$ and $\mathbf{J}_{K2}$ both of the same size, $K-1 \times K$

$$\mathbf{J}_{K1} \triangleq \begin{bmatrix} 1 & 0 & 0\ldots & 0 & 0 \\ 0 & 1 & 0\ldots & 0 & 0 \\ \vdots & \vdots & \vdots & \ddots & \vdots & \vdots \\ 0 & 0 & 0\ldots & 1 & 0 \end{bmatrix} \tag{B.1}$$

and

$$\mathbf{J}_{K1} \triangleq \begin{bmatrix} 0 & 1 & 0\ldots & 0 & 0 \\ 0 & 0 & 1\ldots & 0 & 0 \\ \vdots & \vdots & \vdots & \ddots & \vdots & \vdots \\ 0 & 0 & 0\ldots & 0 & 1 \end{bmatrix} \tag{B.2}$$

respectively. It is clear from (B.1) that $\mathbf{J}_{K1}$ selects the first $K-1$ components of a vector of size $K \times 1$ when multiplied it from the left side. Similarly $\mathbf{J}_{K2}$ selects the last $K-1$ components.

Using the selection matrices $\mathbf{J}_{K1}$ and $\mathbf{J}_{K2}$, the steering vector defined in (A.58) satisfy the shift invariance property [135], i.e.,

$$e^{j\frac{2\pi}{\lambda}d_x\mu}\mathbf{J}_{K1}\mathbf{a}_K(\mu) = \mathbf{J}_{K2}\mathbf{a}_K(\mu), \tag{B.3}$$

for $\mu = \mu_1, \ldots, \mu_P$, and $\nu = \nu_1, \ldots, \nu_P$, Let us multiply both sides of (B.3) by $\mathbf{Q}_K\mathbf{Q}_K^H$, so that

$$e^{j\frac{2\pi}{\lambda}d_x\mu}\mathbf{J}_{K1}\mathbf{Q}_K\mathbf{Q}_K^H\mathbf{a}_K(\mu) = \mathbf{J}_{K2}\mathbf{Q}_K\mathbf{Q}_K^H\mathbf{a}_K(\mu), \tag{B.4}$$

where, $\mathbf{Q}_K$ is unitary matrix in (A.66). Using definition of $\mathbf{d}_K(\mu)$ from (A.68), we can write

$$e^{j\frac{2\pi}{\lambda}d_x\mu}\mathbf{J}_{K1}\mathbf{Q}_K\mathbf{d}_K(\mu) = \mathbf{J}_{K2}\mathbf{Q}_K\mathbf{d}_K(\mu). \tag{B.5}$$

In the next step, we multiply both sides of (B.5) by $\mathbf{Q}_{K-1}^H$ from the left then we have

$$e^{j\frac{2\pi}{\lambda}d_x\mu}\mathbf{Q}_{K-1}^H\mathbf{J}_{K1}\mathbf{Q}_K\mathbf{d}_K(\mu) = \mathbf{Q}_{K-1}^H\mathbf{J}_{K2}\mathbf{Q}_K^H\mathbf{d}_K(\mu). \tag{B.6}$$

It should be noted that $\mathbf{J}_{K1}$ and $\mathbf{J}_{K2}$ satisfy the following relationship

$$\mathbf{\Pi}_{K-1}\mathbf{J}_{K2}\mathbf{\Pi}_K = \mathbf{J}_{K1}. \tag{B.7}$$

Using section A.6 and equation (B.7), the fact that

$$\mathbf{Q}_K\mathbf{\Pi}_K = \mathbf{Q}_K^*, \tag{B.8}$$

we can derive the following relation:

$$\begin{aligned}\mathbf{Q}_{K-1}^H\mathbf{J}_{K2}\mathbf{Q}_K^H &= \mathbf{Q}_{K-1}^H\mathbf{\Pi}_{K-1}\mathbf{\Pi}_{K-1}\mathbf{J}_{K2}\mathbf{Q}_{K-1}^H\mathbf{\Pi}_K\mathbf{\Pi}_K \\ &= \mathbf{Q}_{K-1}^T\mathbf{J}_{K1}\mathbf{Q}_K^* \\ &= (\mathbf{Q}_{K-1}^T\mathbf{J}_{K1}\mathbf{Q}_K)^*. \end{aligned}\tag{B.9}$$

Taking the real and imaginary parts of (B.9), we define

$$\mathbf{F_1} \triangleq \Re\{\mathbf{Q}_{K-1}^H\mathbf{J}_{K2}\mathbf{Q}_K^H\} \tag{B.10}$$

$$\mathbf{F_2} \triangleq \Im\{\mathbf{Q}_{K-1}^H\mathbf{J}_{K2}\mathbf{Q}_K^H\}. \tag{B.11}$$

Therefore, (B.4) becomes

$$e^{j\frac{2\pi}{\lambda}d_x\mu}(\mathbf{F_1} - j\mathbf{F_2})\mathbf{d}_K(\mu) = (\mathbf{F_1} + j\mathbf{F_2})\mathbf{d}_K(\mu). \tag{B.12}$$

From (B.12) we obtain

$$(e^{j\frac{2\pi}{\lambda}d_x\mu/2} - e^{-j\frac{2\pi}{\lambda}d_x\mu/2})\mathbf{F_1}\mathbf{d}_K(\mu) = j(e^{j\frac{2\pi}{\lambda}d_x\mu/2} + e^{-j\frac{2\pi}{\lambda}d_x\mu/2})\mathbf{F_2}\mathbf{d}_K(\mu). \tag{B.13}$$

Then (B.13) can be reformulated as

$$\tan(\frac{2\pi}{\lambda}\mathrm{d_x}\mu/2)\mathbf{F_1}\mathbf{d}_\mathrm{K}(\mu)\mathbf{d}_\mathrm{L}^\mathrm{T}(\nu) = \mathbf{F_2}\mathbf{d}_\mathrm{K}(\mu)\mathbf{d}_\mathrm{L}^\mathrm{T}(\nu). \tag{B.14}$$

For $P < K$ sources, let us define matrix $\mathcal{D}$ as

$$\mathcal{D}(\mu, \nu) = \mathbf{d}_K(\mu)\mathbf{d}_L^T(\nu). \tag{B.15}$$

It was observed that $\mathbf{d}_K(\mu_P)$ and $\mathbf{d}_L(\nu_P)$ satisfy invariance relationship in $(B.14)$ and $(B.24)$, respectively. Therefore,

$$\tan(\frac{2\pi}{\lambda}\mathrm{d_x}\mu/2)\mathbf{F_1}\mathcal{D}(\mu, \nu) = \mathbf{F_2}\mathcal{D}(\mu, \nu). \tag{B.16}$$

An important property of vectorization operator is given as

$$\mathrm{vec}\left\{\mathbf{ABC}\right\} = (\mathbf{C} \otimes \mathbf{A})\mathrm{vec}\left\{\mathbf{B}\right\}. \tag{B.17}$$

Using this vectorization operator property, (B.16) can be written as

$$\tan(\frac{2\pi}{\lambda}\mathrm{d_x}\mu/2)\mathbf{F}_{\mu\mathbf{1}}\mathbf{d}(\mu, \nu) = \mathbf{F}_{\mu\mathbf{2}}\mathbf{d}(\mu, \nu), \tag{B.18}$$

where, $\mathbf{F}_{\mu\mathbf{1}}$ is a $(K-1)L \times KL$ matrix

$$\mathbf{F}_{\mu\mathbf{1}} = (\mathbf{I}_K \otimes \mathbf{F_1}), \tag{B.19}$$

$\mathbf{F}_{\mu\mathbf{2}}$ is a $(K-1)L \times KL$ matrix

$$\mathbf{F}_{\mu\mathbf{2}} = (\mathbf{I}_K \otimes \mathbf{F_2}), \tag{B.20}$$

and using (B.17), we have

$$\mathbf{d}(\mu, \nu) = \mathrm{vec}(\mathcal{D}(\mu, \nu)). \tag{B.21}$$

The same procedure can be performed for other dimension as well, as we did for steering vector defined in (A.58). Consider two selection matrices $\mathbf{J}_{L1}$ and $\mathbf{J}_{L2}$ both of the same size, i.e., $L-1 \times L$ but $\mathbf{J}_{L1}$ selects the first $L-1$ component of a steering vector $\mathbf{a}_L(\nu)$ and $\mathbf{J}_{L2}$ selects the last $L-1$ component of the same steering vector. Using these selection matrices, $\mathbf{F_3}$ and $\mathbf{F_4}$ are defined using the same procedure as for $\mathbf{a}_L(\nu)$ in (B.4), (B.5), (B.6), and (B.9)

$$\mathbf{F_3} = \Re\{\mathbf{Q}_{L-1}^H\mathbf{J}_{L3}\mathbf{Q}_L^H\} \tag{B.22}$$

$$\mathbf{F_4} = \Im\{\mathbf{Q}_{L-1}^H\mathbf{J}_{L4}\mathbf{Q}_L^H\}. \tag{B.23}$$

Using the same reasoning as (B.12), and (B.13), we obtain

$$\{\tan(\frac{2\pi}{\lambda}\mathrm{d_y}\nu/2)\mathbf{F_3}\mathbf{d_L}(\nu)\mathbf{d_L}(\nu)^{\mathrm{T}}\}^{\mathrm{T}} = \{\mathbf{F_4}\mathbf{d_L}(\nu)\mathbf{d_L}(\nu)^{\mathrm{T}}\}^{\mathrm{T}}, \tag{B.24}$$

where, $\mathbf{d}_K(\mu)$ and $\mathbf{d}_L(\nu)$ are real-valued steering vectors defined in (A.68) and (A.69), respectively.

Since $\mathbf{d}_L(\nu)$ satisfy the invariance relation in (B.24), we can write

$$\tan(\frac{2\pi}{\lambda}\mathrm{d_y}\nu/2)\mathcal{D}(\mu,\nu)\mathbf{F_3}^{\mathrm{T}} = \mathcal{D}(\mu,\nu)\mathbf{F_4}^{\mathrm{T}}. \tag{B.25}$$

We can use the vectorization operator as in (B.18), it can be seen that

$$\tan(\frac{2\pi}{\lambda}\mathrm{d_y}\mu/2)\mathbf{F}_{\nu\mathbf{3}}\mathbf{d}(\mu,\nu) = \mathbf{F}_{\nu\mathbf{4}}\mathbf{d}(\mu,\nu), \tag{B.26}$$

where, $\mathbf{d}(\mu,\nu)$ is defined in (B.21), $\mathbf{F}_{\nu\mathbf{3}}$ and $\mathbf{F}_{\nu\mathbf{3}}$ are $K(L-1)\times KL$ matrices given as

$$\mathbf{F}_{\nu\mathbf{3}} = (\mathbf{F_3}\otimes\mathbf{I}_L), \tag{B.27}$$

$$\mathbf{F}_{\nu\mathbf{4}} = (\mathbf{F_4}\otimes\mathbf{I}_L). \tag{B.28}$$

Defining $\mathbf{D}(\mu,\nu)$ as a matrix containing vectors $\mathbf{d}(\mu,\nu)$ for all sources

$$\mathbf{D}(\mu,\nu) = [\mathbf{d}(\mu_1,\nu_1),\mathbf{d}(\mu_2,\nu_2),\ldots,\mathbf{d}(\mu_P,\nu_P)], \tag{B.29}$$

we can see that

$$\mathbf{F}_{\mu\mathbf{1}}\mathbf{D}(\mu,\nu)\mathbf{\Phi}_\mu = \mathbf{F}_{\mu\mathbf{2}}\mathbf{D}(\mu,\nu) \tag{B.30}$$

where,

$$\mathbf{\Phi}_\mu = \mathrm{diag}\{\tan(\frac{2\pi}{\lambda}\mathrm{d_x}\mu_1/2),\tan(\frac{2\pi}{\lambda}\mathrm{d_x}\mu_2/2),\ldots,\tan(\frac{2\pi}{\lambda}\mathrm{d_x}\mu_\mathrm{P}/2)\}. \tag{B.31}$$

Similarly, (B.26) indicates the shift invariance property for steering matrix $\mathbf{D}(\mu,\nu)$ satisfies

$$\mathbf{F}_{\nu\mathbf{3}}\mathbf{D}(\mu,\nu)\mathbf{\Phi}_\nu = \mathbf{F}_{\nu\mathbf{4}}\mathbf{D}(\mu,\nu) \tag{B.32}$$

where,

$$\mathbf{\Phi}_\nu = \mathrm{diag}\{\tan(\frac{2\pi}{\lambda}\mathrm{d_y}\nu_1/2),\tan(\frac{2\pi}{\lambda}\mathrm{d_y}\nu_2/2),\ldots,\tan(\frac{2\pi}{\lambda}\mathrm{d_y}\nu_\mathrm{P}/2)\}. \tag{B.33}$$

Considering the signal model defined in (A.55), where $\mathbf{x}(t)$ is a $KL\times 1$ received signal for the t-th, for $t=1,\ldots,T$. Taking array output for T snapshots results, in T number of $\mathbf{x}(t)$ vectors. Use of vectorization operator can be made to place the $(KL\times 1)$ vectors as columns of $(KL\times T)$ complex-valued matrix $\mathbf{X}$ such that

$$\mathbf{X} = [\mathbf{x}(1),\mathbf{x}(1),\ldots,\mathbf{x}(T)]. \tag{B.34}$$

$\mathbf{X}$ can be transformed into a real-valued $\mathbf{Y}$ by the following relationship using vectorization operator, i.e.,

$$\mathbf{Y} = (\mathbf{Q}_L^H\otimes\mathbf{Q}_K^H)\mathbf{X} \tag{B.35}$$

A covariance matrix $\mathbf{R}_{yy}$ from (A.70) is formed from $\mathbf{Y}$. Eigen Using eigen-decomposition, $\mathbf{R}_{yy}$ is partitioned into signal space matrix $\mathbf{E}_S$ containing eigenvectors for signal eigenvalues and noise space matrix $\hat{\mathbf{E}}_N$ from (A.72). Since $\mathbf{E}_S$ and $\mathcal{D}(\mu, \nu)$ span the same subspace [122]

$$\mathbf{E_s} = \mathbf{D}(\mu, \nu)\mathbf{T}, \tag{B.36}$$

where, $\mathbf{T}$ is a non-singular $P \times P$ matrix.
From (B.36) we have

$$\mathbf{D}(\mu, \nu) = \mathbf{E_s}\mathbf{T}^{-1} \tag{B.37}$$

Plugging (B.37) into (B.30) and (B.32), and considering the x-axis, we obtain the following

$$\mathbf{F}_{\mu\mathbf{1}}\mathbf{E_s}\mathbf{\Phi}_\mu = \mathbf{F}_{\mu\mathbf{2}}\mathbf{E_s}, \tag{B.38}$$

where, $\mathbf{\Phi}_\mu$ is a $(K-1)L \times P$ matrix

$$\mathbf{\Phi}_\mu = \mathbf{T}^{-1}\mathbf{\Phi}_\mu\mathbf{T}. \tag{B.39}$$

The same relation can be written for the other dimension y-axis, i.e.,

$$\mathbf{F}_{\nu\mathbf{3}}\mathbf{E_s}\mathbf{\Phi}_\nu = \mathbf{F}_{\nu\mathbf{4}}\mathbf{E_s}, \tag{B.40}$$

where, $\mathbf{\Phi}_\nu$ is a $(L-1)K \times P$ matrix

$$\mathbf{\Phi}_\nu = \mathbf{T}^{-1}\mathbf{\Phi}_\nu\mathbf{T} \tag{B.41}$$

It is clear that $\mathbf{\Phi}_\mu$ and $\mathbf{\Phi}_\nu$ contain parameters of interest (μ, ν) to be estimated. Therefore (B.38) and (B.40) are solved for $\mathbf{\Phi}_\mu$ and $\mathbf{\Phi}_\nu$ and we have

$$\mathbf{\Phi}_\mu = \mathbf{F}_{\mu\mathbf{1}}{}^\dagger\mathbf{E_s}{}^\dagger\mathbf{F}_{\mu\mathbf{2}}\mathbf{E_s}, \tag{B.42}$$

and

$$\mathbf{\Phi}_\nu = \mathbf{F}_{\nu\mathbf{3}}{}^\dagger\mathbf{E_s}{}^\dagger\mathbf{F}_{\nu\mathbf{4}}\mathbf{E_s}. \tag{B.43}$$

Pairing $\mathbf{\Phi}_\mu$ and $\mathbf{\Phi}_\nu$ together through the following definition

$$\mathbf{\Phi} \triangleq \mathbf{\Phi}_\mu + j\mathbf{\Phi}_\nu. \tag{B.44}$$

It can be seen that the eignenvalues of $P \times P$ matrix, denoted by ξ_i, for $i = 1, \ldots, P$, contain our parameter of interest, μ and ν, then these parameter of interest can be calculated from

$$\mu_i = \frac{\lambda}{\pi d_x}\tan^{-1}(\Re\{\xi_\mathrm{i}\}) \tag{B.45}$$

and

$$\nu_i = \frac{\lambda}{\pi d_y}\tan^{-1}(\Im\{\xi_\mathrm{i}\}). \tag{B.46}$$

In practice, we use sample covariance matrix $\hat{\mathbf{R}}_{yy}$ and the estimated signal subspace $\hat{\mathbf{E}}_s$ to perform 2D ESPRIT DOA estimation, where,

$$\hat{\mathbf{R}}_{yy} = \frac{1}{T}\sum_{t=1}^{T}\mathbf{y}\mathbf{y}^H, \text{for } \mathbf{y} = \text{vec}\{\mathbf{Y}\} \tag{B.47}$$

Appendix C

LTE UE event Measurement Reporting-Event A1,A2,A3,A4,A5,B1,B2

In the LTE system, the RRC connection reconfiguration message is used to configure UE measurement reporting. It replaces the measurement control message used in the UMTS system. The standard defines 5 intra-system and 2 inter-system measurement reporting events, as described below.

The LTE events A1, A2, A3, A4 and A5 are based upon either RSRP or RSRQ messages. Inter-system LTE events B1 and B2 are based upon CPICH RSCP or CPICH Ec/Io for UMTS system, RSSI for GSM and pilot strength for CDMA2000.

The criteria for triggering and subsequently cancelling each event are evaluated after layer-3 filtering has been applied. The criteria for each event must be satisfied at least during the time it takes to trigger. The time to trigger can be configured independently fpr each reporting event. The values are as follows: 0,40,64,80,100,128,160,256,320,480,512,640,1024,1280.

Layer-3 filtering is applied prior to evaluate whether or not any measurement reporting events have been triggered.

$Fn = (1 - a) * Fn - 1 + (a * MEASn)$.

Here, Fn = updated filtered measurement result.
$Fn - 1$ = previous filtered measurement result.
$a = (1/2)k/4$, where k is appropriate filter coefficient.

$MEASn$ = latest measurement result received from PHYSICAL layer.

Filter coefficient can be configured independently for LTE RSRP, LTE RSRQ, UMTS CPICH RSCP, UMTS CPICH Ec/Io and GSM RSSI.

LTE Event A1: The LTE Event A1 is triggered when the serving cell becomes better than a threshold. The event is triggered when the following condition is true:

$$MEAs_{serv} - Hyst > Threshold.$$

Triggering of the event is subsequently cancelled when the following condition is true:

$$MEAs_{serv} + Hyst < Threshold$$

The hysteresis can be configured with a value between 0 and 30 dB.
Event A2: The LTE Event A2 is triggered when the serving cell becomes worse than a threshold. The event is triggered when the following condition is true:

$$MEAs_{serv} + Hyst < Threshold$$

Triggering of the event is subsequently cancelled when the following condition is true.

$$MEAs_{serv} - Hyst > Threshold$$

The hysteresis can be configured with a value between 0 and 30 dB.

Event A3: The LTE Event A3 is triggered when a neighbouring cell becomes better than the serving cell by an offset. The offset can be either positive or negative. The event is triggered when the following condition is true:

$$MEAS_{neigh} + O_{neigh,freq} + O_{neigh,cell} - Hyst > MEAs_{serv} + O_{neigh,freq} + Oserv, cell + Offset$$

$$MEAS_{neigh} + O_{neigh,freq} + O_{neigh,cell} + Hyst < MEAs_{serv} + O_{neigh,freq} + Oserv, cell + Offset$$

Event A4: The LTE Event A4 is triggered when a neighbouring cell becomes better than a threshold.

$$MEAS_{neigh} + O_{neigh,freq} + O_{neigh,cell} - Hyst > Threshold$$

Triggering of the event is subsequently cancelled when the following condition is true:

$$MEAS_{neigh} + O_{neigh,freq} + O_{neigh,cell} + Hyst < Threshold$$

Event A5: LTE Event A5 is triggered when the serving cell becomes worse than threshold-1 while a neighbouring cell becomes better than threshold-2. The event is triggered when both of the following conditions are true:

$$MEAs_{serv} + Hyst < Threshold - 1$$

$$MEAS_{neigh} + O_{neigh,freq} + O_{neigh,cell} - Hyst > Threshold - 2$$

Triggering of the event is subsequently cancelled when either of the following conditions are true:

$$MEAs_{serv} - Hyst > Threshold - 1$$

$$MEAS_{neigh} + O_{neigh,freq} + O_{neigh,cell} + Hyst < Threshold - 2$$

LTE Event B1: The LTE Event B1 is triggered when a neighbouring inter-system cell becomes better than a threshold. The event is triggered when the following condition is true:

$$MEAS_{neigh} + O_{neigh,freq} - Hyst > Threshold$$

Triggering of the event is subsequently cancelled when the following condition is true:

$$MEAS_{neigh} + O_{neigh,freq} + Hyst < Threshold$$

Event B2: The LTE Event B2 is triggered when the serving cell becomes worse than threshold-1 while a neighbouring inter-system cell becomes better than threshold-2. The event is triggered when both of the

following conditions are true:

$MEAs_{serv} + Hyst < Threshold - 1$

$MEAS_{neigh} + O_{neigh,freq} - Hyst > Threshold - 2$

Triggering of the event is subsequently cancelled when either of the following conditions are true:

$MEAs_{serv} - Hyst > Threshold - 1$

$MEAS_{neigh} + O_{neigh,freq} + Hyst < Threshold - 2$

Bibliography

[1] Z. Ma, Z. Zhang, Z. Ding, P. Fan, and H. Li, "Key techniques for 5g wireless communications: network architecture, physical layer, and mac layer perspectives," *Science China Information Sciences*, vol. 58, no. 4, pp. 1–20, 2015.

[2] P. Demestichas, A. Georgakopoulos, D. Karvounas, K. Tsagkaris, V. Stavroulaki, J. Lu, C. Xiong, and J. Yao, "5g on the horizon: key challenges for the radio-access network," *Vehicular Technology Magazine, IEEE*, vol. 8, no. 3, pp. 47–53, 2013.

[3] J. Mundy, "What Is Massive MIMO Technology?." https://5g.co.uk/guides/what-is-massive-mimo-technology/. [Online; accessed 10-March-2018].

[4] D. Brenner, "FCC vote will pave the path for 5G advancements to mobilize mmWave [UPDATED]." https://www.qualcomm.com/news/onq/2016/07/12/upcoming-fcc-vote-will-pave-path-5g-advancements-mobilize-mmwave, JUL 13, 2016, Qualcomm Technologies, Inc. [Online; accessed 10-March-2018].

[5] N. Bhushan, J. Li, D. Malladi, R. Gilmore, D. Brenner, A. Damnjanovic, R. Sukhavasi, C. Patel, and S. Geirhofer, "Network densification: the dominant theme for wireless evolution into 5g," *Communications Magazine, IEEE*, vol. 52, no. 2, pp. 82–89, 2014.

[6] "Cloud RAN: A Centralized Solution for Mobile Operators Seeking Improved Network Efficiency." https://www.sdnzone.com. [Online; accessed 26-January-2016].

[7] B. Wang and K. R. Liu, "Advances in cognitive radio networks: A survey," *IEEE Journal of selected topics in signal processing*, vol. 5, no. 1, pp. 5–23, 2011.

[8] H. Mehta, "Recent Advances in Cognitive Radios." https://www.cse.wustl.edu/~jain/cse574-14/ftp/cr/index.html#Beibei, Last Modified: April 30, 2014. [Online; accessed 12-March-2018].

[9] J. G. Andrews, S. Buzzi, W. Choi, S. V. Hanly, A. Lozano, A. C. Soong, and J. C. Zhang, "What will 5g be?," *Selected Areas in Communications, IEEE Journal on*, vol. 32, no. 6, pp. 1065–1082, 2014.

[10] E. Hossain, M. Rasti, H. Tabassum, and A. Abdelnasser, "Evolution toward 5g multi-tier cellular wireless networks: An interference management perspective," *Wireless Communications, IEEE*, vol. 21, no. 3, pp. 118–127, 2014.

[11] A. Asadi, Q. Wang, and V. Mancuso, "A survey on device-to-device communication in cellular networks," *Communications Surveys & Tutorials, IEEE*, vol. 16, no. 4, pp. 1801–1819, 2014.

[12] H. Ullah, "Multi-antenna aided positioning in lte networks," Master's thesis, Technische Universitaet Darmstadt, 2013.

[13] J. Lim and D. Hong, "Mobility and handover management for heterogeneous networks in lte-advanced," *Wireless personal communications*, vol. 72, no. 4, pp. 2901–2912, 2013.

[14] O. N. Yilmaz, Z. Li, K. Valkealahti, M. A. Uusitalo, M. Moisio, P. Lundén, and C. Wijting, "Smart mobility management for d2d communications in 5g networks," in *Wireless Communications and Networking Conference Workshops (WCNCW), 2014 IEEE*, pp. 219–223, IEEE, 2014.

[15] G. Jaheon, S. J. Bae, S. F. Hasan, and M. Y. Chung, "A combined power control and resource allocation scheme for d2d communication underlaying an lte-advanced system," *IEICE Transactions on Communications*, vol. 96, no. 10, pp. 2683–2692, 2013.

[16] K.-C. Chen, W.-E. Chen, W.-C. Chung, Y.-C. Chung, Q. Cui, C.-H. Hsu, S.-Y. Lien, Z. Niu, Z. Tian, J. Wang, *et al.*, "Efficient network structure of 5g mobile communications," in *Wireless Algorithms, Systems, and Applications*, pp. 19–28, Springer, 2015.

[17] M. Kurk, "Fast-forward to the future with 5g networks." https://www.commscope.com/5g/article-fast-forward-to-the-future-with-5G-networks/, 2017 CommScope. [Online; accessed 09-March-2018].

[18] "A Look into the Future: The Applications Behind 5G, white paper." https://ssl.lvl3.on24.com/event/16/20/75/4/rt/1/documents/resourceList1480528353064/alookintothefutureapplicationsof5gyost1519402928842.pdf, March 7, 2018 IEEE Communications Society sponsored by National Instruments. [Online; accessed 09-March-2018].

[19] S. Barua, S. C. Lam, P. Ghosa, S. Xing, and K. Sandrasegaran, "A survey of direction of arrival estimation techniques and implementation of channel estimation based on scme," in *2015 12th International Conference on Electrical Engineering/Electronics, Computer, Telecommunications and Information Technology (ECTI-CON)*, pp. 1–5, June 2015.

[20] S. Barua and R. Braun, "Direction of arrival (doa) and channel estimation," in *Self-Organized Mobile Communication Technologies and Techniques for Network Optimization*, pp. 216–235, IGI Global, 2016.

[21] S. Barua and R. Braun, "A novel approach of mobility management for the d2d communications in 5g mobile cellular network system," in *Network Operations and Management Symposium (APNOMS), 2016 18th Asia-Pacific*, pp. 1–4, IEEE, 2016.

[22] S. Barua and R. Braun, "Mobility management of d2d communication for the 5g cellular network system: A study and result," in *2017 17th International Symposium on Communications and Information Technologies (ISCIT)*, pp. 1–6, Sept 2017.

[23] S. Barua and R. Braun, "A markovian approach to the mobility management for the d2d communication in 5g cellular network system," in *The 5th Asia Pacific International Conference on Computer Assisted and System Engineering (APCASE 2017)*, Springer, (accepted and presented), 2017.

[24] "Timeline of Telecommunications." [Online; accessed 20-January-2016].

[25] "The History of Telecommunication." https://www.au.shoretel.com. [Online; accessed 20-January-2016].

[26] " Radiolinja's History." http://corporate.elisa.com/. [Online; accessed 20-January-2016].

[27] "ITU, "IMT-2000 Project - ITU"," 4 July 2002.

[28] Z. Niu, "Tango: traffic-aware network planning and green operation," *Wireless Communications, IEEE*, vol. 18, no. 5, pp. 25–29, 2011.

[29] "FP7 European Project 317669 METIS (Mobile and WIreless Communications Enablers for the Twenty-Twenty Information Society)." www.metis2020.com/. [Online; accessed 19-January-2016].

[30] "FP7 European Project 318555 5G NOW (5th Generation Non-Orthogonal Waveforms for Asynchronous Signalling)." www.5gnow.eu/. [Online; accessed 19-January-2016].

[31] F. Boccardi, R. W. Heath, A. Lozano, T. L. Marzetta, and P. Popovski, "Five disruptive technology directions for 5g," *Communications Magazine, IEEE*, vol. 52, no. 2, pp. 74–80, 2014.

[32] Huawei, "The second phase of lte-advanced, lte-b: 30-fold capacity boosting of lte," *Huawei Technologies Co. Ltd.*, pp. 1–20, 2013.

[33] A. Osseiran, F. Boccardi, V. Braun, K. Kusume, P. Marsch, M. Maternia, O. Queseth, M. Schellmann, H. Schotten, H. Taoka, *et al.*, "Scenarios for 5g mobile and wireless communications: the vision of the metis project," *Communications Magazine, IEEE*, vol. 52, no. 5, pp. 26–35, 2014.

[34] J. Xu, J. Wang, Y. Zhu, Y. Yang, X. Zheng, S. Wang, L. Liu, K. Horneman, and Y. Teng, "Cooperative distributed optimization for the hyper-dense small cell deployment," *Communications Magazine, IEEE*, vol. 52, no. 5, pp. 61–67, 2014.

[35] Y. Kishiyama, A. Benjebbour, T. Nakamura, and H. Ishii, "Future steps of lte-a: evolution toward integration of local area and wide area systems," *Wireless Communications, IEEE*, vol. 20, no. 1, pp. 12–18, 2013.

[36] L. Lu, G. Y. Li, A. L. Swindlehurst, A. Ashikhmin, and R. Zhang, "An overview of massive mimo: Benefits and challenges," *Selected Topics in Signal Processing, IEEE Journal of*, vol. 8, no. 5, pp. 742–758, 2014.

[37] E. Larsson, O. Edfors, F. Tufvesson, and T. Marzetta, "Massive mimo for next generation wireless systems," *Communications Magazine, IEEE*, vol. 52, no. 2, pp. 186–195, 2014.

[38] J. Hoydis, S. Ten Brink, and M. Debbah, "Massive mimo in the ul/dl of cellular networks: How many antennas do we need?," *Selected Areas*

in Communications, IEEE Journal on, vol. 31, no. 2, pp. 160–171, 2013.

[39] F. Rusek, D. Persson, B. K. Lau, E. G. Larsson, T. L. Marzetta, O. Edfors, and F. Tufvesson, "Scaling up mimo: Opportunities and challenges with very large arrays," *Signal Processing Magazine, IEEE*, vol. 30, no. 1, pp. 40–60, 2013.

[40] Z. Xiang, M. Tao, and X. Wang, "Massive mimo multicasting in noncooperative cellular networks," *Selected Areas in Communications, IEEE Journal on*, vol. 32, no. 6, pp. 1180–1193, 2014.

[41] N. Sidiropoulos, T. Davidson, and Z. Luo, "Transmit beamforming for physical-layer multicasting," *Signal Processing, IEEE Transactions on*, vol. 54, no. 6, pp. 2239–2251, 2006.

[42] A. Lozano, "Long-term transmit beamforming for wireless multicasting," in *Acoustics, Speech and Signal Processing, 2007. ICASSP 2007. IEEE International Conference on*, vol. 3, pp. III–417, IEEE, 2007.

[43] B. Hassibi and B. M. Hochwald, "How much training is needed in multiple-antenna wireless links?," *Information Theory, IEEE Transactions on*, vol. 49, no. 4, pp. 951–963, 2003.

[44] N. Jindal and A. Lozano, "A unified treatment of optimum pilot overhead in multipath fading channels," *Communications, IEEE Transactions on*, vol. 58, no. 10, pp. 2939–2948, 2010.

[45] Y. Zeng, R. Zhang, and Z. N. Chen, "Electromagnetic lens-focusing antenna enabled massive mimo: Performance improvement and cost reduction," *Selected Areas in Communications, IEEE Journal on*, vol. 32, no. 6, pp. 1194–1206, 2014.

[46] S. Wu, C.-X. Wang, E.-H. M. Aggoune, M. M. Alwakeel, and Y. He, "A non-stationary 3-d wideband twin-cluster model for 5g massive mimo channels," *Selected Areas in Communications, IEEE Journal on*, vol. 32, no. 6, pp. 1207–1218, 2014.

[47] A. Kammoun, H. Khanfir, Z. Altman, M. Debbah, and M. Kamoun, "Preliminary results on 3d channel modeling: From theory to standardization," *Selected Areas in Communications, IEEE Journal on*, vol. 32, no. 6, pp. 1219–1229, 2014.

[48] A. Adhikary, E. Al Safadi, and G. Caire, "Massive mimo and inter-tier interference coordination," in *Information Theory and Applications Workshop (ITA), 2014*, pp. 1–10, IEEE, 2014.

[49] J. Chen and V. K. Lau, "Two-tier precoding for fdd multi-cell massive mimo time-varying interference networks," *Selected Areas in Communications, IEEE Journal on*, vol. 32, no. 6, pp. 1230–1238, 2014.

[50] A. Adhikary, E. Al Safadi, M. K. Samimi, R. Wang, G. Caire, T. S. Rappaport, and A. F. Molisch, "Joint spatial division and multiplexing for mm-wave channels," *Selected Areas in Communications, IEEE Journal on*, vol. 32, no. 6, pp. 1239–1255, 2014.

[51] Z. Pi and F. Khan, "An introduction to millimeter-wave mobile broadband systems," *Communications Magazine, IEEE*, vol. 49, no. 6, pp. 101–107, 2011.

[52] T. S. Rappaport, S. Sun, R. Mayzus, H. Zhao, Y. Azar, K. Wang, G. N. Wong, J. K. Schulz, M. Samimi, and F. Gutierrez, "Millimeter wave mobile communications for 5g cellular: It will work!," *Access, IEEE*, vol. 1, pp. 335–349, 2013.

[53] C. Mobile, "C-ran: the road towards green ran," *White Paper, ver*, vol. 2, 2011.

[54] V. N. Ha, L. B. Le, and N.-D. Dao, "Cooperative transmission in cloud ran considering fronthaul capacity and cloud processing constraints," in *Wireless Communications and Networking Conference (WCNC), 2014 IEEE*, pp. 1862–1867, IEEE, 2014.

[55] Z. Zhu, P. Gupta, Q. Wang, S. Kalyanaraman, Y. Lin, H. Franke, and S. Sarangi, "Virtual base station pool: towards a wireless network cloud for radio access networks," in *Proceedings of the 8th ACM international conference on computing frontiers*, p. 34, ACM, 2011.

[56] "Network Function VirtualisationAn Introduction, Benefit, Enablers, Challenges and Call for Action, white paper." https://portal.etsi.org/NFV/NFV_White_Paper.pdf, October 22-24, 2012 at the SDN and OpenFlow World Congress, Darmstadt-Germany. [Online; accessed 26-January-2016].

[57] "Network Function VirtualisationNetwork Operator Perspectives on Industry Progress, white paper." https://portal.etsi.org/NFV/

NFV_White_Paper2.pdf, October 22-24, 2012 at the SDN and OpenFlow World Congress, Darmstadt-Germany. [Online; accessed 26-January-2016].

[58] S. Sezer, S. Scott-Hayward, P.-K. Chouhan, B. Fraser, D. Lake, J. Finnegan, N. Viljoen, M. Miller, and N. Rao, "Are we ready for sdn? implementation challenges for software-defined networks," *Communications Magazine, IEEE*, vol. 51, no. 7, pp. 36–43, 2013.

[59] E. Aryafar, A. Keshavarz-Haddad, M. Wang, and M. Chiang, "Rat selection games in hetnets," in *INFOCOM, 2013 Proceedings IEEE*, pp. 998–1006, IEEE, 2013.

[60] S. Hong, M. Sagong, C. Lim, S. Cho, K. Cheun, and K. Yang, "Frequency and quadrature-amplitude modulation for downlink cellular ofdma networks," *Selected Areas in Communications, IEEE Journal on*, vol. 32, no. 6, pp. 1256–1267, 2014.

[61] A. Sahin, I. Guvenc, and H. Arslan, "A survey on multicarrier communications: Prototype filters, lattice structures, and implementation aspects," *Communications Surveys & Tutorials, IEEE*, vol. 16, no. 3, pp. 1312–1338, 2014.

[62] H. S. Dhillon, Y. Li, P. Nuggehalli, Z. Pi, and J. G. Andrews, "Fundamentals of heterogeneous cellular networks with energy harvesting," *Wireless Communications, IEEE Transactions on*, vol. 13, no. 5, pp. 2782–2797, 2014.

[63] N. Golrezaei, P. Mansourifard, A. F. Molisch, and A. G. Dimakis, "Base-station assisted device-to-device communications for high-throughput wireless video networks," *Wireless Communications, IEEE Transactions on*, vol. 13, no. 7, pp. 3665–3676, 2014.

[64] N. Golrezaei, A. G. Dimakis, and A. F. Molisch, "Device-to-device collaboration through distributed storage," in *Global Communications Conference (GLOBECOM), 2012 IEEE*, pp. 2397–2402, IEEE, 2012.

[65] A. Asadi and V. Mancuso, "Energy efficient opportunistic uplink packet forwarding in hybrid wireless networks," in *Proceedings of the fourth international conference on Future energy systems*, pp. 261–262, ACM, 2013.

[66] A. Asadi and V. Mancuso, "On the compound impact of opportunistic scheduling and d2d communications in cellular networks," in *Proceedings of the 16th ACM international conference on Modeling, analysis & simulation of wireless and mobile systems*, pp. 279–288, ACM, 2013.

[67] Q. Wang and B. Rengarajan, "Recouping opportunistic gain in dense base station layouts through energy-aware user cooperation," in *World of Wireless, Mobile and Multimedia Networks (WoWMoM), 2013 IEEE 14th International Symposium and Workshops on a*, pp. 1–9, IEEE, 2013.

[68] K. Doppler, M. Rinne, C. Wijting, C. B. Ribeiro, and K. Hugl, "Device-to-device communication as an underlay to lte-advanced networks," *Communications Magazine, IEEE*, vol. 47, no. 12, pp. 42–49, 2009.

[69] L. Wei, R. Hu, Y. Qian, and G. Wu, "Enable device-to-device communications underlaying cellular networks: challenges and research aspects," *Communications Magazine, IEEE*, vol. 52, no. 6, pp. 90–96, 2014.

[70] L. Song, D. Niyato, Z. Han, and E. Hossain, "Wireless device-to-device communications and networks," 2015.

[71] C. Xu, L. Song, and Z. Han, "Resource management for device-to-device underlay communication," 2014.

[72] K. J. Zou, M. Wang, K. W. Yang, J. Zhang, W. Sheng, Q. Chen, and X. You, "Proximity discovery for device-to-device communications over a cellular network," *Communications Magazine, IEEE*, vol. 52, no. 6, pp. 98–107, 2014.

[73] L. Lei, Y. Zhang, X. Shen, C. Lin, and Z. Zhong, "Performance analysis of device-to-device communications with dynamic interference using stochastic petri nets," *Wireless Communications, IEEE Transactions on*, vol. 12, no. 12, pp. 6121–6141, 2013.

[74] J. Hong, S. Park, H. Kim, S. Choi, and K. B. Lee, "Analysis of device-to-device discovery and link setup in lte networks.," in *PIMRC*, pp. 2856–2860, 2013.

[75] M. N. Tehrani, M. Uysal, and H. Yanikomeroglu, "Device-to-device communication in 5g cellular networks: challenges, solutions, and future directions," *Communications Magazine, IEEE*, vol. 52, no. 5, pp. 86–92, 2014.

[76] P.-K. Huang, E. Qi, M. Park, and A. Stephens, "Energy efficient and scalable device-to-device discovery protocol with fast discovery," in *Sensor, Mesh and Ad Hoc Communications and Networks (SECON), 2013 10th Annual IEEE Communications Society Conference on*, pp. 1–9, IEEE, 2013.

[77] G. Fodor, E. Dahlman, G. Mildh, S. Parkvall, N. Reider, G. Miklós, and Z. Turányi, "Design aspects of network assisted device-to-device communications," *Communications Magazine, IEEE*, vol. 50, no. 3, pp. 170–177, 2012.

[78] K. Doppler, C. B. Ribeiro, and J. Kneckt, "Advances in d2d communications: Energy efficient service and device discovery radio," in *Wireless Communication, Vehicular Technology, Information Theory and Aerospace & Electronic Systems Technology (Wireless VITAE), 2011 2nd International Conference on*, pp. 1–6, IEEE, 2011.

[79] L. Lei, Z. Zhong, C. Lin, and X. Shen, "Operator controlled device-to-device communications in lte-advanced networks," *IEEE Wireless Communications*, vol. 19, no. 3, p. 96, 2012.

[80] X. Lin, J. Andrews, A. Ghosh, and R. Ratasuk, "An overview of 3gpp device-to-device proximity services," *Communications Magazine, IEEE*, vol. 52, no. 4, pp. 40–48, 2014.

[81] "Study on LTE Device to Device Proximity services (Release 12, 3GPP standard TR 36.843)." https://www.3gpp.org, 2013. [Online; accessed 30-January-2016].

[82] L. Lei, X. Shen, M. Dohler, C. Lin, and Z. Zhong, "Queuing models with applications to mode selection in device-to-device communications underlaying cellular networks," *Wireless Communications, IEEE Transactions on*, vol. 13, no. 12, pp. 6697–6715, 2014.

[83] F. Sanchez Moya, V. Venkatasubramanian, P. Marsch, and A. Yaver, "D2d mode selection and resource allocation with flexible ul/dl tdd for 5g deployments," in *Communication Workshop (ICCW), 2015 IEEE International Conference on*, pp. 657–663, IEEE, 2015.

[84] M. Jung, K. Hwang, and S. Choi, "Joint mode selection and power allocation scheme for power-efficient device-to-device (d2d) communication," in *Vehicular Technology Conference (VTC Spring), 2012 IEEE 75th*, pp. 1–5, IEEE, 2012.

[85] J. Seppälä, T. Koskela, T. Chen, and S. Hakola, "Network controlled device-to-device (d2d) and cluster multicast concept for lte and lte-a networks," in *Wireless Communications and Networking Conference (WCNC), 2011 IEEE*, pp. 986–991, IEEE, 2011.

[86] K. Doppler, C.-H. Yu, C. B. Ribeiro, and P. Jänis, "Mode selection for device-to-device communication underlaying an lte-advanced network," in *Wireless Communications and Networking Conference (WCNC), 2010 IEEE*, pp. 1–6, IEEE, 2010.

[87] S. Hakola, T. Chen, J. Lehtomäki, and T. Koskela, "Device-to-device (d2d) communication in cellular network-performance analysis of optimum and practical communication mode selection," in *Wireless Communications and Networking Conference (WCNC), 2010 IEEE*, pp. 1–6, IEEE, 2010.

[88] T. D. Hoang, L. B. Le, and T. Le-Ngoc, "Joint subchannel and power allocation for d2d communications in cellular networks," in *Wireless Communications and Networking Conference (WCNC), 2014 IEEE*, pp. 1338–1343, IEEE, 2014.

[89] C.-H. Yu, O. Tirkkonen, K. Doppler, and C. Ribeiro, "Power optimization of device-to-device communication underlaying cellular communication," in *Communications, 2009. ICC'09. IEEE International Conference on*, pp. 1–5, IEEE, 2009.

[90] B. Guo, S. Sun, and Q. Gao, "Downlink interference management for d2d communication underlying cellular networks," in *Communications in China-Workshops (CIC/ICCC), 2013 IEEE/CIC International Conference on*, pp. 193–196, IEEE, 2013.

[91] J. Shin, J. P. Choi, and J.-W. Choi, "An autonomous interference avoidance scheme for d2d communications through frequency overhearing," in *ICT Convergence (ICTC), 2013 International Conference on*, pp. 1074–1075, IEEE, 2013.

[92] S. Shalmashi, G. Miao, and B. Slimane, "Interference management for multiple device-to-device communications underlaying cellular networks," in *2013 IEEE 24th Annual International Symposium on Personal, Indoor, and Mobile Radio Communications, PIMRC 2013; London; United Kingdom; 8 September 2013 through 11 September 2013*, pp. 223–227, IEEE, 2013.

[93] W. Xu, L. Liang, H. Zhang, S. Jin, J. C. Li, and M. Lei, "Performance enhanced transmission in device-to-device communications: Beamforming or interference cancellation?," in *Global Communications Conference (GLOBECOM), 2012 IEEE*, pp. 4296–4301, IEEE, 2012.

[94] H. Min, J. Lee, S. Park, and D. Hong, "Capacity enhancement using an interference limited area for device-to-device uplink underlaying cellular networks," *Wireless Communications, IEEE Transactions on*, vol. 10, no. 12, pp. 3995–4000, 2011.

[95] X. Xiao, X. Tao, and J. Lu, "A qos-aware power optimization scheme in ofdma systems with integrated device-to-device (d2d) communications," in *Vehicular Technology Conference (VTC Fall), 2011 IEEE*, pp. 1–5, IEEE, 2011.

[96] J. Gu, S. J. Bae, B.-G. Choi, and M. Y. Chung, "Dynamic power control mechanism for interference coordination of device-to-device communication in cellular networks," in *Ubiquitous and Future Networks (ICUFN), 2011 Third International Conference on*, pp. 71–75, IEEE, 2011.

[97] F. Wang, L. Song, Z. Han, Q. Zhao, and X. Wang, "Joint scheduling and resource allocation for device-to-device underlay communication," in *Wireless Communications and Networking Conference (WCNC), 2013 IEEE*, pp. 134–139, IEEE, 2013.

[98] L. Song, D. Niyato, Z. Han, and E. Hossain, "Game-theoretic resource allocation methods for device-to-device communication," *Wireless Communications, IEEE*, vol. 21, no. 3, pp. 136–144, 2014.

[99] L. Lei, Y. Kuang, X. Shen, C. Lin, and Z. Zhong, "Resource control in network assisted device-to-device communications: solutions and challenges," *Communications Magazine, IEEE*, vol. 52, no. 6, pp. 108–117, 2014.

[100] D. Zhu, J. Wang, A. L. Swindlehurst, and C. Zhao, "Downlink resource reuse for device-to-device communications underlaying cellular networks," *Signal Processing Letters, IEEE*, vol. 21, no. 5, pp. 531–534, 2014.

[101] M. Hasan, E. Hossain, and D. I. Kim, "Resource allocation under channel uncertainties for relay-aided device-to-device communication underlaying lte-a cellular networks," *Wireless Communications, IEEE Transactions on*, vol. 13, no. 4, pp. 2322–2338, 2014.

[102] D. Wu, J. Wang, R. Hu, Y. Cai, and L. Zhou, "Energy-efficient resource sharing for mobile device-to-device multimedia communications," *Vehicular Technology, IEEE Transactions on*, vol. 63, no. 5, pp. 2093–2103, 2014.

[103] D. H. Lee, K. W. Choi, W. S. Jeon, and D. G. Jeong, "Two-stage semi-distributed resource management for device-to-device communication in cellular networks," *Wireless Communications, IEEE Transactions on*, vol. 13, no. 4, pp. 1908–1920, 2014.

[104] R. Zhang, X. Cheng, L. Yang, and B. Jiao, "Interference-aware graph based resource sharing for device-to-device communications underlaying cellular networks," in *Wireless Communications and Networking Conference (WCNC), 2013 IEEE*, pp. 140–145, IEEE, 2013.

[105] H. Zhang, T. Wang, L. Song, and Z. Han, "Radio resource allocation for physical-layer security in d2d underlay communications," in *Communications (ICC), 2014 IEEE International Conference on*, pp. 2319–2324, IEEE, 2014.

[106] Y. Peng, Q. Gao, S. Sun, and Z. Yan-Xiu, "Discovery of device-device proximity: Physical layer design for d2d discovery," in *2013 IEEE/CIC International Conference on Communications in China-Workshops (CIC/ICCC)*, 2013.

[107] Y. Zhang, L. Song, W. Saad, Z. Dawy, and Z. Han, "Exploring social ties for enhanced device-to-device communications in wireless networks," in *Global Communications Conference (GLOBECOM), 2013 IEEE*, pp. 4597–4602, IEEE, 2013.

[108] "Feasibility study on proximity based services (ProSe), 3GPP TR 22.803 V12.2.0,2013." https://www.3gpp.org, 2013. [Online; accessed 5-January-2016].

[109] "Feasibility study on proximity based services (ProSe), 3GPP TR 23.703 V0.7.1, 2013." https://www.3gpp.org, 2013. [Online; accessed 5-January-2016].

[110] B. Van Veen and K. Buckley, "Beamforming: a versatile approach to spatial filtering," *ASSP Magazine, IEEE*, vol. 5, no. 2, pp. 4–24, 1988.

[111] G. Bienvenu and L. Kopp, "Optimality of high resolution array processing using the eigensystem approach," *Acoustics, Speech and Signal Processing, IEEE Transactions on*, vol. 31, no. 5, pp. 1235–1248, 1983.

[112] F. Rasheed, "Beamforming doa estimation for a uniform linear array," tech. rep., Electrical and Computer Engineering Department, Drexel University.

[113] G. Y. Y. Chen, Z. Gokeda, *Introduction to Direction-of-Arrival Estimation*. Academic Press, 2009.

[114] H. Krim and M. Viberg, "Two decades of array signal processing research: the parametric approach," *Signal Processing Magazine, IEEE*, vol. 13, no. 4, pp. 67–94, 1996.

[115] J. Capon, "High-resolution frequency-wavenumber spectrum analysis," *Proceedings of the IEEE*, vol. 57, no. 8, pp. 1408–1418, 1969.

[116] N. A. M. Tayem, "Direction of arrival angel estimation schemes for wireless communication system," Master's thesis, Wichita University, 2005.

[117] R. Schmidt, "Multiple emitter location and signal parameter estimation," *Antennas and Propagation, IEEE Transactions on*, vol. 34, no. 3, pp. 276–280, 1986.

[118] F. Gross, *Smart antennas for wireless communication*. McGraw-Hill, 2012.

[119] A. Khallaayoun, "High resolution direction of arrival estimation analysis and implementation in a smart antenna system," tech. rep., MONTANA STATE UNIVERSITY.

[120] P. Parvazi, *Sensor Array Processing In Difficult And Non-Idealistic Conditions*. PhD thesis, TU Darmstadt, Darmstadt, March 2012.

[121] A. Paulraj, R. Roy, and T. Kailath, "A subspace rotation approach to signal parameter estimation," *Proceedings of the IEEE*, vol. 74, no. 7, pp. 1044–1046, 1986.

[122] M. Zoltowski, M. Haardt, and C. P. Mathews, "Closed-form 2-d angle estimation with rectangular arrays in element space or beamspace via unitary esprit," *Signal Processing, IEEE Transactions on*, vol. 44, no. 2, pp. 316–328, 1996.

[123] S. Ren, X. Ma, S. Yan, and C. Hao, "2-d unitary esprit-like direction-of-arrival (doa) estimation for coherent signals with a uniform rectangular array," *Sensors*, vol. 13, no. 4, pp. 4272–4288, 2013.

[124] T.-J. Shan, M. Wax, and T. Kailath, "On spatial smoothing for direction-of-arrival estimation of coherent signals," *Acoustics, Speech and Signal Processing, IEEE Transactions on*, vol. 33, no. 4, pp. 806–811, 1985.

[125] M. Haardt and J. Nossek, "Unitary esprit: how to obtain increased estimation accuracy with a reduced computational burden," *Signal Processing, IEEE Transactions on*, vol. 43, no. 5, pp. 1232–1242, 1995.

[126] M. Pesavento, C. F. Mecklenbräuker, and J. F. Böhme, "Multidimensional rank reduction estimator for parametric mimo channel models," *EURASIP J. Appl. Signal Process.*, vol. 2004, pp. 1354–1363, Jan. 2004.

[127] D. Wu, L. Zhou, Y. Cai, R. Hu, and Y. Qian, "The role of mobility for d2d communications in lte-advanced networks: Energy vs. bandwidth efficiency," *Wireless Communications, IEEE*, vol. 21, no. 2, pp. 66–71, 2014.

[128] J. R. Norris, *Markov chains*. No. 2, Cambridge university press, 1998.

[129] C. M. Grinstead and J. L. Snell, *Introduction to probability*. American Mathematical Soc., 2012.

[130] D. Aldous and J. Fill, "Reversible markov chains and random walks on graphs," 2002.

[131] S. Ross, *A first course in probability*. Pearson, 2014.

[132] G. Grimmett and D. Stirzaker, *Probability and random processes*. Oxford university press, 2001.

[133] E. Tuncer and B. Friedlander, *Classical and Modern Direction-of-Arrival Estimation*. Academic Press, 2009.

[134] M. L. Rocca, "RSRP and RSRQ Measurement in LTE." https://www.laroccasolutions.com/78-rsrp-and-rsrq-measurement-in-lte/, 4th April 2016, Sponsored by Laroccasolutions. [Online; accessed 10-March-2018].

[135] R. Roy and T. Kailath, "Esprit-estimation of signal parameters via rotational invariance techniques," *Acoustics, Speech and Signal Processing, IEEE Transactions on*, vol. 37, no. 7, pp. 984–995, 1989.